



DE84002414

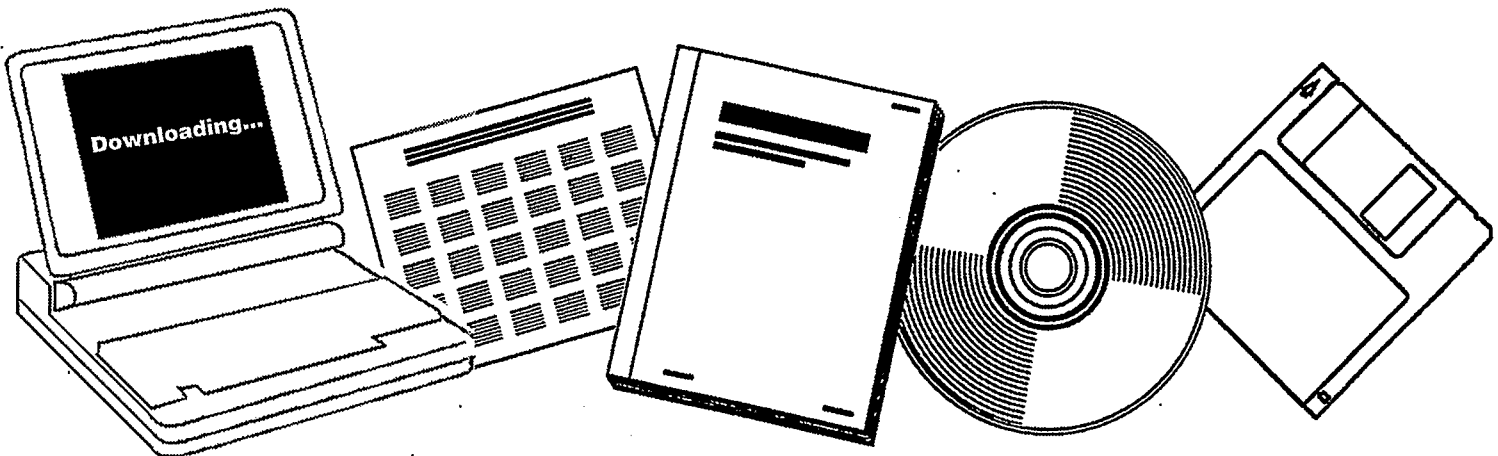
NTIS

One Source. One Search. One Solution.

SITE ACTIVITIES OF ZEOLITE-SUPPORT RU FOR CO HYDROGENATION. FINAL REPORT

PITTSBURGH UNIV., PA. DEPT. OF CHEMICAL
AND PETROLEUM ENGINEERING

01 OCT 1983



U.S. Department of Commerce
National Technical Information Service

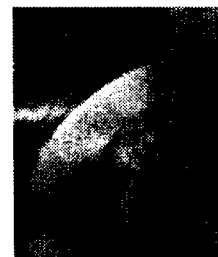
One Source. One Search. One Solution.

NTIS



Providing Permanent, Easy Access to U.S. Government Information

National Technical Information Service is the nation's largest repository and disseminator of government-initiated scientific, technical, engineering, and related business information. The NTIS collection includes almost 3,000,000 information products in a variety of formats: electronic download, online access, CD-ROM, magnetic tape, diskette, multimedia, microfiche and paper.



Search the NTIS Database from 1990 forward

NTIS has upgraded its bibliographic database system and has made all entries since 1990 searchable on www.ntis.gov. You now have access to information on more than 600,000 government research information products from this web site.

Link to Full Text Documents at Government Web Sites

Because many Government agencies have their most recent reports available on their own web site, we have added links directly to these reports. When available, you will see a link on the right side of the bibliographic screen.

Download Publications (1997 - Present)

NTIS can now provides the full text of reports as downloadable PDF files. This means that when an agency stops maintaining a report on the web, NTIS will offer a downloadable version. There is a nominal fee for each download for most publications.

For more information visit our website:

www.ntis.gov



U.S. DEPARTMENT OF COMMERCE
Technology Administration
National Technical Information Service
Springfield, VA 22161

DOE/PC/40774-T1

(DE84002414)

Distribution Category UC-90d

DE84002414



Final Report

SITE ACTIVITIES OF
ZEOLITE-SUPPORTED Ru
FOR CO HYDROGENATION

DOE Grant No. DE-FG22-81PC40774

by

James G. Goodwin, Jr.

Department of Chemical and Petroleum Engineering
University of Pittsburgh
Pittsburgh, PA 15261

October 1, 1983

TABLE OF CONTENTS

| | <u>Page</u> |
|--|-------------|
| I. OBJECTIVE AND SCOPE OF WORK..... | 1 |
| II. SUMMARY OF ACCOMPLISHMENTS..... | 2 |
| III. ARTICLES AND PRESENTATIONS..... | 4 |
| IV. RESULTS AND DISCUSSIONS..... | 7 |
| <u>Chemisorption Characteristics</u> | |
| "Reversible Chemisorption on Highly Dispersed Ru Catalysts"..... | 9 |
| "Particle Size Dependence for CO Chemisorption on Supported Ru Catalysts"..... | 27 |
| "Hydrogen Chemisorption Suppression in Ru-Zeolite Catalysts"..... | 37 |
| <u>Electronic State of Ru</u> | |
| "The Electronic Properties of Ru in Y Zeolites as Determined by ESCA"..... | 56 |
| <u>Hydrogenolysis Properties of NaY-Supported Ru</u> | |
| "Structure and Properties of Zeolite-Supported Ru ₃ (CO) ₁₂ Catalysts"..... | 87 |
| "Characterization of Ru Zeolite Catalysts by a Hydrogenolysis Test Reaction Network"..... | 105 |
| <u>Fischer-Tropsch Synthesis</u> | |
| "The Influence of the Support on K Promotion of Ru for the F-T Synthesis"..... | 128 |
| "Effect of Preparation Method on the Catalytic Properties of Zeolite-Supported Ru in the F-T Synthesis"..... | 135 |
| "F-T Synthesis over Zeolite-Supported Ru Catalysts Derived from Ru ₃ (CO) ₁₂ "..... | 171 |
| "Support Effects on CO Hydrogenation over Ru/Zeolite Catalysts"..... | 190 |

I. OBJECTIVE AND SCOPE OF WORK

The research program entitled "Site Activities of Zeolite-Supported Ruthenium for CO Hydrogenation" was performed for DOE by the University of Pittsburgh under grant no. DE-FG22-81PC40774. Work on the program was initiated on February 1, 1981.

The objective of the program was to identify the catalytic activity, selectivity and stability of three types of ruthenium sites in RuY-zeolite catalysts." The main emphasis was to be directed toward examining these catalysts under Fischer-Tropsch and methanation reaction conditions.

To accomplish the objective, three sequential program tasks were established.

Task 1: Construction of Apparatus

Construction of a differential reactor system, gas volumetric system, and IR cells.

Task 2: Catalyst Preparation/Characterization

Preparation of RuY catalysts was to be done by 3 methods (impregnation by a solution of RuCl_3 , vapor impregnation by $\text{Ru}_3(\text{CO})_{12}$, and ion exchange with a $\text{Ru}(\text{NH}_3)_6\text{Cl}_3$). Catalysts prepared were to be characterized by atomic absorption, gas volumetry, IR, and other pertinent techniques.

Task 3: Catalyst Testing

The activities of the catalyst preparations were to be determined for both methanation and Fischer-Tropsch synthesis in a differential reactor.

II. SUMMARY OF ACCOMPLISHMENTS

The work supported by this grant can be grouped under three headings: a comprehensive study of RuY, Ru supported on zeolites having a range of Si/Al values, and alkali promotion of Ru. NaY-supported Ru catalysts have been prepared by incipient-wetness (I.W.) [using RuCl_3], ion-exchange (I.E.) [using $\text{Ru}(\text{NH}_3)_6\text{Cl}_3$], and vapor-impregnation (V.I.) [using $\text{Ru}_3(\text{CO})_{12}$]. The resulting catalysts were extensively studied by chemisorption, atomic absorption, IR, ESCA, and catalytic reaction (especially F-T). Significant differences were found depending on the method of preparation. These differences were exhibited in both the physical and chemical characteristics of the catalysts. By variation of the preparation method and Si/Al ratio of the zeolite it is possible to develop a better understanding of how metal particle size and location, metal-zeolite interactions, neutralizing cation type and concentration, and the presence of zeolite acid sites can influence the catalytic properties of the supported metal.

Some of the important conclusions from this research are:

1. Highly dispersed (ca. 100% dispersion) NaY-supported Ru catalysts are able to be prepared by I.E. and V.I. The metal particles are dispersed throughout the zeolite support. Catalysts prepared by I.W. are poorly dispersed with large particles primarily on the external surfaces of the zeolites.
2. The fraction of reversible (weak) H_2 chemisorption on Ru catalysts in general is a function of average metal particle diameter, reaching a maximum at an average diameter of 1.6 nm. This suggests that adsorption on intermediately coordinated surface sites are responsible for the weak chemisorption.

3. Significant suppression of hydrogen chemisorption occurs at ambient temperature for ion-exchanged zeolite-supported Ru catalysts as the Si/Al ratio of the zeolite increases. It is suggested that an interaction with the acidic hydroxyl groups is involved in this suppression of chemisorption.
4. While both V.I. and I.E. catalysts have similar dispersions, they exhibit different stoichiometries for CO chemisorption and different IR spectra for adsorbed CO.
5. ESCA results corroborate previous IR results which indicated that ion-exchanged Ru/zeolite catalysts have a number of different type of Ru sites. The binding energy of $3p_{3/2}$ core electrons of Ru appears to be more sensitive to the nature of the different types of Ru present than the $3d_{5/2}$ binding energy.
6. Based on hydrogenolysis reaction studies using RuY catalysts, it appears that the electrostatic field present in the zeolite does not affect the hydrogenolysis of linear species but does facilitate tremendously the rate of cyclopropane ring opening.
7. The observed changes in adsorption and catalytic properties with preparation method for Ru/zeolite catalysts appear to result from differences produced in metal location in/on the zeolite, metal particle size, and zeolite-metal interactions.
8. The activity for F-T over the various catalysts correlates with the ratios of irreversibly (strongly) chemisorbed CO to that of H_2 .
9. The lowest methane selectivity and the highest olefin selectivity is exhibited for highly dispersed catalysts prepared by the vapor impregnation of $Ru_3(CO)_{12}$, provided the carbonyl is able to diffuse into the zeolite (such as is not the case for NaX).

10. Methane selectivity for highly dispersed Ru/zeolite catalysts appears to be influenced by the type and concentration of alkali cations remaining in the zeolite.
11. Olefin selectivity does not appear to be a function of the zeolite support but is a function of the method of catalyst preparation.
12. The formation of isobutane, which occurs only over ion-exchanged catalysts, is probably a function of the acid strength of the OH groups present.

Experimental results, upon which these and other conclusions are based, are given in Section IV of this report

III. ARTICLES AND PRESENTATIONS

The following is a list of articles and presentations based upon research funded in total or in part by this research grant:

Articles

1. C. H. Yang and J. G. Goodwin, Jr., "Particle Size Dependence for CO Chemisorption on Supported Ru Catalysts," *Reaction Kinetics and Catalysis Lett.* 20, 13 (1982).
2. C. H. Yang, Y. W. Chen, I. Wender, and J. G. Goodwin, Jr., "The Influence of the Support on K Promotion of Ru for the Fischer-Tropsch Synthesis," *Symposium on Coal Liquefaction, Preprints of Fuel Chemistry Division (ACS), Kansas City, Sept., 12-17, 1982.*
3. C. H. Yang, and J. G. Goodwin, Jr., "Reversible Chemisorption on Highly Dispersed RuY Catalyst," *J. of Catalysis* 78, 182 (1982).
4. J. G. Goodwin, Jr., Y. W. Chen; H. T. Wang, and J. Z. Shyu, "Zeolite-

Supported Ru in the F-T Synthesis: Effect of Zeolite Type," Proc. of the 1982 DOE Contractors Conf. on Indirect Liquefaction, Greentree, PA, Sept. 8-9, 1982.

5. Y. W. Chen, H. T. Wang, and J. G. Goodwin, Jr., "The Effect of Preparation Method on the Catalytic Properties of Zeolite-Supported Ru in the Fischer-Tropsch Synthesis," J. of Catalysis, in press.
6. Y. W. Chen, H. T. Wang, and J. G. Goodwin, Jr., "Support Effects on CO Hydrogenation over Ru/Zeolite Catalysts," J. of Catalysis, in press.
7. H. T. Wang, Y. W. Chen, and J. G. Goodwin, Jr., "Hydrogen Chemisorption Suppression in Ru-Zeolite Catalysts," Zeolites, in press.
8. Y. W. Chen, H. T. Wang, J. G. Goodwin, Jr., and W. K. Shiflett, "Fischer-Tropsch Synthesis over Zeolite-Supported Ru Derived from $Ru_3(CO)_{12}$," submitted for publication.
9. D. J. Sajkowski, J. Schwank, and J. G. Goodwin, Jr., "Characterization of Ru Zeolite Catalysts by a Set of Hydrogenolysis Test Reactions," submitted for publication.
10. J. Z. Shyu, D. M. Hercules, and J. G. Goodwin, Jr., "The Electronic Properties of Ru in Y Zeolites as Determined by ESCA," submitted for publication.

PRESENTATIONS

1. "Reversible Chemisorption on Highly Dispersed Zeolite-Supported Ruthenium Catalysts," Seventh N. American Meeting of the Catalysis Society, Boston, MA, Oct. 11-15, 1981.
2. "Surface Studies of Zeolite-Supported Ru Catalysts," 33rd Pittsburgh Conference and Exposition on Analytical Chemistry and Applied

- Spectroscopy, Atlantic City, N.J., March 8-13, 1982. Paper 308 (presented by J. Z. Shyu).
3. "Some Aspects of Zeolite-Supported Ru Fischer-Tropsch Catalysts," Pittsburgh Energy Technology Center (DOE), March 18, 1982. Invited Seminar.
 4. "Investigation of Zeolite-Support Effects on Ru-Zeolite Catalysts by ESCA," 21st Pittsburgh Catalysis Society Spring Symp., May 5-7, 1982 (presented by J. Z. Shyu).
 5. "Effects of Preparation Method on the Catalytic Properties of Zeolite-Supported Ru in the Fischer-Tropsch Synthesis," 21st Pittsburgh Catalysis Society Spring Symp., May 5-7, 1982.
 6. "Zeolite-Supported Ru for F-T Synthesis: Effect of Zeolite-Type," DOE Contractors Conference on Indirect Coal Liquefaction, Greentree, Sept. 8-9, 1982, Invited Talk.
 8. "The Influence of the Support on K Promotion of Ru for the Fischer-Tropsch Synthesis," Symp. on Coal Liquefaction, Fuel Chemistry Division, ACS Meeting, Kansas City, Sept. 12-17, 1982 (presented by C. H. Yang).
 9. "Fischer-Tropsch Synthesis over Ru Catalysts Derived from Ru Carbonyls," A.I.Ch.E. Nat. Meeting, Los Angeles, Nov. 14-18, 1982 (presented by W. Shiflett).
 10. "Parameters Affecting the Catalytic Properties of Zeolite-Supported Fisher-Tropsch Catalysts," Tri-State Catalysis Society, Lexington, Ky, March 16, 1983, Invited Talk.
 11. "Parameters Affecting the Catalytic Properties of Zeolite-Supported Fischer-Tropsch Catalysts," Department of Chemical Engineering, Queen's University, Kingston, Ontario, March 25, 1983, Invited Seminar.

12. "Deactivation by Metal Loss," 8th N. Am. Catalysis Society Meeting, Philadelphia, PA, May 1-4, 1983.
13. "Parameters Affecting the Catalytic Properties of Zeolite-Supported Fischer-Tropsch Catalysts," Kimya Mühendisliği Bölümü, Anadolu Üniversitesi, Eskişehir, Turkey, May 23, 1983, Invited Seminar.
14. "Ibid," Kimya Mühendisliği Bölümü, İstanbul Teknik Üniversitesi, İstanbul, Turkey, May 25, 1983, Invited Seminar.
15. "Ibid," Institut de Recherches sur la Catalyse, Villeurbanne, France, June 23, 1983, Invited Seminar.

IV. RESULTS AND DISCUSSIONS

Included in this section are all the major results and conclusions stemming from studies supported by this grant. These studies can be grouped as follows:

Chemisorption Characteristics

"Reversible Chemisorption on Highly Dispersed Ru Catalysts"

"Particle Size Dependence for CO Chemisorption on Supported Ru Catalysts"

"Hydrogen Chemisorption Suppression in Ru-Zeolite Catalysts"

Electronic State of Ru

"The Electronic Properties of Ru in Y Zeolites as Determined by ESCA"

Hydrogenolysis Properties of NaY-Supported Ru

"Structure and Properties of Zeolite-Supported $\text{Ru}_3(\text{CO})_{12}$ Catalysts"

"Characterization of Ru Zeolite Catalysts by a Hydrogenolysis Test Reaction Network"

Fischer-Tropsch Synthesis

"The Influence of the Support on K Promotion of Ru for the F-T Synthesis"

"Effect of Preparation Method on the Catalytic Properties of Zeolite-Supported Ru in the F-T Synthesis"

"F-T Synthesis over Zeolite-Supported Ru Catalysts Derived from $\text{Ru}_3(\text{CO})_{12}$ "

"Support Effects on CO Hydrogenation over Ru/Zeolite Catalysts"

The write-ups for all of these studies are given on the following pages.

REVERSIBLE CHEMISORPTION ON HIGHLY DISPERSED Ru CATALYSTS

Chau-Hwa Yang and James G. Goodwin, Jr.

ABSTRACT

Hydrogen and carbon monoxide adsorption have been studied by static gas volumetric measurement on a range of highly dispersed Y-zeolite supported ruthenium catalysts prepared by ion-exchange. At ambient temperature, the adsorption isotherms indicated two distinct types of adsorption - reversible (composed of both physisorption and weak chemisorption) and irreversible (strongly chemisorbed). The catalysts were highly dispersed and had average particle diameters ranging from 0.9 - 1.6 nm. Reversible hydrogen chemisorption was found to be a function of average particle diameter and dispersion. On the other hand, reversible carbon monoxide chemisorption seemed to be mainly due to interaction with the support.

INTRODUCTION

The recent interest in the hydrogenation of CO has encouraged particular interest in Ru since it is catalytically very active for this reaction.⁽¹⁻³⁾ In general, zeolites offer great possibilities as supports because of their ion-exchange capabilities, shape selectivity, and catalytic properties. Obviously, in order to benefit from all these properties, the metal must be retained in large part within the zeolite and thus remain highly dispersed. Nijs et al.⁽⁴⁾ have found Ru to be the only Fischer-Tropsch active metal that can be easily kept in the zeolite supercages.

In most cases, maintaining supported metal catalysts in a highly dispersed form (60 - 100% Dispersion, $d_{ave} < 2\text{nm}$) necessitates good characterization since the distribution of sites on small crystallites vary greatly with size and shape. Goodwin and Naccache⁽⁵⁾ have found that highly dispersed zeolite Y supported Ru catalysts contain several different types of identifiable active Ru sites - probably existing on atomically dispersed Ru atoms, Ru clusters, and Ru particles greater than 1 nm in diameter. In addition, at high dispersions, there is an enhanced possibility that support-metal interactions may be significant. For the most part, these interactions can make surface characterization more difficult.

Chemisorption measurements can be used to determine adsorptive properties, metal surface area, dispersion, and average particle size for supported metal catalysts. Other techniques, such as E.M., SAXS, STEM, etc., are tricky, expensive and time consuming, and give only physical characterizations. The standard chemisorption technique, while giving both chemical and physical characteristics of a catalyst, does not

distinguish between catalysts at 100% dispersion and having various types of surface sites.

In characterizing by chemisorption RuY catalysts known by E.M. to have dispersions of 100%, Goodwin⁽⁶⁾ found significant quantities of reversible (weak) hydrogen chemisorption at room temperature. McVicker et al.⁽⁷⁾ have found that, on 100% dispersed iridium catalysts, reversible chemisorbed hydrogen is a linear function of the wt% of Ir suggesting that reversible H₂ chemisorption results from interaction with the metal surface.

The objective of the present study was to investigate reversible chemisorption at room temperature, its validity for surface characterization, and the factors which might affect its quantities for RuY catalysts having a range of metal loadings and various dispersions.

EXPERIMENTAL

RuY catalysts containing 0.19 to 3 wt% Ru were prepared by ion-exchange of hexamine ruthenium (III) chloride. The Ru(NH₃)₆Cl₃, obtained from Strem Chemical Co., was dissolved in an acidic hydrochloride solution (pH = 4.5). This solution was then mixed with NaY zeolite and stirred continuously for 50 hours at room temperature. Excess solution was used for this purpose to maintain approximately a constant pH during ion exchange.

After the exchange reaction, the catalysts were filtered and washed several times in deionized water and dried in air for 18 hours at 40°C. Ru metal loading was determined by atomic absorption spectrometry.

Prior to chemisorption measurements in a conventional gas volumetric apparatus, approximately one gram of the supported complex was decomposed

slowly under vacuum (10^{-6} Torr) by heating (at approximately $1^{\circ}\text{C}/\text{min}$) to 420°C and holding at that temperature for two hours. A Stanton Redcroft 3077 programmable linear rate temperature controller was used. The catalyst was reduced in pure H_2 ($p = 20$ kPa) at 420°C for two hours and then heated at the same temperature to desorb the hydrogen.

Air Products UPC grade hydrogen and helium were passed through a liquid nitrogen trap before being admitted to the gas reservoirs. Helium was used for dead volume determination. Carbon monoxide of 99.99% purity was used as received for adsorption measurements.

The hydrogen adsorption measurements were made at 25°C and isotherms of total H_2 adsorption on the fresh catalyst were determined from 50 Torr to 400 Torr. The time for the equilibration at each pressure was about four hours. The catalysts were then evacuated for ten minutes at the same temperature and a second adsorption was carried out in the same manner. However, there was no significant difference in the quantity of adsorbed species removed for evacuation times ranging between 2 and 20 minutes.

Carbon monoxide uptakes at 25°C on the same samples were made after desorption of H_2 at 420°C for two hours under vacuum. The same procedure as in H_2 adsorption was used. However, twelve hours were required for each measurement. Studies indicated that adsorption and desorption of H_2 did not cause sintering of the Ru provided no prior exposure of the catalyst to O_2 or CO had occurred.

RESULTS AND DISCUSSION

A typical set of hydrogen adsorption isotherms is shown in Figure 1 for the RuY catalyst. Two separate isotherms, designated as a and b, indicate the total and reversible adsorption, respectively. The linear region of isotherm a above 120 Torr indicates complete coverage of the ruthenium surface by hydrogen. Following evacuation for 10 minutes, isotherm b was obtained. The two isotherms were parallel, as expected. The observed increasing amount of adsorbed hydrogen with increasing pressure above the point of complete coverage of the ruthenium surface was due to physical adsorption on the catalyst.

Extrapolation of the hydrogen adsorption isotherms to zero pressure gives the amount of total and reversible chemisorbed hydrogen, namely, $H_{2(T)}$ and $H_{2(r)}$. The net irreversible hydrogen uptake, $H_{2(ir)}$, at zero pressure was obtained by subtracting the reversible contribution from the initial uptake.

$$H_{2(ir)} = H_{2(T)} - H_{2(r)}$$

It is evident that on ruthenium two distinct types of hydrogen chemisorption occur at room temperature: a rather strong, activated chemisorption (designated here as "irreversible") and a weak, non-activated chemisorption (designated as "reversible") which is rapidly removed under vacuum.

Earlier work⁽⁶⁾ on highly-dispersed NaY-supported Ru utilizing both chemisorption and T.E.M. has shown that such catalysts can be accurately characterized using H_2 chemisorption by assuming a stoichiometry of $H_{(ir)}/Ru_{(s)} = 1$. Characteristics of the Ru catalysts studied here were thus determined from the irreversible hydrogen chemisorption and are shown in Table 1. The ruthenium surface area per gram of metal, S, was calculated from hydrogen adsorption assuming an average Ru area of

8.17 Å² per Ru atom. Dispersion, D, is defined according to the following:

$$D = \frac{\text{number of surface metal atoms}}{\text{number of total metal atoms}} \times 100\%$$

Average particle size, d, was calculated from the surface area data employing the relation $d = 5/S \cdot \rho$, assuming the particle to be cubic with five sides exposed to the gas phase and where ρ is the density of bulk ruthenium. It should be noted that the particle size thus obtained represents a good estimation of the average Ru size range since zeolites usually provide a rather uniform distribution for metal particles due to their crystalline cage structure, although some larger particles tend to exist on the external surfaces of the zeolite. Thus, Ru particles having diameters less than 16 Å, are sufficiently small to remain in the zeolite cages.^(4,8) The catalysts in this range, therefore, are designated as highly dispersed.

In order to determine the catalyst characteristics from H₂ chemisorption it was not possible to use the intersection of the extrapolated total adsorption isotherm at zero pressure. It has been reported earlier⁽⁶⁾ that, on totally dispersed RuY catalysts (as determined by electron microscopy), employing the extrapolated total hydrogen adsorption isotherm produced a stoichiometry ratio, H_(T)/Ru_(s), as high as 1.94. Since the stoichiometric ratio for irreversibly (strongly) chemisorbed hydrogen, H_(ir)/Ru_(s), was found to be approximately unity, it was suggested that an assumption of H_(ir)/Ru_(s) = 1 would be a better approximation for the purpose of characterization. It is felt that this quantity is more constant with varying particle size than H_(T)/Ru_(s). For a more complete discussion of the earlier work on the determination of values for H_(T)/Ru_(s) using Ru powder and of the relationship of this

ratio to the characteristics of highly dispersed NaY-supported Ru please refer to Goodwin.⁽⁶⁾

Similar adsorption isotherms were obtained for carbon monoxide on RuY, such as shown in Figure 2. $CO_{(T)}$, $CO_{(rev)}$, and $CO_{(ir)}$, given in Table 2, were determined in an identical manner as those values for H_2 . The values found for $CO_{(ir)}/H_{(ir)}$ imply that CO molecules were multiply chemisorbed on the surface Ru atoms for all the samples investigated. These results for CO adsorption are in agreement with previous findings of multiple adsorption of CO on highly dispersed Ru.^(1,9,10)

Reversibly adsorbed hydrogen which desorbs upon evacuating at ambient was found to be significant. This reversibly adsorbed hydrogen includes the hydrogen molecules in the physisorbed state and the hydrogen species in the weakly chemisorbed state, either a transition state at total surface coverage or an adsorption state on low energy sites. Taylor⁽¹¹⁾ has noted reversible chemisorption of H_2 on 1% Ru/ Al_2O_3 following evacuation of the catalyst for one hour. As high as 75% of the hydrogen initially adsorbed was found to be reversible at ambient. Kubicka and Kuźnika⁽¹²⁾ have also observed 25% reversibly adsorbed hydrogen on Ru/ Al_2O_3 at 25°C. While at 400°C, 80% of the total chemisorption became reversible.

Obviously, all chemisorption is reversible if one evacuates long enough or at high enough temperatures. Desorption occurs when the adsorbate-adsorbant bond acquires the activation energy for desorption in the form of vibrational energy. TPD spectra of hydrogen and CO adsorption from 20°C to 500°C indicates considerable nonhomogeneity of chemisorbed molecules or atoms on highly dispersed Ru surfaces.⁽¹³⁾ For certain metals, i.e. Co, chemisorption may be so weak that all can be removed

fairly fast by evacuation at room temperature. For hydrogen adsorption on RuY surfaces, however, two distinct types of chemisorption co-exist at room temperature: reversible and irreversible. Each type is associated with a specific average activation energy and kinetics. It is believed that, at total surface coverage and equilibrium, some factors which might influence the reversibility of hydrogen adsorption are metal dispersion, particle size, and support-metal interactions.

In this study, for the highly dispersed RuY catalysts, the quantity of reversibly bound hydrogen varied from 1.4 to 35.8 micromoles per gram of catalyst while that of CO was relatively constant for all the RuY catalysts studied (as shown in Figure 3). This behavior is similar to the reversible chemisorption results for Ir found by McVicker et al.⁽⁷⁾ As can be seen in Figure 3, reversibly bound CO does not vary greatly as the Ru weight percent (and consequently surface area) increases suggesting that this quantity is mainly due to the interaction with the total catalyst surface, including the zeolite support's surface. On the other hand, reversible bound hydrogen would seem to be a linear function of the Ru weight percent. Certainly, the Ru surface area increased with increasing Ru metal loading (see Table 1). However, in order to prevent all properties from varying directly with metal loading, slight differences in the rate of temperature programmed decomposition (0.5°C - 1.5°C/min) were used. This produced a variety of Ru dispersions not directly related to metal loading.

The fraction of reversibly chemisorbed H₂, R_H, was observed to increase from 13 to 32% of the initial as the average Ru particle size increased from 0.87 to 1.59 nm (Figure 4). A similar variance was also observed as to be expected when metal dispersion was plotted instead of

average particle size (Figure 5). This indicates that a greater portion of hydrogen is strongly chemisorbed on smaller Ru particles than on larger ones. From the concept that the extent of reversibility is associated with lower energy sites and/or sites for multiple hydrogen chemisorption, such sites on the larger Ru particles would be predominantly responsible for the reversible chemisorption.⁽¹³⁾ It is evident that the small Ru particles must possess a greater fraction of sites which do not chemisorb hydrogen weakly at room temperature. It is as yet difficult to say whether this is a structural effect solely or an effect due to support-metal interactions having a greater influence on the properties of the smaller clusters. Based on previously compared E.M. and chemisorption results⁽⁶⁾ where $H/Ru_{(s)} = 1$ was found (based on $H_{(ir)}$), it would seem highly likely that at least some of the reversibly chemisorbed hydrogen at room temperature is due to multiple hydrogen chemisorption on certain Ru sites.

Another possibility to be considered for the appearance of reversible chemisorption is hydrogen spillover. An unoccupied site on the Y zeolite in the vicinity of a Ru particle may function as a hydrogen-acceptor site.^(14,15) Thus the amount of hydrogen spillover onto the support would be directly proportional to the quantity of neighboring sites and to the surface area and particle size of the metal. However, it has been suggested that hydrogen spillover should only be significant beyond ambient temperature.⁽¹⁴⁾ In the present case, hydrogen spillover would seem to be of minor importance.

CONCLUSIONS

A detailed picture of reversible adsorptive properties of ion-exchanged RuY catalysts has been obtained. For highly dispersed RuY catalysts prepared by ion-exchange, the fraction of reversibly (weakly) chemisorbed hydrogen is directly related to average particle size and dispersion. This fraction increases approximately linearly with average Ru particle diameter for diameters between 0.9 and 1.6 nm; however, it probably eventually attains a constant value for large particles. This reversible hydrogen chemisorption may be related to multiple chemisorption on certain Ru sites. These results for reversible H₂ chemisorption are surprising since one might expect that highly uncoordinated sites on smaller particles would be more likely to exhibit multiple chemisorption.

Reversible (weak) CO chemisorption, unlike that of H₂, is a function only of total catalyst surface area. In other words, it seems due to an interaction with both the metal and the support.

The reversibility of hydrogen chemisorption may depend upon other factors besides particle diameter. Preliminary results of chemisorption on zeolite supported Co catalysts indicate that the fraction of reversibly chemisorbed hydrogen is sensitive to the preparation method. Several other factors which might affect reversible hydrogen chemisorption are the temperature of adsorption, the presence of impurities, and support-metal interactions.

REFERENCES

1. Dalla Betta, R. A., J. Phys. Chem. 79, 2519 (1975).
2. Dalla Betta, R. A., Piken, A. G., and Shelef, M., J. Catal. 40, 173 (1975).
3. Vannice, M. A., Adv. in Chem. Ser. 163, 15 (1972).
4. Nijs, H. H., Jacobs, P. A., and Uytterhoeven, J. B., J. C. S. Chem. Comm., 1095 (1979).
5. Goodwin, J. G. Jr., and Naccache, C., J. Catal. 64, 482 (1980).
6. Goodwin, J. G., Jr., J. Catal. 68, 227 (1981).
7. McVicker, G. B., Baker, R. T. K., Garten, R. L., and Kugler, E. L., J. Catal. 65, 207 (1980).
8. Pederson, L. A., and Lunsford, H., J. Catal. 61, 39 (1980).
9. Kobayashi, M., and Shirasaki, T., J. Catal. 28, 289 (1973).
10. Kobayashi, M., and Shirasaki, T., J. Catal. 32, 254 (1974).
11. Taylor, K. C., J. Catal. 38, 299 (1975).
12. Kubicka, H., and Kuźnika, B., React. Kin. Catal. Lett. 8, 131 (1978).
13. Yang, C. -H., M. S. Thesis, University of Pittsburgh, 1980.
14. Sermon, S. A., and Bond, G. C., Catal. Rev. 8, 211 (1973).
15. Neikam, W. C., and Vannice, M. A., in Proceedings of Fifth International Congress on Catalysis, Vol. 1, North Holland, Amsterdam, 1972, pp. 609.

ACKNOWLEDGEMENTS

This research was supported in part by the Department of Energy via Grant No. DE-FG22-81PC40774.

TABLE 1: Catalyst Characteristics (1)

| Wt % Ru | S.A. (2) (m ² Ru/g.cat.) | d _{ave} (3) (nm) | D, % (4) |
|---------|--|------------------------------|----------|
| 0.19 | 0.89 | 0.87 | 95.8 |
| 0.38 | 0.95 | 1.59 | 52.0 |
| 0.76 | 2.86 | 1.07 | 77.4 |
| 1.5 | 4.03 | 1.50 | 55.3 |
| 3.0 | 9.56 | 1.27 | 65.5 |

- (1) Based on A.A. and gas volumetry
(2) 8.17 Å²/Ru surface atom, H_(ir)/Ru(s) = 1
(3) d_{ave} = 5/S·ρ, S = m²/g·Ru
(4) D = (# Ru(s)/# Ru(T)) x 100%

Table 2: Comparison of Hydrogen and Carbon Monoxide Chemisorption on RuY Catalysts

| Sample (wt.% Ru) | H ₂ uptakes, 10 ⁻⁶ mol/g | | | CO uptakes, 10 ⁻⁶ mol/g | | | Ratio |
|---------------------|--|--------------------|---------------------|------------------------------------|-------|--------|-------|
| | H ₂ (T) | H ₂ (r) | H ₂ (1r) | CO(T) | CO(r) | CO(1r) | |
| 0.19 | 10.4 | 1.4 | 9.0 | 108.0 | 20 | 88.0 | 0.13 |
| 0.38 | 13.8 | 4.1 | 9.7 | 112.5 | 25 | 87.5 | 0.30 |
| 0.76 | 37.2 | 8.1 | 29.1 | 276.1 | 22 | 254.1 | 0.22 |
| 1.5 | 60.0 | 19.0 | 41.0 | -- | -- | -- | 0.32 |
| 3.0 | 133.0 | 35.8 | 97.2 | 927.0 | 30 | 897.0 | 0.27 |

^aFraction of reversibly chemisorbed H₂, R_H = H(r)/H(T) = H₂(r)/H₂(T)

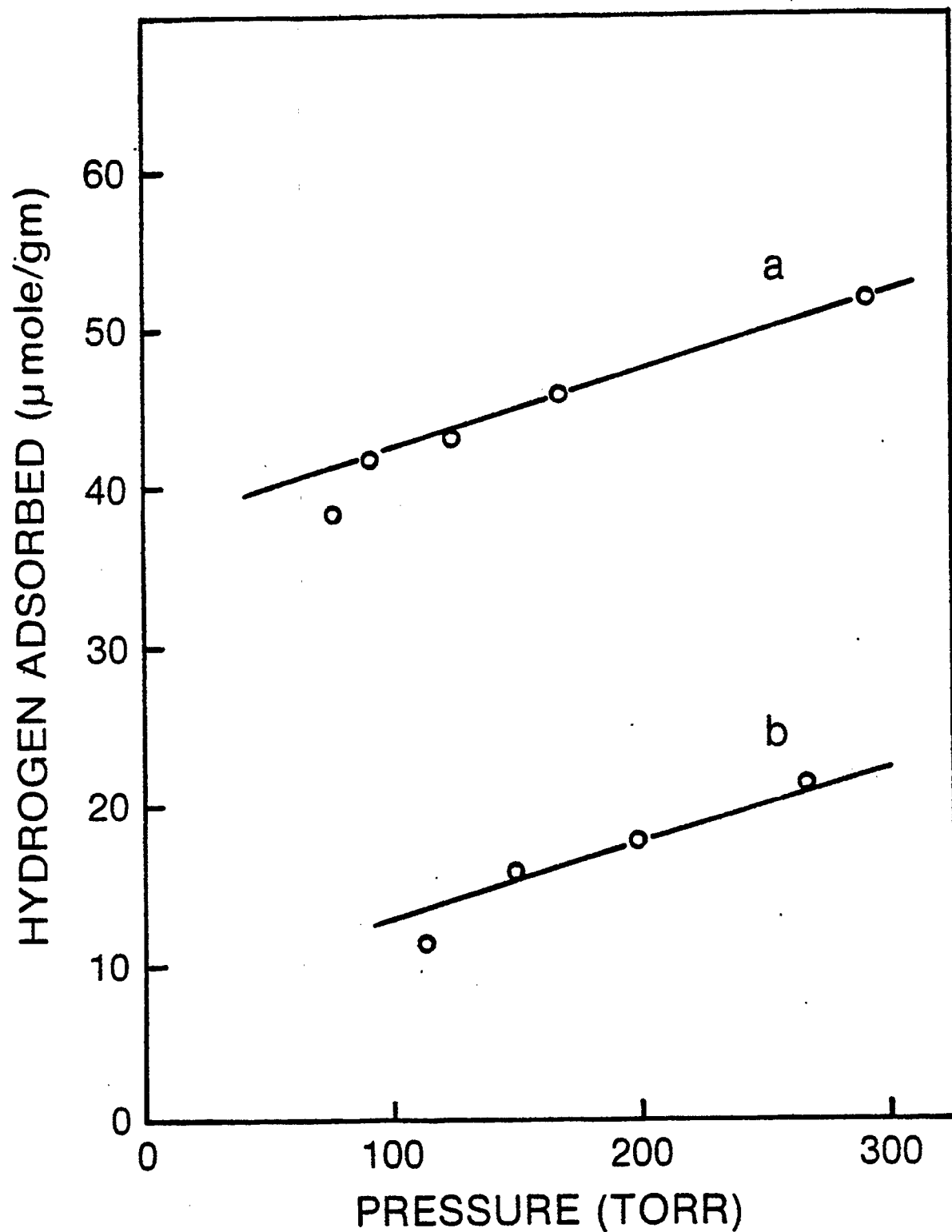


Figure 1: Hydrogen Adsorption Isotherms on 0.76 wt% RuY at 25°C
(a) Total Adsorption (b) Reversible Adsorption.

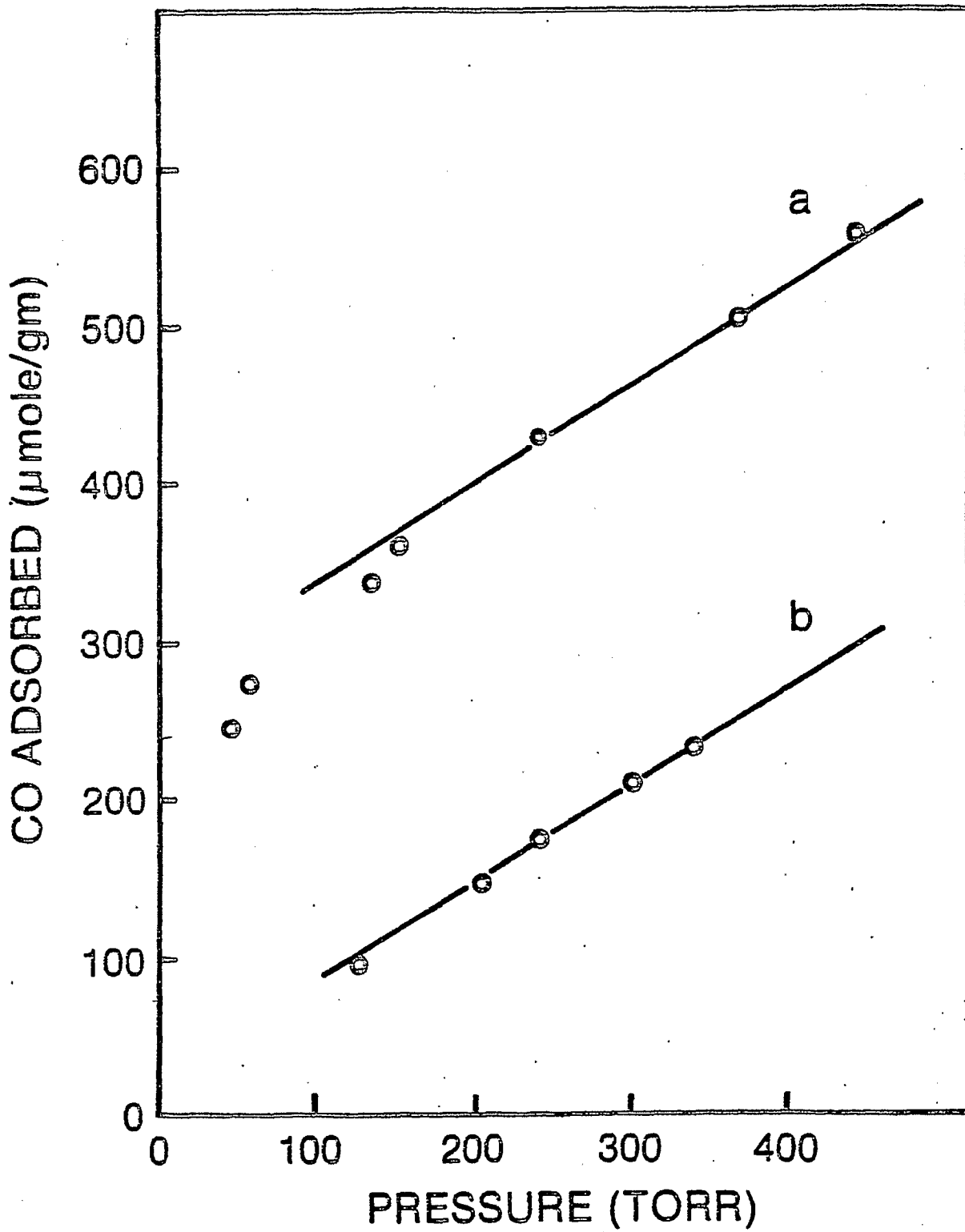


Figure 2: CO Adsorption Isotherms on 0.76 wt% RuY at 25°C
(a) Total Adsorption (b) Reversible Adsorption.

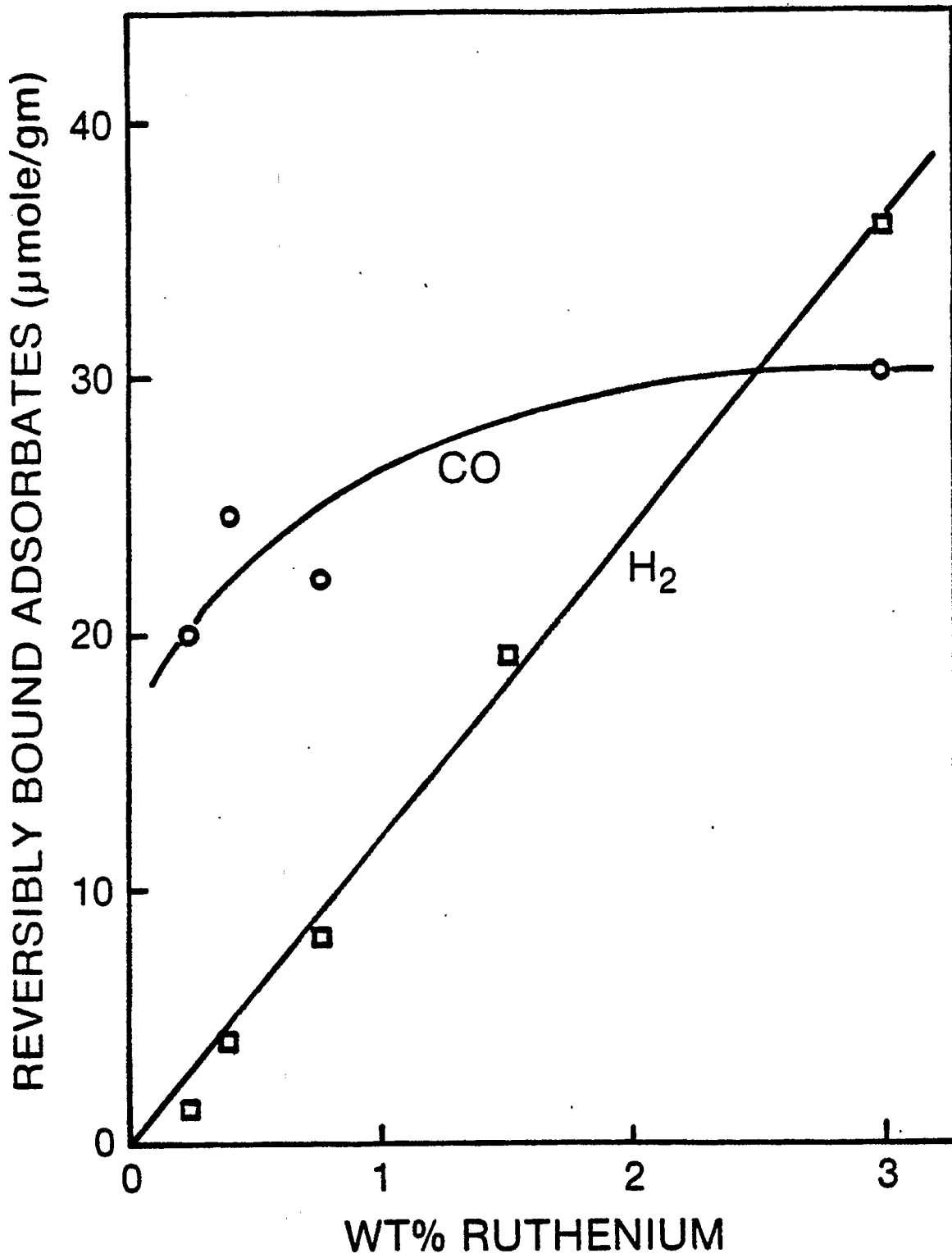


Figure 3: The Effect of Ru Metal Loading on the Reversible Quantities of H_2 and CO Chemisorption from RuY Catalysts at 25°C .

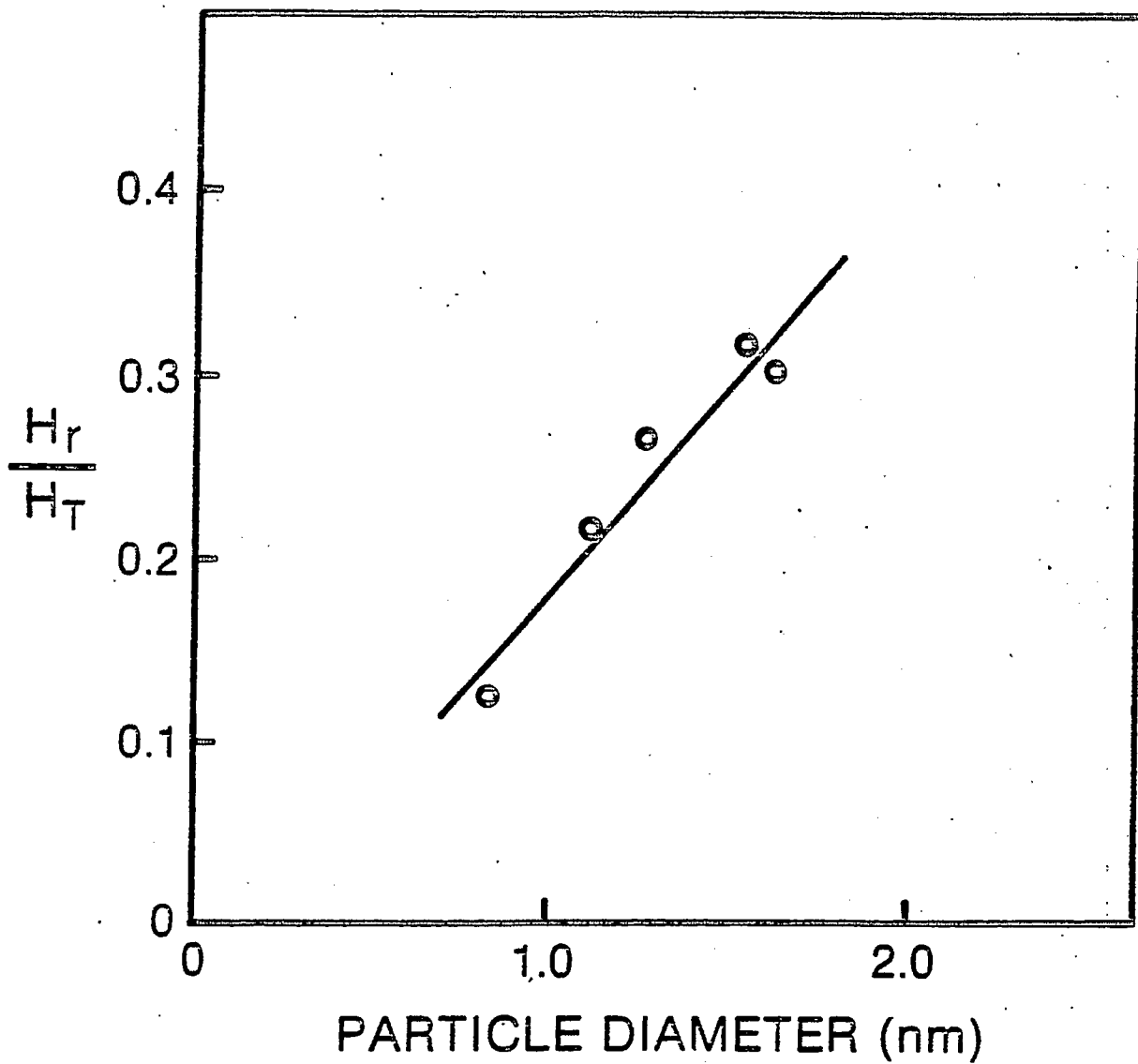


Figure 4: The Effect of Particle Size on Reversibility of Hydrogen Chemisorption on RuY Catalysts.

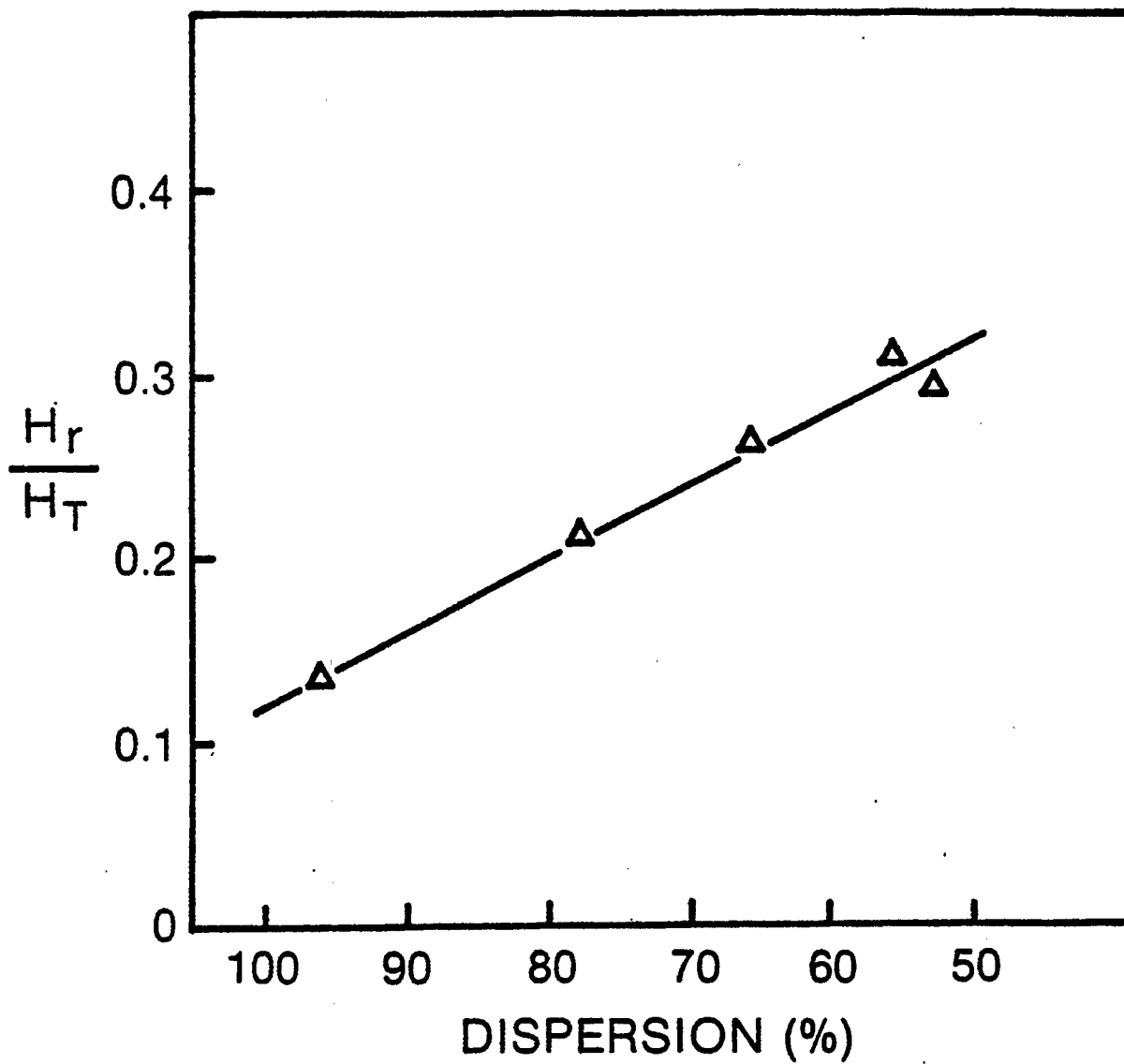


Figure 5: The Effect of Dispersion on Reversibility of Hydrogen Chemisorption on RuY Catalysts.

PARTICLE SIZE DEPENDENCE FOR CO CHEMISORPTION ON SUPPORTED Ru CATALYSTS

Chau-Hwa Yang and James G. Goodwin, Jr.

ABSTRACT

The stoichiometry of CO chemisorption on highly dispersed zeolite-supported Ru has been investigated. This stoichiometry, which can be expressed as CO/H, increases with decreasing Ru particle diameter. For diameters < 1.6 nm this ratio approached a limiting value of 4-5, indicating the formation of surface carbonyls. No direct influence of the support on this ratio could be detected.

INTRODUCTION

CO chemisorption has been used successfully for the surface area determination of certain supported metals. For Ru, however, CO chemisorption can result in the adsorption of several molecules for each Ru surface atom.⁽¹⁻⁴⁾ Because the stoichiometry of CO chemisorption can vary, the chemisorption of CO has not been useful for the determination of Ru surface area or the number of Ru surface sites in supported Ru catalysts. For this purpose, the use of H₂ chemisorption has proved to be more satisfactory since it appears that the ratio H/Ru_(surface) is independent of metal particle size and has a value of approximately one.⁽⁵⁻⁷⁾

Interestingly, Dalla Betta⁽³⁾ found that ratio CO/H, based on separate chemisorptions of H₂ and CO, varied with particle size. This ratio increased from a value of 0.63 for an average Ru particle diameter, d_{Ru} , of 10³ nm to 3.8 for d_{Ru} equal to 1.4 nm before increasing to 3.1 for d_{Ru} = 1.1 nm.

An investigation was undertaken to study the stoichiometry of CO adsorption on supported Ru as the average metal particle size was decreased below 2.5 nm average diameter. It was felt that this ratio of CO/H might be of use in the characterization of the particulate structures. In particular, it was desired to find out if the CO/H ratio does in fact exhibit a maxima as found by Dalla Betta⁽³⁾ and what part the support might play in affecting this ratio as the average Ru particle diameter decreases:

EXPERIMENTAL.

RuY catalysts containing 0.19 to 3.2 wt% Ru were prepared by ion-exchange of $\text{Ru}(\text{NH}_3)_6\text{Cl}_3$ with NaY zeolite. The Ru metal loading was determined by atomic absorption spectrometry.

The prepared catalysts were decomposed slowly under vacuum on heating at a rate of 0.5-1.5 k/min to 420 K. They were then reduced in H_2 at that maximum temperature for 2 hours and then desorbed under vacuum for 2 hours while maintaining the temperature.

Chemisorption measurements were made using a conventional gas volumetric apparatus. Detailed description of the methodology is given elsewhere.⁽⁹⁾ The hydrogen adsorption measurements were made at 25°C and isotherms of the total H_2 adsorption on the fresh catalysts were determined from 50 to 400 torr. The time for the equilibration at each pressure was about 4 hrs. The catalysts were then evacuated for 10 minutes and a second adsorption was carried out in the same manner.

Carbon monoxide adsorption at 25°C on the same samples were made after desorption of H_2 at 420°C for 2 hrs under vacuum. The same procedure as in H_2 adsorption measurement was used. However, 12 hours were required for equilibrium at each pressure on the total CO adsorption isotherms.

DISCUSSION OF RESULTS

Figures 1 and 2 show typical H_2 and CO isotherms. The amounts irreversibly chemisorbed at 298 K, the difference between the total isotherm and the reversible isotherm, were used in the calculations. This quantity has been shown for H_2 to best reflect $\text{H}/\text{Ru}_{(\text{surface})} = 1$.⁽⁷⁾ For CO

chemisorption, the reversible quantity, that which is easy to be removed by evacuation at temperature, seems to be due to interaction of CO with the support.⁽⁸⁾ The characteristics of each catalyst and its determined CO/H ratio are given in Table 1.

A plot of CO/H versus average Ru particle diameter is shown in Figure 3. It can immediately be seen that the CO/H ratio exceeds 1 for all $d_{\text{Ru}} < 3$ nm. For the RuY catalysts, a limiting value of CO/H between 4 and 5 is reached below 1.6 nm. It may be noted that one of the Ru/Al₂O₃ catalysts (that at the highest dispersion) appears to deviate somewhat from the general trend found for the RuY and other Ru/Al₂O₃ catalysts. This might be attributed to an effect of the Al₂O₃ support on highly dispersed Ru; however, it is most likely due either to an experimental error or to the fact that Dalla Betta⁽³⁾ used the zero pressure intercept of the total adsorption isotherm to characterize his catalysts. Previous work has shown, that for highly dispersed RuY catalysts, the use of the total isotherm can introduce significant error into the calculation if $H/\text{Ru}_{(\text{surface})} = 1$ is being assumed.⁽⁷⁾

As supported metal particle sizes become smaller and smaller, support-metal interactions can play a greater role in affecting the properties of the metal. It would be expected, based on steric considerations and the existence of various Ru carbonyls, that as Ru particles decrease in size a greater number of CO molecules would be chemisorbed. Strong interaction of the Ru with the acidic support, however, would be expected to weaken CO adsorption and perhaps decrease the number of CO molecules able to be adsorbed. No such decrease was detected. Since the results for Al₂O₃-supported Ru also appear to follow approximately the same trend as those for zeolite-supported Ru, no direct evidence of support effects is detectable in this process.

Finally, metallic Ru clusters or particles less than 1.6 nm have the ability to irreversibly bind between four and five CO molecules per exposed metal atom. Evidently, carbonyl species such as $\text{Ru}(\text{CO})_4$ and $\text{Ru}(\text{CO})_5$ may exist on highly dispersed Ru catalysts. While Ru carbonyls are known to exist having these stoichiometries [$\text{Ru}_3(\text{CO})_{12}$ and $\text{Ru}(\text{CO})_5$], it may be hard to picture from a steric point of view 5 CO molecules adsorbed per surface Ru atom on 1.6 nm particles. A small portion of this bound CO, however, may be interacting with the zeolite instead of with the Ru since carbonate bands can be seen by IR spectroscopy for the zeolite exposed to CO. It also must be remembered that the Ru particle diameter used is an average value. As IR study of CO adsorption on RuY has shown,⁽⁴⁾ many different Ru surface structures can exist simultaneously on these catalysts at high dispersion. Thus, while the average particle diameter may be 1.0-1.5 nm, many very small clusters of Ru atoms and, possibly, isolated single atoms may also exist. Such small clusters could easily produce $\text{Ru}(\text{CO})_4$ or $\text{Ru}(\text{CO})_5$ following CO adsorption.

CONCLUSIONS

CO chemisorption at 298 K on highly dispersed Ru is a function of metal particle size. The CO/H ratio exceeds 1 for Ru catalysts having an average particle diameter, $d_{\text{Ru}} < 3$ nm. The ratio increases rapidly as average particle size decreases and approaches a limit of between 4 and 5 for $d_{\text{Ru}} < 1.6$ nm. It is obvious that surface species of the form $\text{Ru}(\text{CO})_4$ or $\text{Ru}(\text{CO})_5$ are formed. Finally, no evidence of a direct support effect on the CO/H ratio was found.

ACKNOWLEDGEMENT

This work was supported in part by the U. S. Department of Energy via Grant Number DE-FG22-81PC40774.

REFERENCES

1. C. R. Guerra and J. A. Schulman, *Surface Sci.* 7, 229 (1967).
2. M. Kobayashi and T. Shirasaki, *J. of Catal.* 32, 254 (1974).
3. R. A. Dalla Betta, *J. Phys. Chem.* 79, 2519 (1975).
4. J. G. Goodwin, Jr., and C. Naccache, *J. of Catal.* 64, 482 (1980).
5. R. A. Dalla Betta, *J. Catal.* 34, 57 (1974).
6. K. C. Taylor, *J. of Catal.* 38, 299 (1975).
7. J. G. Goodwin, Jr., *J. of Catal.* 68, 227 (1981).
8. C.-H. Yang and J. G. Goodwin, Jr., submitted for publication.
9. C.-H. Yang, M. S. Thesis, University of Pittsburgh, 1980.

TABLE 1: Characteristics of Catalysts

| Catalyst | wt.% | d_{Ru} (nm) [*] | CO/H | Ref. |
|---|-------|----------------------------|------|------------|
| Ru powder & Al ₂ O ₃ | -- | 10 ³ | 0.63 | (3) |
| Ru/Al ₂ O ₃ | 5% | 9.6 | 0.52 | (3) |
| Ru/Al ₂ O ₃ | 5% | 6.0 | 0.87 | (3) |
| RuY | 3.2% | 2.8 | 2.07 | this paper |
| Ru/Al ₂ O ₃ | 5% | 2.5 | 2.3 | (3) |
| RuY | 3.2% | 2.0 | 4.0 | this paper |
| RuY | 0.38% | 1.6 | 4.51 | this paper |
| Ru/Al ₂ O ₃ | 0.5% | 1.4 | 3.8 | (3) |
| RuY | 3% | 1.3 | 4.61 | this paper |
| Ru/Al ₂ O ₃ | 0.23% | 1.1 | 3.1 | (3) |
| RuY | 0.76% | 1.1 | 4.38 | this paper |
| RuY | 0.19 | 0.9 | 4.89 | this paper |

* average value--determined by H₂ chemisorption

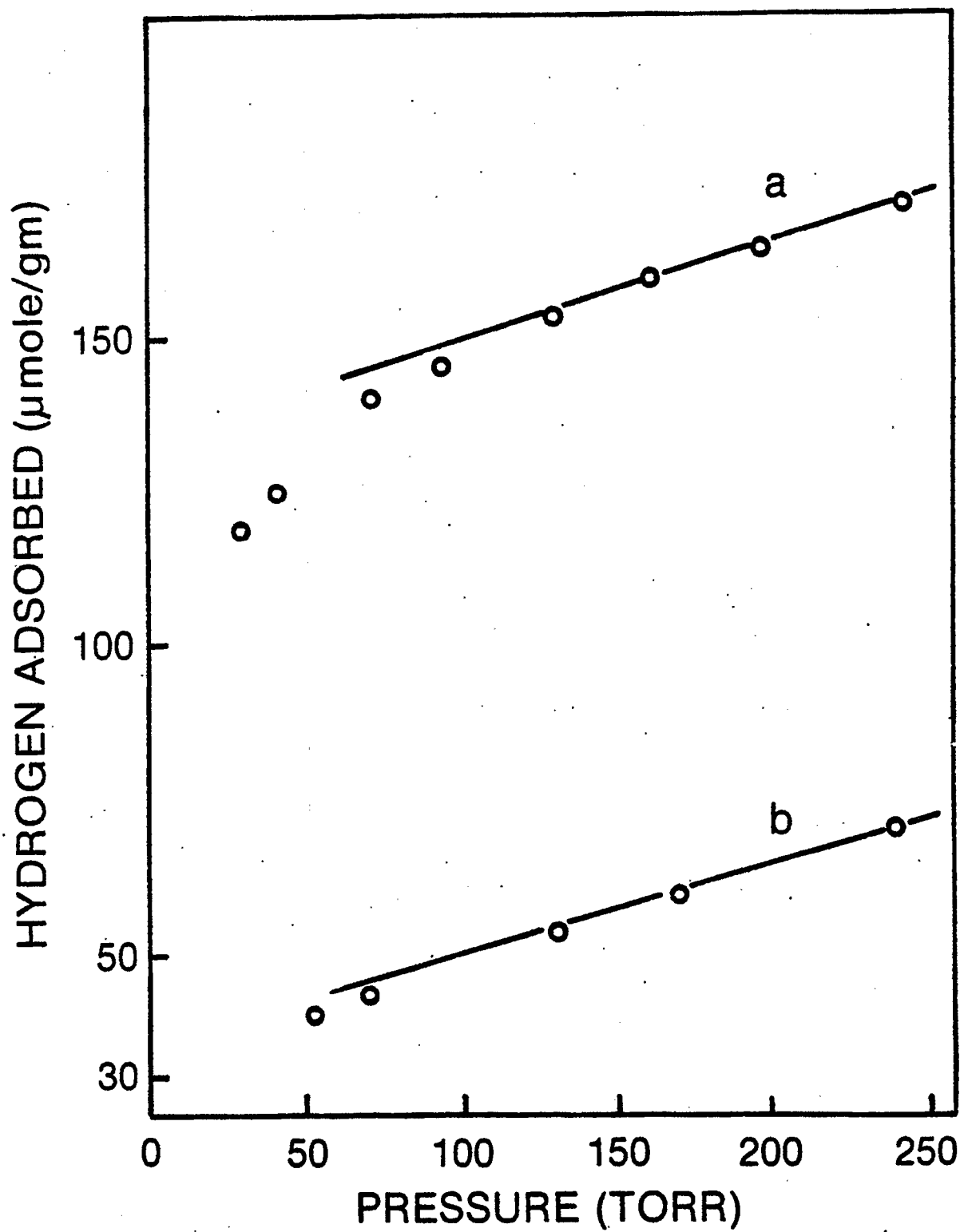


FIGURE 1: Hydrogen Adsorption Isotherms on 3 wt% RuY at 25°C.

- a. total adsorption
- b. reversible adsorption

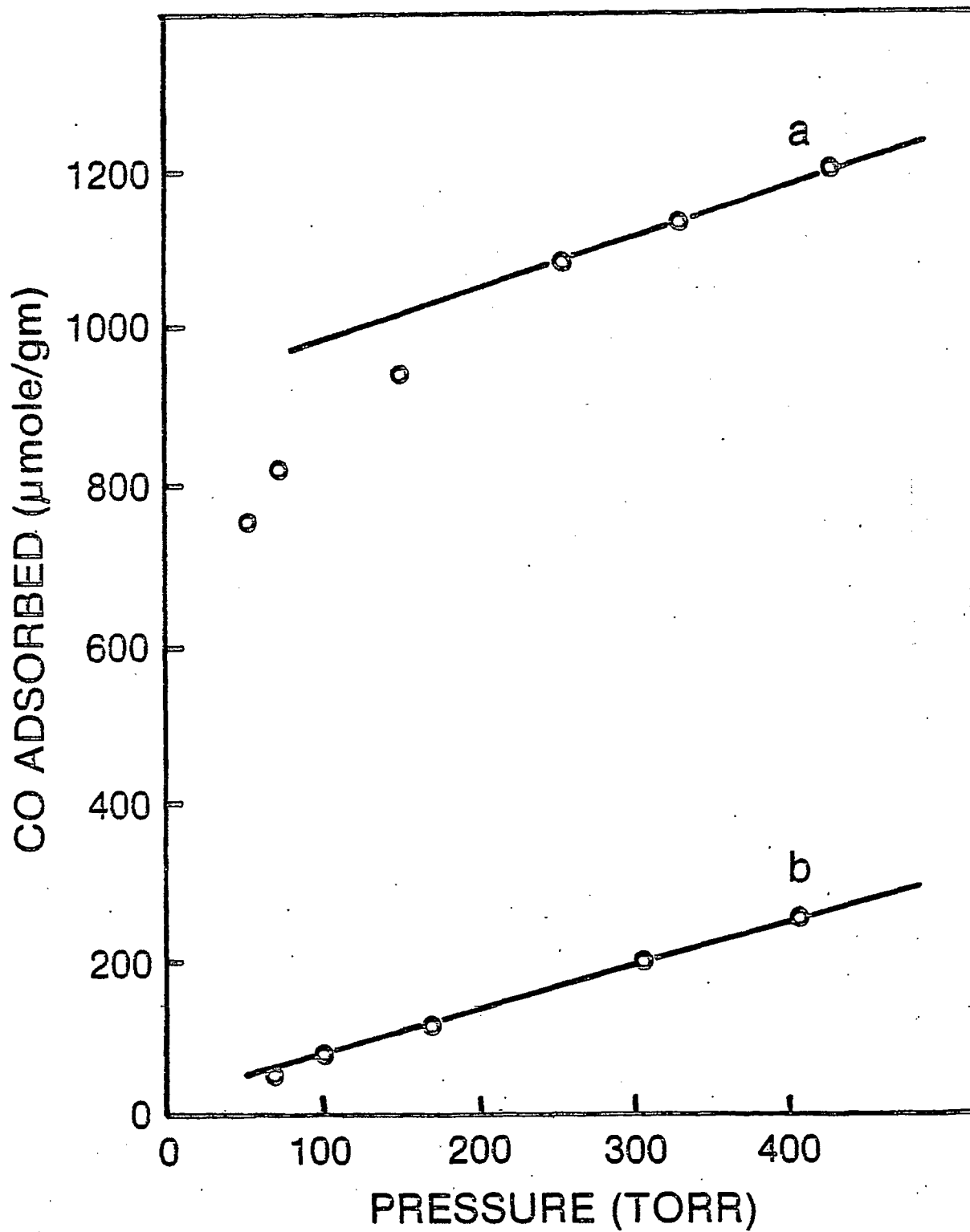


FIGURE 2: CO Adsorption Isotherms on 3 wt% RuY at 25°C

- a. total adsorption
- b. reversible adsorption

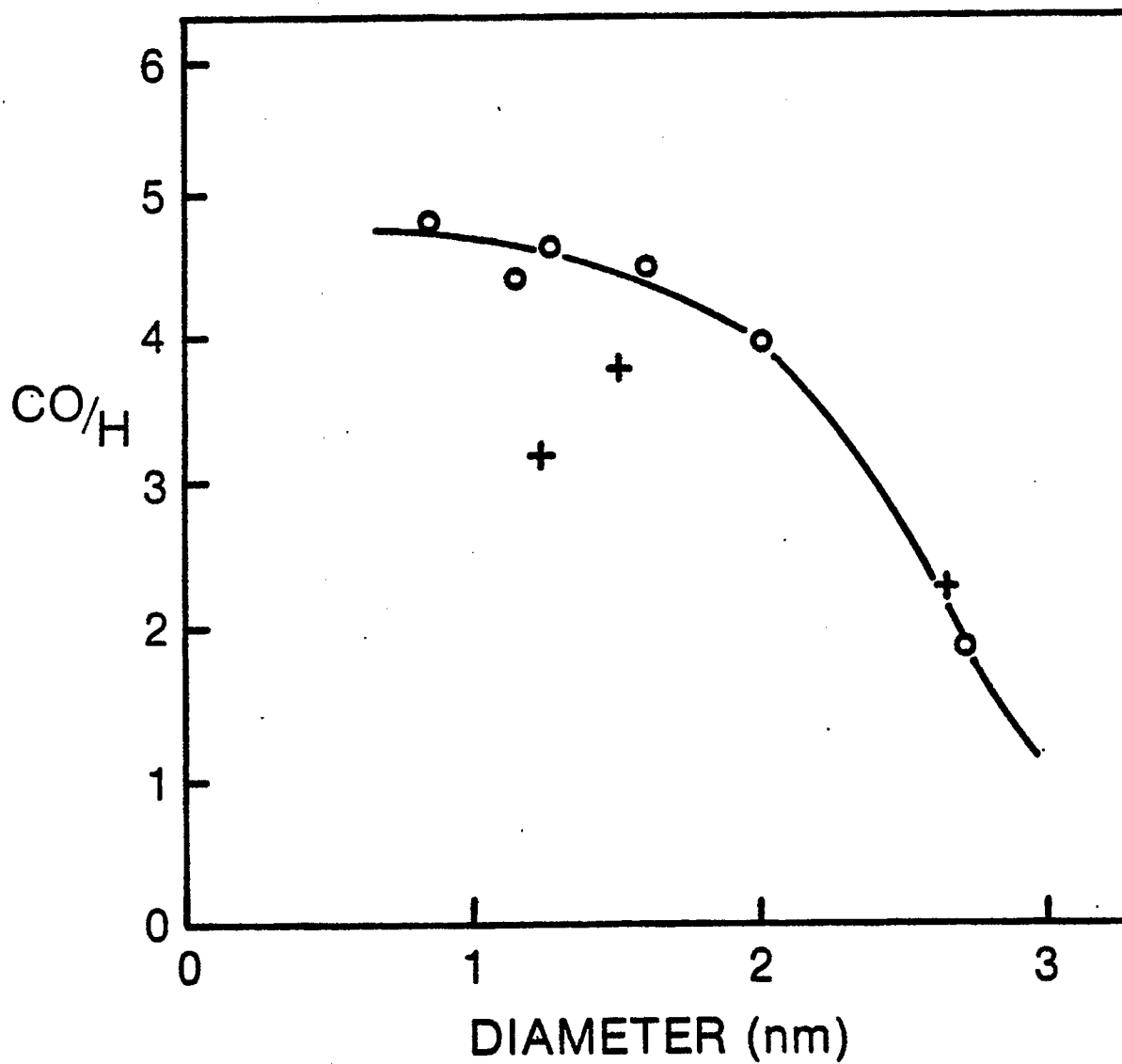


FIGURE 3: Number of CO Molecules Adsorbed per Ru Surface Atom vs. Average Ru Particle Diameter

(o) from this study of RuY
 (+) from Dalla Betta⁽³⁾ for Ru/Al₂O₃

HYDROGEN CHEMISORPTION SUPPRESSION IN Ru-ZEOLITE CATALYSTS

H. T. Wang, Y. W. Chen, and James G. Goodwin, Jr.

ABSTRACT

Ru catalysts prepared using NaX, NaY, KL and NaMordenite as supports have been characterized by H₂ and CO chemisorption. Significant suppression of hydrogen chemisorption was found for the ion-exchanged catalysts as the Si/Al ratio of the zeolite support increased. Chemical interactions between the metal and the support are considered the main cause of this hydrogen chemisorption suppression. It is suggested that the acidic hydroxyl groups are involved in these interactions. These interactions are greatly affected by method of preparation and metal loading.

INTRODUCTION

In recent years, the selective chemisorption of gases has been extensively used to estimate the degree of dispersion of supported Group VIII metal catalysts. Hydrogen and CO have both been used for estimation of Ru metal surface area (1). Dalla Betta (2) studied hydrogen adsorption on unsupported and supported Ru catalysts whose particle size distributions had been measured by electron microscopy, and he found good agreement between average particle sizes calculated from hydrogen adsorption and the particle size distribution observed by electron microscopy. Taylor (3) used three methods (hydrogen chemisorption, oxygen chemisorption, and hydrogen-oxygen titration) to measure the specific surface area of alumina-supported ruthenium catalysts. The results showed that these three methods are in agreement when average Ru crystallite sizes are greater than 4 nm. The selective chemisorption of hydrogen and H_2-O_2 titration were applied to three types of Ru catalysts prepared by two different techniques on two different supports (4). It was found that H_2 chemisorption method was the best method to determine the dispersion of highly dispersed Ru catalysts provided irreversible hydrogen chemisorption was used.

CO chemisorption on Ru was compared to H_2 chemisorption by Dalla Betta (5), and he found CO/H ratios as high as 4 on Ru particles of 1.1 nm diameter. Yang and Goodwin (6) showed that the CO/H ratio is a function of Ru particle size for RuNaY catalysts.

An investigation into the chemisorption properties of zeolite-supported ruthenium catalysts in general has been carried out. Preliminary results had suggested that significant zeolite-metal interactions were in effect.

EXPERIMENTAL

Catalysts Preparation

Materials

The zeolites were obtained from Strem Chemicals, Inc. (NaX, NaY, and KL) and Norton (NaZeolon = large port NaMordenite). NH_4Y was prepared by ion-exchange of NaY with NH_4Cl . The extent of exchange was 84%. RuCl_3 , $\text{Ru}(\text{NH}_3)_6\text{Cl}_3$, and $\text{Ru}_3(\text{CO})_{12}$ were also obtained from Strem Chemicals, Inc.

Ion-Exchange Method (I.E.)

For preparing the ion-exchanged catalysts, $\text{Ru}(\text{NH}_3)_6\text{Cl}_3$ was dissolved in a weakly acidic hydrochloride solution ($\text{pH} = 4.5$). This solution was then mixed with the zeolite and stirred continuously for 50 hours at ambient temperature. Excess solution was used to maintain an approximately constant pH during ion-exchange. After the ion-exchange reaction, the catalysts were filtered and washed several times in deionized water and dried in air overnight at 40°C . The catalysts were then bottled and stored.

Vapor Impregnation Method (V.I.)

Ru carbonyl cluster catalysts were prepared by sublimating $\text{Ru}_3(\text{CO})_{12}$ under vacuum and adsorbing the vapor on the zeolite, previously activated under vacuum at 450°C . This impregnation process took place in an evacuated, sealed Pyrex cell held at a temperature of 80°C for several weeks. This temperature ensured that the vapor pressure of $\text{Ru}_3(\text{CO})_{12}$ was high enough for reasonably rapid adsorption of it on the zeolite but was not high enough to cause decomposition of the carbonyl.

Catalyst Characterization

Metal Loading Measurement

The metal loading of the catalysts were determined by atomic absorption using the method of Fabec (7).

Chemisorption Measurement

Hydrogen (99.995%) was purified further by passing it through a liquid nitrogen trap before being used for both catalyst reduction and chemisorption measurements. Carbon monoxide (99.8%) was dried by passing through a trap thermostatted at -78°C (dry ice trap). He (99.997%), used for dead space determination, was also purified by passing it through a liquid nitrogen trap.

The V.I. and I.E. catalysts were usually decomposed under vacuum (ca. 4×10^{-5} Pa) by heating to 420°C ($0.5^{\circ}\text{C}/\text{min}$) and holding at that temperature for two hours. Reduction in and desorption of hydrogen was carried out at the same temperature. H_2 reduction was not necessary for the V.I. catalysts.

Gas adsorption measurements were performed in a conventional Pyrex-glass volumetric adsorption apparatus. An ultimate vacuum of about 4×10^{-5} Pa was obtained by means of oil diffusion and mechanical pumps isolated from the adsorption system by a liquid-nitrogen cooled trap. Each I.E. catalyst (ca. 1g) was placed in a Pyrex cell to enable decomposition under vacuum and reduction of samples in static hydrogen prior to the chemisorption measurement. The V.I. catalysts were decomposed in the same specially designed cell used in their preparation. This avoided exposure of the supported carbonyl to the air.

Hydrogen and carbon monoxide uptakes were determined separately at ambient temperature on the reduced and desorbed catalysts. One day was sufficient to reach equilibrium for hydrogen chemisorption at this temperature and 2 days was sufficient for carbon monoxide chemisorption. The total amount of chemisorbed hydrogen or carbon monoxide was determined by extrapolation of the linear part of the first isotherm to zero pressure corresponding to the method described by Benson and Boudart (8) and Wilson and Hall (9). A second isotherm was measured after evacuation of the sample for 2 min following the

first isotherm. The second isotherm provided a measure of the reversibly bound hydrogen or carbon monoxide (both chemisorbed and physisorbed). The difference between these two isotherms gave the amount of irreversibly (strongly) chemisorbed hydrogen or carbon monoxide.

The dispersion of Ru was calculated from the hydrogen measurements, assuming a stoichiometry of $H_{1rr}/Ru(s) = 1$ (4). The crystallite sizes were calculated by assuming the particle to be cubic with five sides exposed to the gas phase and an average area per surface Ru atom of 8.17\AA^2 (2).

RESULTS AND DISCUSSION

The results of the H_2 and CO chemisorption studies are summarized in Table 1 along with CO/H ratios of the samples. Figures 1 and 2 show representative H_2 and CO chemisorption isotherms. From H_2 chemisorption at $22 \pm 2^\circ\text{C}$, average Ru particle diameters and dispersions were calculated.

In metal zeolite catalysts the initial location of the metal in the porous framework is an important factor to be considered. As described in a previous study (10), ruthenium supported on the external surface of zeolites via the incipient wetness method is easily sintered into large particles during reduction, resulting in average particles sizes in the range of 3.0-8.5 nm for metal loadings between 1 and 3 weight percent. However, as can be seen in Table 1, the average particle size calculated from H_2 chemisorption for ion-exchanged catalysts with metal loadings larger than 1 weight percent, with the exception of RuHY, RuKL, RuNaM, was exclusively below 1.6 nm. The average particle size for catalysts prepared by the vacuum impregnation method, with metal loadings less than 1 weight percent, was below 1.1 nm. A 0.49% RuNaY (I.E.) catalyst had, however, an average calculated particle size of 2.3 nm. This might have been due to incomplete reduction. However, high dispersions

of the Ru were found for all V.I. and I.E. NaX and NaY catalysts. As can be seen by T.E.M. (4), most of the particles are inside the zeolite cavities.

From the data in Table 1 and Figure 3, it is obvious that there are higher CO/H ratios for NaY-supported catalysts prepared by ion-exchange method than for CO/H ratios for catalysts prepared by the vapor-impregnation method. Since ruthenium can coordinate no more than four CO molecules if it is bonded to other Ru atoms (to five other CO molecules if it is in the form of $\text{Ru}(\text{CO})_5$), it is reasonable to have CO/H ratios between 2 and 3 for vapor-impregnation catalysts prepared via a $\text{Ru}_3(\text{CO})_{12}$ precursor since during decomposition there can be some sintering of the Ru clusters (11).

Matsuo and Klabunde (12) have studied a series of Ni catalysts supported on MgO having different metal loadings and showed that CO/H ratios increase as Ni loading decreases. They indicated that H_2 chemisorption is seriously suppressed, especially in the samples with low metal loadings. Bartholomew and Pannell (13) have studied hydrogen and carbon monoxide chemisorption on alumina- and silica-supported nickel. They also found that the CO/H ratio varied inversely with metal loading. CO/H ratios were 28 and 9.8 for 0.5% Ni/ Al_2O_3 and 1% Ni/ Al_2O_3 , respectively. These values were unexpectedly high. One reason for these differences may lie with increased support-metal interaction at low loadings. Catalysts with low metal loadings have been found (14,15) to be hard to reduce. Hence, the higher CO/H ratio for 0.49 RuNaY (I.E.) compared to that for 0.24% and 0.68% Ru_3NaY (V.I.) may have been due to less hydrogen chemisorption, which thereby increased the CO/H ratio, as a result of stronger zeolite-metal interactions. In all cases, vapor-impregnated catalysts appear to have less zeolite-metal interactions than ion-exchange catalysts. Due to the high dispersions calculated from H_2 chemisorption, it can be assumed that there is no significant H_2 chemisorption

suppression for the Ru/NaY catalysts prepared by vapor-impregnation of $\text{Ru}_3(\text{CO})_{12}$.

It would appear that as the Si/Al ratio of the zeolite support increases larger average particle diameters results (Table 1). However, it becomes apparent from a consideration of the CO/H ratios that suppression of hydrogen chemisorption takes place at ambient temperature on the Ru catalysts with higher Si/Al ratios (it is impossible for 1 Ru atom to bond to 12 CO ligands) (Table 1, Figure 4). Since the stoichiometry of CO adsorption on Ru is determined by the metal particle size (5,6), it is difficult to use CO to determine metal surface areas. However, CO chemisorption can at least serve to compare relative metal dispersions. The CO/Ru_T ratios in Table 1 would seem to indicate that the Ru dispersions in the various catalysts were similar and probably on the order of 70-90%.

At this point, let us consider what may be the cause of suppression of hydrogen chemisorption at high Si/Al ratios for the ion-exchanged catalysts. One phenomenon which must be considered is encapsulation of the metal particles in the catalysts following reduction. This would make the metal inaccessible to sorbing gases regardless of particle size. We consider this explanation to be unlikely, however, for the following reasons. First, the X-ray diffraction patterns of the reduced catalysts were similar to those of the original supports. Thus, no significant collapse of the zeolite supports and encapsulation of the metal accompanied reduction. Coughlan et al. (16) have studied Ru supported on A, X, Y, L and mordenite zeolites. They also reported that all the zeolites retained their crystalline structure after outgassing and reduction. Second, if encapsulation of the metal were responsible for the suppression of H₂, one would not expect similar CO/Ru_T ratios for all the catalysts. Thus, the possibility of occlusion of particles in the zeolite

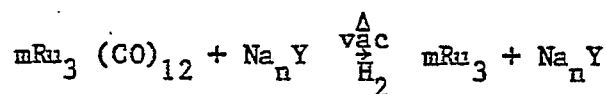
matrix is excluded because of the high dispersion in RuNaX (NaX being the least stable of these zeolites) and the similar CO/Ru_T ratios for all the catalysts.

Poisoning of the metals following reduction is also unlikely to explain the unusual sorption properties of the zeolite-supported metal. Koopman et al. (17) have reported that surface contamination of chlorine on Ru/SiO₂ catalysts (prepared from RuCl₃) caused a decrease in dispersion. However, in this case, the ion-exchange catalysts were washed several times in deionized water to remove all the chloride from the zeolite. Certainly, RuNaX did not seem to exhibit any H₂ chemisorption suppression and it was prepared in the same way as all the ion-exchanged catalysts. Clausen and Good (18) have investigated the decomposition of [Ru(NH₃)₅N₂]²⁺ ions in a Y-type zeolite. They found that all of the coordinated N₂ and NH₃ was removed if the sample was heated to 400°C and 10⁻³ Pa. As a result of this decomposition procedure, a highly reactive ruthenium species was formed in the zeolite. Hence, it is unlikely that Cl⁻ ions or coordinated NH₃ influence the amount of H₂ chemisorption.

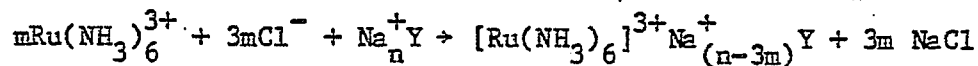
Brooks and Christopher (19) have investigated alumina- and zeolite-supported nickel. They found very high CO/H₂ ratios (between 46 and 59) for Zeolon-supported Ni and suggested that these results were due to dissociative hydrogen adsorption occurring only on Ni crystallites of sufficient size so as to offer adjacent hydrogen adsorption sites. Shimizu et al. (20) have also suggested that ensembles of up to 5-10 adjacent Ru atoms are involved in hydrogen chemisorption, and small amounts of Cu on the Ru surface can suppress the hydrogen adsorption capacity drastically. From the data in Table 1, catalysts prepared via vapor-impregnation have average calculated particle diameters of 1.0 nm. RuNaX prepared via ion-exchange had an average calculated

particle size of 1.0 nm, and part of the reduced Ru in the ion-exchanged RuNaX catalyst was possibly dispersed atomically in the zeolite cavities. This suggests that very small particles of reduced Ru metal are still active for hydrogen chemisorption and adsorb reasonable quantities of H₂. Hence, it is not likely that ensemble size influences the H₂ chemisorption or CO/H ratio for Ru.

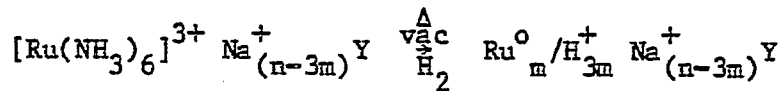
Let us consider differences between catalysts prepared by vapor impregnation and ion-exchange since one (V.I.) results in no H₂ chemisorption suppression and the other (I.E.) does. For the vapor impregnation case, decomposition and reduction can be represented schematically as



and the zeolite is seen to undergo no change in its chemistry. On the other hand, during ion-exchange some Na⁺ is replaced by the cationic Ru:



Upon reduction



The neutralizing protons associate with zeolite oxygens to produce OH groups. The greatest chemical difference between the V.I. and the I.E. catalysts thus lies with the formation of hydroxyl groups in the I.E. catalysts.

The results in Table 1 show that catalysts prepared by I.E. from HY have larger calculated average particle diameters than catalysts prepared from NaY and a slightly lower ratio of CO/Ru_T. However, the CO/H ratio is about the same as the CO/H ratio of RuNaY. Since an increase in particle size in this range should be compensated by a decrease in the number of CO adsorbing per Ru surface atom and a decrease in the CO/H ratio, one is led to consider these two catalysts to have similar dispersions but with more H₂ chemisorption suppression on RuHY. Suzuki et al. (21) in studies of a series of nickel-zeolites (A, X, Y and Mordenite) reported that the degree of nickel ion reduction and the dispersion of reduced nickel were affected by the extent of nickel-exchange and by the types of parent-cations in zeolites. RuHY and RuNaY have similar structures, but they are different in concentrations of Na⁺ ions and acidic protons produced during reduction at 400°C. The lower concentration of Na⁺ and the higher concentration of H⁺ may be factors affecting H₂ chemisorption suppression in the RuHY catalyst. However, 3.1% RuNaY, 2.5% RuNaX, 2.8% RuKL and 2.2% RuNaMordenite have very similar loadings of ruthenium. Since hydroxyl groups are formed when protons interact with framework oxygen atoms during the reduction of the ruthenium ions (22), 3.1% RuNaY, 2.5% RuNaX, 2.8% RuKL and 2.2% RuNaMordenite will have similar concentrations of acidic protons. It is thus obvious that the concentration of acidic hydroxyl protons seems unlikely to completely explain the H₂-chemisorption suppression in 2.2% RuNaMordenite. Hence, we must also consider the implication of the strength of the acidic hydroxyl protons.

In Figure 4, the CO/H ratios of RuNaX, RuNaY, RuKL, and RuNaMordenite seem to correlate to the Si/Al ratio. Significantly more hydrogen chemisorption suppression occurs as the Si/Al ratio of zeolite support increases. There is a good linear relationship between the hydroxyl frequency

(near 3650 cm^{-1}) and the Si/Al composition, independent of any structural influence (23). The shift to lower frequencies observed as the Si/Al ratio increases is related to an increase in the acid strength of the protons (24). Moreover, the catalytic activity of reduced nickel is decreased by the increase in acidic hydroxyl groups in mordenites (25). Thus, the increase in H_2 suppression as the Si/Al ratio is increased for ion-exchanged Ru/zeolite may be explained on the basis of increasing acid strength of the zeolite hydroxyls.

The influence of Si/Al ratio on CO adsorption on the reduced metal has also been found in a previous IR study (26). The IR investigation of these zeolites catalysts at 25°C showed that, in general, as the Si/Al ratio of the support increases, the frequency of the adsorbed CO also tends to increase indicating weaker CO chemisorption, which correlates well with the increase in the acid strength of the zeolites. Recent studies (27,28) of supported carbonyls have shown that the evolution of CH_4 during temperature-programmed decomposition is due to a reaction between the initially zero-valent carbonyl and the surface hydroxyl groups of the support. Therefore, it is suggested that hydrogen suppression is due to the interaction of the zeolite hydroxyls with the Ru, and this interaction increases with the strength of the acidic hydroxyl protons. The reason for the change in the acid strength of the hydroxyl protons is not clear. It may result from a change in the local electric charge in the zeolite framework caused by ion-exchange or from direct interaction of structural hydroxyls with cations. The one case that deviated slightly in Figure 4 was that of RuKL. It is felt that the slight deviation to a higher CO/H ratio was due to the presence of K^+ in the zeolite as opposed

to Na^+ in all the other zeolites studied. This would seem to be reasonable given the relatively greater ability of K compared to Na to destabilize CO in alkali promoted F-T catalysts.

CONCLUSIONS

Hydrogen chemisorption suppression has been found for zeolite-supported Ru prepared by ion-exchange. Hydrogen chemisorption suppression appeared to be a function of the Si/Al ratio of the support. However, the presence and strength of acidic hydroxyl protons and their possible interaction with the residual cations (Na^+ or K^+) are suggested to be the reason for hydrogen chemisorption suppression. It would appear that the amount of H_2 chemisorption suppression for ion-exchanged catalysts may be an inverse function of metal loading. Catalysts prepared via vapor-impregnation of $\text{Ru}_3(\text{CO})_{12}$ did not exhibit H_2 chemisorption suppression, probably as a result of the absence of significant concentrations of acidic hydroxyl groups. No evidence for CO chemisorption suppression was seen.

ACKNOWLEDGMENTS

Funding for this study was provided by the Office of Fossil Energy of the Department of Energy under grant #DE-FG22-81PC40774.

REFERENCES

1. Farrauto, R. J., *AIChE Symp. Ser.* 70, 9 (1975).
2. Dalla Betta, R. A., *J. Catal.* 34, 57 (1974).
3. Taylor, K. C., *J. Catal.* 38, 299 (1975).
4. Goodwin, J. G., Jr., *J. Catal.* 68, 227 (1981).
5. Dalla Betta, R. A., *J. Phys. Chem.* 79, 2519 (1975).
6. Yang, C.-H., and Goodwin, J. G., Jr., *React. Kin. and Catal. Lett.* 20, 13 (1982).
7. Fabec, J. L., *Atomic Spec.* 4, 46 (1983).
8. Benson, J. E., and Boudart, M., *J. Catal.* 4, 704 (1965).
9. Wilson, G. R., and Hall, W. K., *J. Catal.* 17, 190 (1970).
10. Chen, Y.-W., Wang, H.-T., and Goodwin, J. G., Jr., submitted for publication.
11. Goodwin, J. G., Jr., and Naccache, C., *Appl. Catal.* 4, 145 (1982).
12. Matsuo, K., and Klabunde, K. J., *J. Catal.* 73, 216 (1982).
13. Bartholomew, C. H., and Pannell, R. B., *J. Catal.* 65, 390 (1980).
14. Brown, M. F., and Gonzalez, R. D., *J. Phys. Chem.* 80, 1731 (1976).
15. Davydov, A. A., and Bell, A. T., *J. Catal.* 49, 332 (1977).
16. Coughlan, B., Narayanan, S., McCann, W. V., and Carroll, W. M., *J. Catal.* 49, 97 (1977).
17. Koopman, P. G. T., Kieboom, A. P. G., and van Beckkum, H., *J. Catal.* 69, 172 (1981).
18. Clausen, C. A., III, and Good, M. L., *Inorg. Chem.* 16, 816 (1977).
19. Brooks, G. B., and Christopher, G.L.M., *J. Catal.* 10, 211 (1968).
20. Shimizu, H., Christmann, K., and Ertl, G., *J. Catal.* 61, 412 (1980).
21. Suzuki, M., Tsutsumi, K., and Takahashi, H., *Zeolites* 2, 185 (1982).
22. Verdonck, J. J., Jacobs, P. A., Genet, M., and Poncelet, G., *J.C.S. Faraday I* 76, 403 (1980).
23. Barthomeuf, D., *J.C.S. Chem. Comm.*, 743 (1977).
24. Bielanski, A., and Datka, J., *J. Catal.* 37, 383 (1975).

25. Suzuki, M., Tsutsumi, K., and Takahashi, H., *Zeolites* 2, 87 (1982).
26. Blackmond, D. G., and Goodwin, J. G., Jr., *J.C.S. Chem. Comm.*, 125 (1981).
27. Brenner, A., and Hucul, D. A., *J. Catal.* 61, 216 (1980).
28. Hucul, D. A., and Brenner, A., *J. Phys. Chem.* 85, 496 (1981).

Table 1
CHARACTERISTICS BASED ON CHEMISORPTION

| Catalyst | Preparation Method | \bar{d}_P^* (nm) | D^* (%) | CO/H _{1T} | CO _{1T} /Ru _{1T} |
|---------------------------|-----------------------|-----------------------|--------------|--------------------|------------------------------------|
| 0.24% Ru ₃ NaY | V.I. | 1.1 | 76 | 3.2 | 2.5 |
| 0.68% Ru ₃ NaY | V.I. | 0.9 | 94 | 2.4 | 2.1 |
| 1.1% Ru ₃ NaY | V.I. | 1.1 | 76 | 2.3 | 1.7 |
| 1.3% Ru ₃ NaY | V.I. | 0.9 | 94 | 2.1 | 2.4 |
| 2.5% RuNaX | I.E. | 1.0 | 83 | 3.0 | 2.5 |
| 0.49% RuNaY | I.E. | 2.3 | 35 | 5.7 | 2.1 |
| 1.1% RuNaY | I.E. | 1.5 | 55 | 5.7 | 3.2 |
| 2.17% RuNaY | I.E. | 1.2 | 67 | 4.5 | 3.1 |
| 3.1% RuNaY | I.E. | 1.6 | 51 | 4.6 | 2.2 |
| 3.9% RuHY | I.E. | 2.8 | 31 | 4.5 | 1.4 |
| 2.8% RuKL | I.E. | 2.6 | 32 | 9.9 | 3.2 |
| 2.2% RuNaM | I.E. | 3.9 | 22 | 12 | 2.6 |

* determined from irrev. H₂ chemisorption

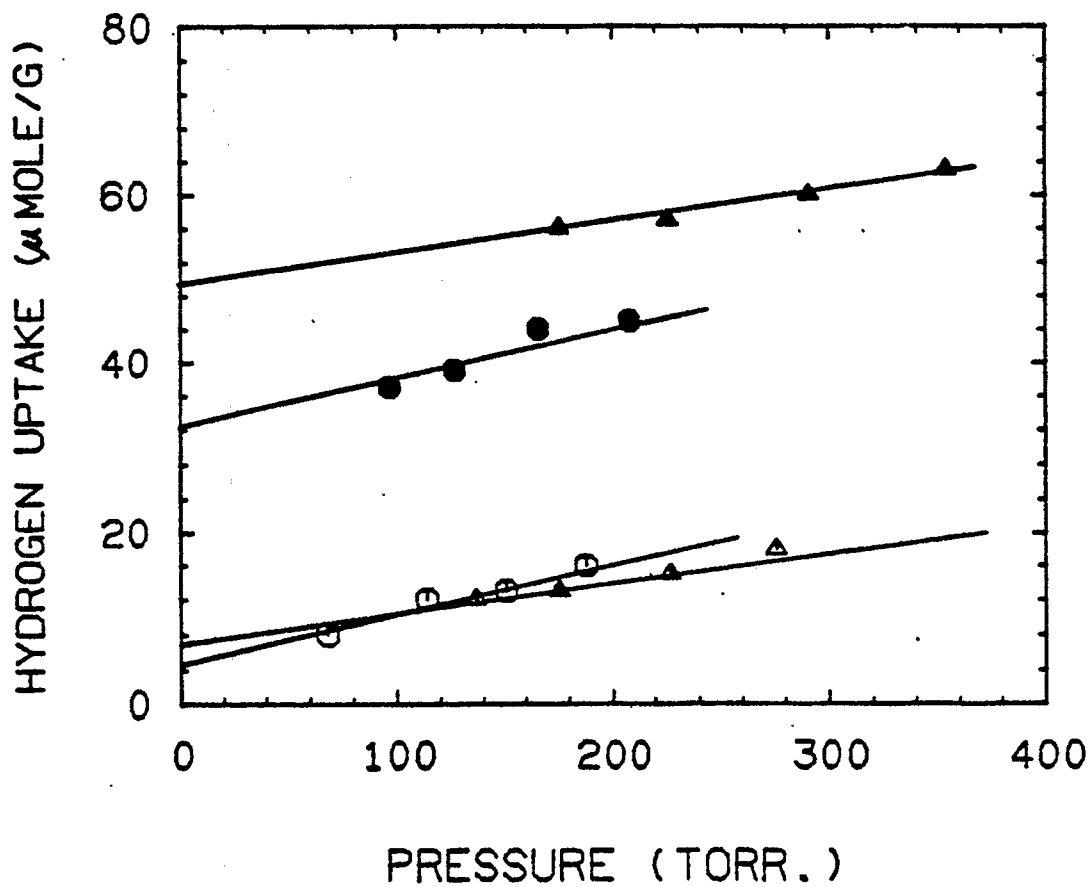


Figure 1: Hydrogen Adsorption Isotherms

1.1% Ru₃NaY (V.I.) (▲) Total
 (△) Reversible

1.1% RuNaY (I.E.) (●) Total
 (○) Reversible

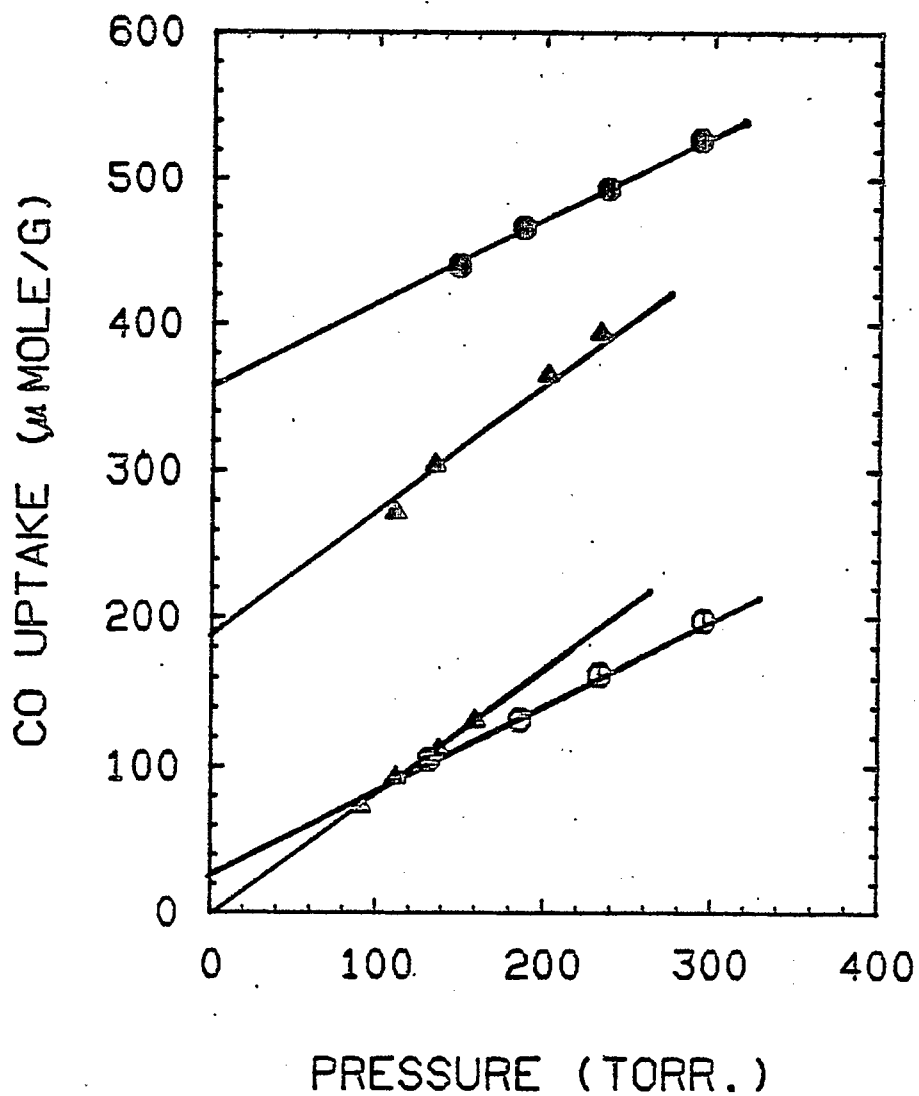


Figure 2: Carbon Monoxide Adsorption Isotherms

1.1% Ru₃NaY (V.I.) (●) Total
 (△) Reversible

1.1% RuNaY (I.E.) (●) Total
 (○) Reversible

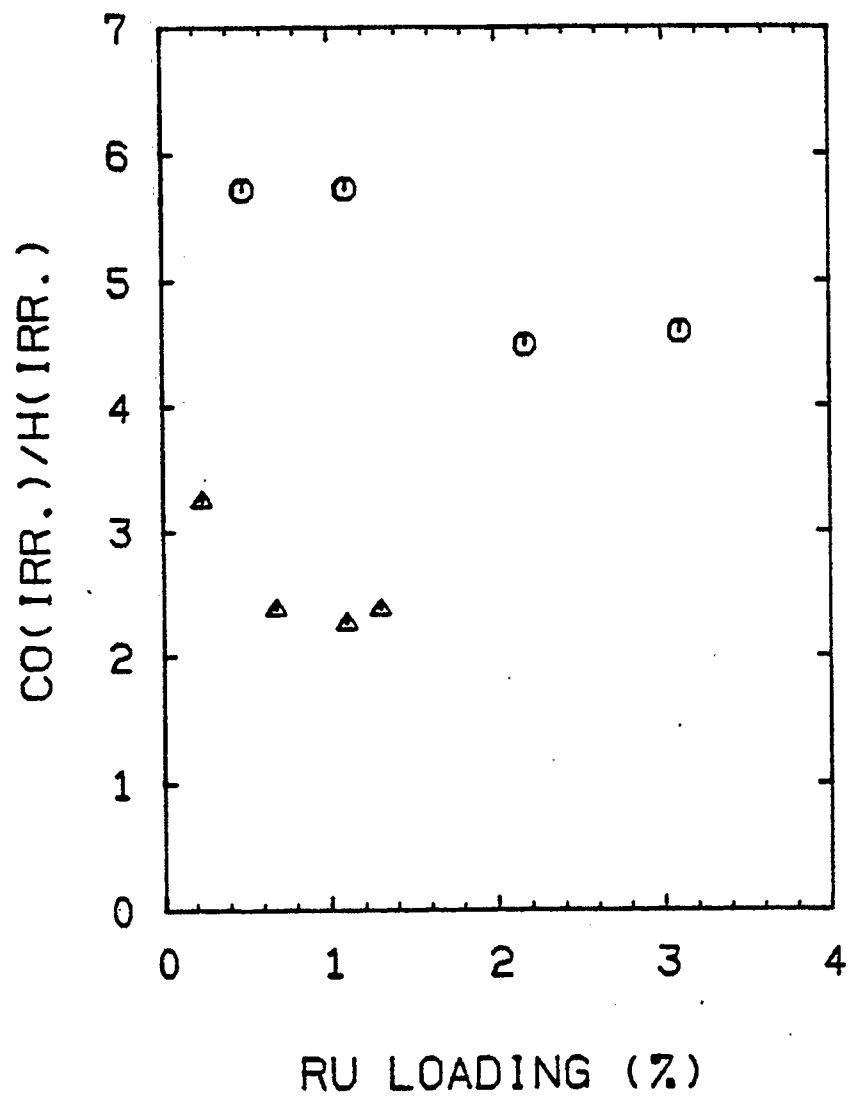


Figure 3: Irreversible (CO/H) vs. Metal Loading

(Δ) Ru₃NaY (V.I.)
 (○) RuNaY (I.E.)

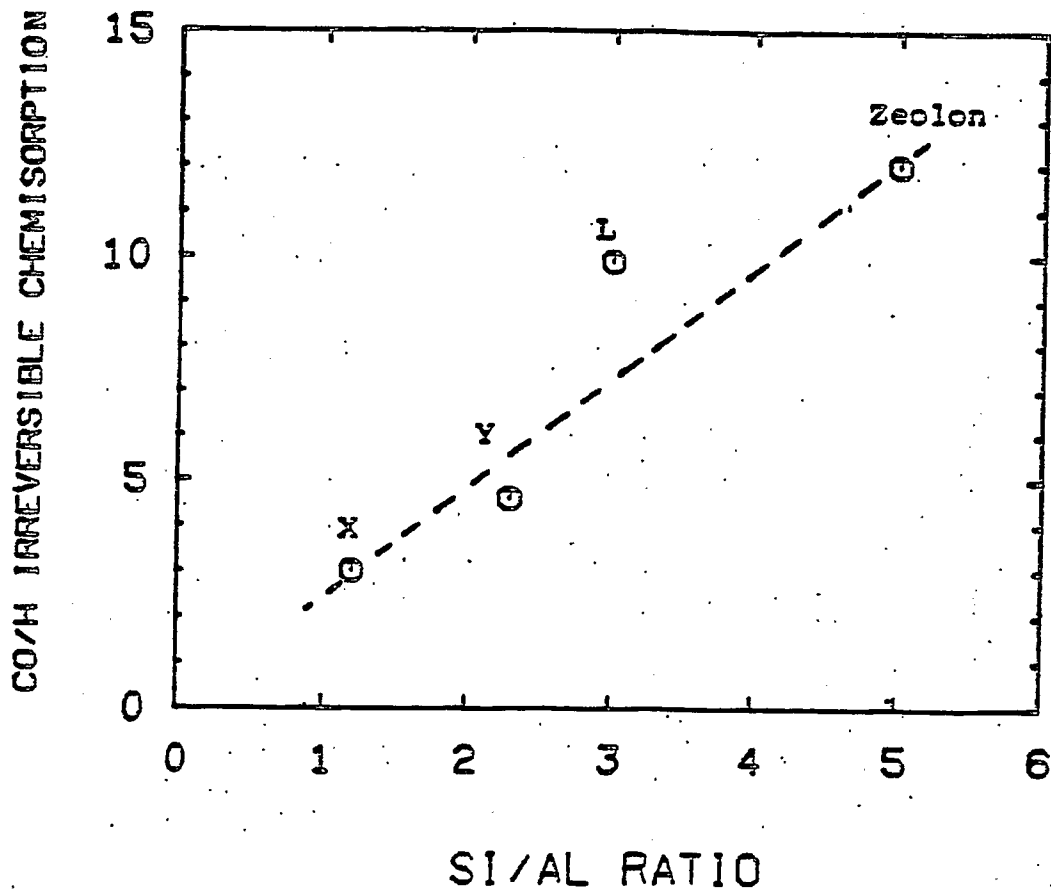


Figure 4: Irreversible (CO/H) vs. Si/Al Ratio

Ru/Zeolite catalysts prepared by ion-exchange

THE ELECTRONIC PROPERTIES OF Ru IN Y ZEOLITES
AS DETERMINED BY ESCA

J. Z. Shyu, D. M. Hercules and James G. Goodwin, Jr.

ABSTRACT

An investigation by ESCA was made of Ru supported in NaY zeolite. Catalysts were prepared by incipient wetness, vapor impregnation by $\text{Ru}_3(\text{CO})_{12}$, and ion-exchange. In addition, a RuHY catalyst was prepared by ion-exchange with NH_4Y . It was found that the Ru $3p_{3/2}$ band was more sensitive to the state of Ru in the zeolite than the Ru $3d_{5/2}$ band that is often used in ESCA studies. This greater sensitivity is probably related to a final state configuration interaction of the Ru 3p electrons with the valence 4d electrons. The results from the Ru $3p_{3/2}$ band were in excellent agreement with previous IR results.

INTRODUCTION

Metal-support interactions are known to play an important role in determining the catalytic properties of supported metal catalysts. This is especially true in the case of zeolite supports. For zeolite-supported Ru, both the method of preparation and the type of zeolite used have been shown to greatly affect the adsorptive and catalytic properties of the Ru (1-8). While the exact causes of all these differences in properties are not known, certain tentative conclusions have been able to be made based on characteristics of the zeolites used, chemisorption results for H₂ and CO (volumetric and IR), T.E.M., and catalytic properties for the Fischer-Tropsch synthesis. However, few studies have been reported dealing with the direct determination of location and electronic structure of the Ru in the zeolite. Two studies of particular note, both dealing with RuNaY catalysts prepared by ion exchange, have been reported. One, using X-ray diffraction (XRD), dealt with the location of Ru species in the zeolite following reduction and/or exposure to oxygen (9). The other used ESCA (Ru 3d_{5/2} band) to explore the electronic properties of Ru following various pretreatments (10).

The earlier ESCA study (10) of ion-exchanged RuNaY showed that, while the Ru 3d_{5/2} band shifted significantly with sample treatment, only one type of Ru seemed to be present at any time. However, IR results for CO adsorption on such catalysts have suggested that a number of different Ru sites can exist simultaneously (2).

While the Ru 3d_{3/2} and 3d_{5/2} bands are the most intense for ESCA, the use of the 3d_{3/2} band is difficult due to the overlap with the C 1s band. This led to the use of the Ru 3d_{5/2} band in the previous ESCA study of RuNaY (10). However, an ESCA study of Ru has indicated that Ru 4p and Ru 3p electrons have a strong configuration interaction with the valence 4d

electrons (11). This implies that the photionized 3p holes experience a strong perturbation by the 4d valence electrons. Thus, the Ru 3p_{3/2} ESCA band should be much more suitable to variations in the Ru oxidation state.

An investigation using ESCA has been made of RuNaY catalysts prepared by ion-exchange, incipient wetness, and vapor impregnation of Ru₃(CO)₁₂. Both Ru 3d_{5/2} and Ru 3p_{3/2} bands were used in the analysis. It was felt that, given the number of studies of the Ru-NaY system available for comparison, there was a greater likelihood of arriving at a better understanding of the nature of Ru i zeolites by use of this system.

EXPERIMENTAL

Apparatus

ESCA spectra of the Ru catalysts were recorded on an AEI ES200 electron spectrometer with a DS100 data system. The spectrometer is equipped with an aluminum anode (Al K α = 1486.6 eV) which was operated routinely at 12 kV and 22 mA. The base pressure of the ESCA chamber was below 5×10^{-8} torr. Binding energies of overlapping peaks were determined using a non-linear least-squares curve fitting technique (12). A sealable probe was used which permitted pretreatment of the catalysts and introduction of them into the spectrometer without exposure to air.

Materials

Ru metal powder, RuCl₃, Ru₃(CO)₁₂, Ru (NH₃)₆Cl₃, RuO₂ and the NaY zeolite were obtained from Stem Chemicals. The composition of dehydrated NaY is Na₅₆(AlO₂)₅₆(SiO₂)₁₃₅. Zeolite NH₄Y was prepared by ion-exchange of NaY with an aqueous solution of NH₄Cl to form NH₄Y. The extent of exchange was 84%.

The wet impregnated RuNaY catalyst (designated as RuNaY-IW) was prepared by the standard incipient wetness method using an aqueous solution of RuCl_3 . Vapor-impregnated RuNaY catalysts (designated as RuNaY-VI) were prepared by vacuum deposition of $\text{Ru}_3(\text{CO})_{12}$ onto NaY (5). For preparing the ion-exchange catalysts, $\text{Ru}(\text{NH}_3)_6\text{Cl}_3$ was dissolved in a weakly acidic solution ($\text{pH} = 4.5$). This solution was mixed with the zeolite NaY or NH_4Y and stirred continuously for 50 hours at ambient temperature (5). Excess solution was used to maintain an approximately constant pH during ion-exchange.

To minimize catalyst sintering all of the catalysts were dried at 40°C overnight and decomposed slowly under vacuum (10^{-6} torr) as the temperature was raised $0.5^\circ/\text{min}$ from room temperature to 400°C . This was followed by reduction in H_2 at 400°C for 2 hours. Pretreatment conditions and the abbreviated names used in the present study are listed in Table 1. ESCA spectra of Ru metal (Ru^0) were obtained from Ru metal powder after the treatment of OxR. The bulk Ru contents of RuNaY and RuHY were 3.1 wt% determined by atomic absorption spectroscopy.

ESCA Measurements

ESCA binding energies (BE's) were referenced to internal standards which were themselves referenced to Au $4f_{7/2}$ (= 83.8 eV) (13-14). For zeolite supported Ru catalysts, BE's were referenced to Si 2p (= 103.0 eV), while BE's of bulk Ru^0 and RuO_2 were adapted from values given in recent publications (15-18), found for Ru supported by SiO_2 (19), and measured directly from reduced Ru metal powder.

The Si/Al ratios of the zeolites at the surfaces of NaY and HY were determined using ESCA. Assuming a homogeneous distribution of silicon and

aluminum atoms on the surface, the Si/Al ratios can be estimated by the equation (20),

$$\left(\frac{\text{Si}}{\text{Al}}\right)_{\text{atomic}} = \frac{I_{\text{Si}}}{\sigma_{\text{Si}} \sqrt{KE_{\text{Si}}}} + \frac{I_{\text{Al}}}{\sigma_{\text{Al}} \sqrt{KE_{\text{Al}}}} \quad (1)$$

where $(\text{Si}/\text{Al})_{\text{atomic}}$ = atomic ratio of Si/Al on the surface

σ_{Si} , σ_{Al} photoelectron cross section for Si 2p and Al 2p respectively (21)

I_{Si} , I_{Al} = integrated peak areas for Si 2p and Al 2p, respectively

KE_{Si} , KE_{Al} = kinetic energies of Si 2p and Al 2p photoelectrons (eV), respectively, used for the correction of photoelectron escape depth

The estimated Si/Al surface ratios based on equation (1), are 2.43 and 2.45 respectively for NaY and HY. These values are within experimental error of the bulk Si/Al ratio of 2.4 typical for Y-type zeolites (22). Therefore, in the present study, an average value of 2.44 was used for the Si/Al ratio of the Y-type zeolites.

Because the Ru 3d lines overlap with the C 1s lines from carbon contamination and the Al 2p line overlaps with the Ru 4s line, Ru 3p_{3/2} and Si 2p lines were used to calculate the atomic ratio of Ru to zeolite, based on the following equation:

$$\left(\frac{\text{Ru}}{\text{zeolite}}\right)_{\text{atomic}} = \frac{I_{\text{Ru}}}{\sigma_{\text{Ru}} \sqrt{KE_{\text{Ru}}}} + \frac{I_{\text{Si}}}{\sigma_{\text{Si}} \sqrt{KE_{\text{Si}}}} \times (1 + N^{-1}) \quad (2)$$

The notations used in equation (2) are the same as for equation (1). N in equation (2) represents the surface Si/Al ratio of the support ($=2.44$). Thus, the term $(1+N^{-1})$ denotes the percentage contribution of Al relative to Si plus the contribution from Si to the ESCA intensity of the zeolite.

ESCA Data for Ru^0 and RuO_2

ESCA BE's for Ru^0 in the Ru $3d_{5/2}$ and Ru $3p_{3/2}$ regions are 280.0 and 461.1 eV, respectively, and those for RuO_2 in the Ru $3d_{5/2}$ and Ru $3p_{3/2}$ regions are 280.6 and 462.3 eV, respectively. These BE's correspond to reported values (15-19) and were used to characterize the bulk Ru^0 and RuO_2 .

RESULTS

RuNaY Prepared by Incipient Wetness

As shown in Table 2, RuNaY-IW-R1 gave Ru $3d_{5/2}$ and Ru $3p_{3/2}$ BE's of 280.0 and 461.0 eV, respectively, which are characteristic of bulk Ru^0 . H_2 chemisorption results (5) showed Ru to be present as large particles (average particle diameter = 6 nm). The variation of average particle diameter with metal loading has suggested that the Ru exists primarily on the external surfaces of the zeolite (5). The BE for the Ru $3d_{5/2}$ band is in good agreement with the results of Pedersen and Lunsford (10) for a similar catalyst. They have suggested that ESCA Ru BE's are essentially the same as bulk Ru^0 for Ru particles larger than 1.5 nm. The BE for Ru $3p_{3/2}$ does not contradict this conclusion.

RuNaY Prepared by Vapor Impregnation with $\text{Ru}_3(\text{CO})_{12}$

RuNaY catalysts prepared in this manner are known to exhibit metal dispersions on the order of 100% (5,23) and to show less metal-zeolite

interaction than ion-exchanged catalysts with similar dispersions, as evidenced by IR studies of CO chemisorption (2,4). Less obvious metal-zeolite interaction is probably the result of 2 conditions: the fact that Ru starts out zero valent in the carbonyl and the fact that the zeolite structure is completely neutralized by Na^+ . ESCA data for RuNaY-VI-R1 are shown in Table 2. The Ru $3d_{5/2}$ and Ru $3p_{3/2}$ BE's of 281.0 and 462.0 eV, respectively, were about 1 eV higher than those for bulk Ru^0 . Such shifts could be due to strong Ru-zeolite interactions or to small Ru particles experiencing strong atomic-relaxation during photoemission. However, given the IR results for CO chemisorption (4) and the lack of H_2 chemisorption suppression (8) for such catalysts, the former explanation seems unlikely. There appears also to be little direct interaction of the Ru with the Na^+ cations, since, according to our previous study of the effect of alkali promotion on the BE's of Ru (19), the Ru BE's would have decreased relative to Ru^0 . Since the average Ru particle size for this catalyst was determined by H_2 chemisorption to be < 1 nm, it is likely that these shifts in BE were due to strong atomic-relaxation during photoemission, which is known to be especially important in very small crystallites. The shift of 1 eV found for the Ru $3d_{5/2}$ BE is consistent with the results previously reported for such small Ru particles (10).

RuNaY Prepared by Ion-Exchange

Ru $3d_{5/2}$ BE

ESCA spectra of ion-exchanged RuNaY catalysts in the Ru 3d region are shown in Figure 1. The decomposed (D) RuNaY catalysts gave a low intensity for the Ru $3d_{5/2}$ line centered at 281.1 eV (Figure 1(a)). After the catalyst was subjected to reduction under R1 and R2 conditions, shifts in the Ru $3d_{5/2}$ BE to 280.5 and 281.1 eV, respectively, (Figure 1 (b),(c) and Table 3) were

observed. However, after oxidation and reduction treatment of the RuNaY catalyst (OxR conditions), the Ru $3d_{5/2}$ peak location shifted to 279.9 eV (Figure 1 (d)), which is essentially that for bulk Ru⁰ (280.0 eV). Pedersen and Lunsford (10) have indicated that, for RuNaY catalysts, Ru will remain inside the zeolite cavities except for catalysts which are treated in O₂ at elevated temperatures. Therefore, the Ru species in RuNaY catalysts pretreated under D, R1 and R2 conditions should be located primarily inside the zeolite cavities, whereas the Ru species in RuNaY-OxR should be Ru⁰ in large particles on the external surface of NaY.

For a RuNaY-D catalyst which was prereduced and then exposed to air (Table 1), the Ru species present would be RuO₂ inside the zeolite cavities. Because RuO₂ is the most easily reducible oxide among the transition metals (15;24-25), after reduction most of the Ru species on RuNaY catalysts should be in the metallic form. However, as can be seen in Table 3 and Figure (b) and (c), deviations of the Ru $3d_{5/2}$ BE's of RuNaY-R1 and RuNaY-R2 from bulk Ru⁰ (dashed line in Figure 1) suggest that the metallic Ru present is substantially different from bulk metal. However, these results are in accord with those of Pedersen and Lunsford (10) for reduced Ru particles in the 1-1.5 nm range. Based on past experience, this is approximately the average particle size expected for treatment R1. The formation of bulk-like Ru⁰ after OxR treatments can be attributed to the sintering of Ru as a result of high temperature oxidation (10). Mossbauer data indicate that oxidation of RuNaY at 400°C in air yields large particles of RuO₂ (26). These large RuO₂ particles can not be accommodated inside the zeolite cavities because of the small diameter of the zeolite cavities (13 Å) (22). Once formed, the RuO₂ is able to migrate to the external surface of NaY. A final reduction in H₂ of

the oxidized RuNaY catalyst leads to formation of bulk-like Ru⁰ on the external surface of the zeolite (10,24).

Ru 3p_{3/2} BE

To investigate the chemical states and surface concentrations of Ru on NaY more precisely, the Ru 3p_{3/2} lines for the RuNaY catalyst were recorded; these are shown in Figure 2 and summarized in Table 3. The Ru3p_{3/2} line has the advantage of being free from carbon interference and is more sensitive to variations in the chemical state of Ru (11).

The decomposed (D) RuNaY catalyst (Figure 2 (a)) gave a peak having a Ru 3p_{3/2} BE of 462.6 eV which can be attributed to RuO₂ inside the zeolite cavities. After reduction of the decomposed RuNaY catalyst by H₂ under R1 or R2 conditions, complex spectral envelopes were observed (Figure 2(b),(c)). The spectra were resolved into three components by a non-linear least-squares curve fitting technique (12). The validity of the curve fit was gauged by the weighted variance of the fit. Judging from the weighted variances of 3.3 and 1.7 for the RuNaY-R1 and RuNaY-R2 spectra respectively (Table 3), the measured spectra (dotted spectra in Figure 2(b),(c)) are not statistically different from those obtained by summation of the three resolved components (solid lines) from the best computer fit. The resolved Ru 3p_{3/2} peaks, having FWHM's of 3.5 eV, give Ru 3p_{3/2} BE's of 465.0, 462.3 and 459.0 ± 0.2 eV for RuNaY-R1 and RuNaY-R2.

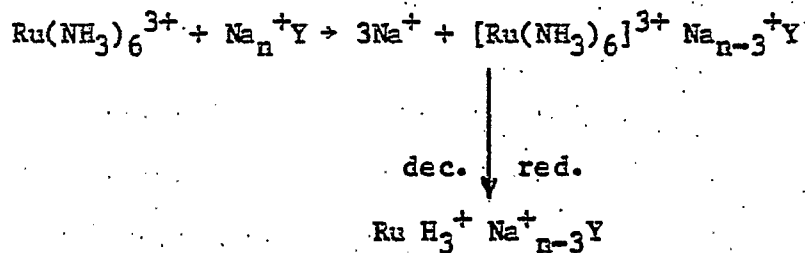
As shown in Figure 2(b) and (c), the Ru 3p_{3/2} ESCA spectrum of RuNaY-R1 is virtually identical to that for RuNaY-R2. This similarity suggests that the Ru species on the reduced RuNaY catalyst are chemically unchanged and thermally stable even for extended reduction periods. The BE's of these three components in the Ru 3p_{3/2} envelope for RuNaY-R1 and RuNaY-R2 are all different from the BE for bulk Ru⁰ (BE = 461.1 eV). It is recalled that the

Ru 3d_{5/2} band exhibited a single peak which could be related to small reduced Ru particles inside the zeolite. It appears, thus, that the Ru 3p_{3/2} BE is truly much more sensitive than that for Ru 3d_{5/2} in that three types of Ru species are able to be distinguished. After oxidation and reduction treatments (OxR), the Ru 3p_{3/2} BE consisted of a single component which is identical with that for bulk Ru⁰ (Figure 2(d)).

Certainly, it is not completely surprising that the Ru may exist in several forms in the reduced catalyst. The results from the Ru 3p_{3/2} band are in agreement with the IR results (2). What is surprising is the tremendous difference in complexity of the Ru 3p_{3/2} band compared to that of the Ru 3d_{5/2} band. It is difficult to consider this complexity to be due only to particle size differences since the ABE's relative to bulk Ru⁰ of the three components are so large and different (+3.9, +1.2, and -2.3 eV). Such ABE's must be related to interactions with the zeolite support. In order to better understand these possible interactions, an ion-exchanged RuHY catalyst was also studied.

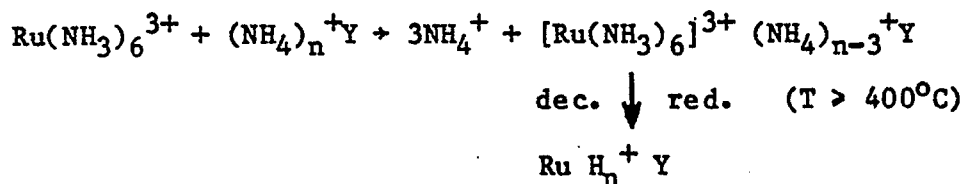
RuHY Prepared by Ion-Exchange

The ion-exchange of Ru(NH₃)₆³⁺ with NaY followed by decomposition and reduction can be expressed schematically by



While this catalyst is designated RuNaY there are theoretically three

neutralizing protons in the zeolite for each reduced Ru atom. By starting with NH_4Y zeolite the catalyst preparation can be represented by the following schematic:



Thus the RuHY catalyst is produced. The extent of bulk exchange of Na^+ by NH_4^+ for the zeolite used in this study was 84%. The remaining 16% of the original Na^+ was probably in the less exchangeable sites of the Y zeolite, such as in the hexagonal prisms (22,27). This, the remaining concentration of Na^+ in the RuHY catalyst was significantly less than in the RuNaY catalyst and the hydroxyl concentration (resulting from an interaction of the H^+ cations with structural oxygen) was much greater.

The ESCA results for RuHY are given in Table 4. The Ru $3p_{3/2}$ region is shown in Figure 3. For RuHY-D the BE's for Ru $3d_{5/2}$ and Ru $3p_{3/2}$ were 281.1 and 463.1 eV, respectively. These bands are shifted 0.5 and 0.8 eV relative to those for RuO_2 (bulk). By comparison, these bands are shifted by 0.5 and 0.3 eV, respectively, for RuNaY-D. In both cases, we can assume that these BE's correspond to small particles of RuO_2 in the zeolite.

Following reduction, the Ru $3d_{5/2}$ BE became 280.8 (R1) and 280.7 eV (R2), indicative of what has been concluded to be small Ru particles 1.0-1.5 nm in diameter (10). However, after reduction of RuHY under R1 conditions, a complex spectral envelope was obtained for Ru $3p_{3/2}$ (Figure 3(b)), which could be resolved into three components having FWHM's of 3.6 eV and BE's of 465.0, 462.6 and 460.5 eV (Table 4). This fitting gives a weighted variance of 1.9

(Table 4) suggesting that the fit is statistically as good as for RuNaY-R1 (w.v. = 3.1). After prolonged reduction in H₂, the Ru 3p_{3/2} ESCA spectrum of RuHY-R2 could be resolved into two components at 464.7 and 461.1 eV respectively, as shown in Figure 3(c). This curve fit is good, as indicated by a weighted variance of 1.0 (Table 4). It should be noted that 70% of Ru in RuHY-R2 shows the characteristics BE of bulk Ru⁰, suggesting sintering of the Ru as a result of prolonged thermal treatment. Comparing RuNaY-R1 and RuHY-R1, it can be seen that the biggest difference lies with the value of the lowest Ru 3p_{3/2} BE, 458.8 versus 461.1 eV, respectively. The ΔBE's for these bands relative to Ru⁰ (bulk) are -2.3 (RuNaY) and -0.6 eV (RuHY). H₂ chemisorption revealed average particle diameters of Ru for RuNaY and RuHY to be ca. 1.6 and 2.7 nm, respectively. Due to the greater suppression of H₂ chemisorption on RuHY (8), its actual average Ru particle size was probably < 2 nm. The values for the Ru 3d_{5/2} BE's are consistent with these facts. It would appear from the ESCA results, that the species related to the highest BE for Ru 3p_{3/2} is the most stable under reducing conditions. After OxR treatment, Ru on RuHY-OxR gave essentially the BE of bulk Ru⁰ (461.2 eV).

DISCUSSIONS

Binding Energies

With regards to the Ru 3p_{3/2} and Ru 3d_{5/2} BE's for RuNaY-R1, RuNaY-R2, and RuHY-R1 (Figures 1, 2, 3 and Tables 3 and 4), it has been shown that, while only a single species of Ru is suggested by the Ru 3d_{5/2} band, three Ru species can be identified from the Ru 3p_{3/2} band.

Comparing the Ru 3p_{3/2} and Ru 3d_{5/2} BE shifts relative to bulk Ru⁰ for RuNaY-R1, RuNaY-R2 and RuHY-R1, it is clear that different shifts are observed for the two photoelectron lines. The effect is especially pronounced for the

Ru $3p_{3/2}$ peak at 459.0 ± 0.2 eV for RuNaY-R1 and RuNaY-R2, which is shifted negative relative to bulk Ru⁰ by 2 eV. No peaks having BE's below bulk Ru metal (280.0 eV) were observed for the Ru $3d_{5/2}$ line. The difference in the BE shifts for different Ru orbitals can not be due to charging effects, because charging effects generate the same BE shift in all spectral regions (19). Rather, the difference must be due to final state effects such as relaxation or final state configuration interactions (FSCI) (11).

Final state effects in the Ru $3p_{3/2}$ region can be caused by modification of the electronic structure of Ru by the Y-type zeolite. One such effect, final state configuration interaction (FSCI) is known to be symmetry-dependent. For example, only the Ni 2p and Ni 3p lines of NiO show characteristic shake-up transitions between nickel and oxygen (28), because the symmetry of the Ni p orbitals favors this transition. An ESCA study of Ru has indicated that Ru 4p and Ru 3p lines have a strong configuration interaction with the valence 4d electrons (11). This implies that photoionized 3p holes experience strong perturbation by the 4d valence electrons and thus the p orbitals would be more sensitive to variation in the Ru oxidation state.

Another final state effect, relaxation of Ru due to polarization of the photoionized holes, can not account for the BE shifts relative to bulk Ru in the present case, because such relaxation effects cause a positive BE shift (11,19). Therefore, only FSCI's are considered to be important for the observed difference in BE shifts of the different Ru orbitals. Because the Ru $3p_{3/2}$ line appears to be more sensitive than the Ru $3d_{5/2}$ line to the Ru-zeolite interaction, assignments of Ru species on the zeolites will be based on the ESCA results for Ru $3p_{3/2}$.

Ru-zeolite interactions may be related to Ru species at different locations on the Y-type zeolites. Verdonck et al. (24) have reported that decomposition of $\text{Ru}(\text{NH}_3)_6^{3+} \text{NaY}$ under vacuum at 623 K results in almost 90% of the Ru ions being reduced to the metallic state. Based on reoxidation results, the Ru was completely reduced upon reduction in H_2 at 623 K. Clausen and Good (26) found by Mossbauer spectroscopy a similar complete reduction of Ru in a $\text{Ru}(\text{NH}_3)_5 \text{N}_2^{2+} \text{NaY}$ catalyst. In a study of the evolution of a $\text{Ru}(\text{NH}_3)_6^{3+} \text{NaY}$ catalyst by XRD, Pearce et al. (9) were able to conclude that, after decomposition under vacuum, most of the Ru was inside the supercages of NaY. However, after reduction of RuNaY catalysts in H_2 , they determined that 19% of Ru was atomically dispersed in the sodalite cages in site II' and 81% of Ru remained in the supercages. Exposure to O_2 at ambient following reduction appeared to cause all the Ru to leave the sodalite cages. The Ru did not return even upon re-reduction under 300 torr of H_2 at 373 K. Unfortunately, it is not known exactly what the situation would be if the re-reduction were carried out in flow at 673 K (condition R1).

In this study, we attribute the Ru species present in RuNaY-D and RuHY-D to highly dispersed RuO_2 . The Ru $3d_{5/2}$ BE for both of these systems was 281.1 eV. This BE is shifted +0.5 eV relative to that of bulk RuO_2 . This can be explained by relaxation effects due to small particle size. The Ru $3p_{3/2}$ BE of RuNaY-D was 462.6 eV, shifted + 0.3 eV relative to bulk RuO_2 . The greater shift exhibited by this band for RuHY-D (+ 0.8) may be related to the greater Bronsted acidity of the HY support and thus stronger RuO_2 - zeolite interactions (29). Some Lewis acid sites may have been formed which could also explain such an interaction (30). These different shifts in the Ru $3p_{3/2}$ band can not just be explained by experimental error (± 0.15 eV) thus indicating the sensitivity of this band to metal-support interactions.

Following reduction R1, both RuNaY and RuHY exhibited BE's for Ru $3d_{5/2}$ (280.5 - 280.8 eV) which suggest the presence of small reduced Ru particles. This is in agreement with previous results (9,10,24,26).

The exact cause of the 3 components of the $3p_{3/2}$ band exhibited by RuNaY-R1 and RuHY-R1 is not so obvious. It would appear that 17-24% of the Ru has a $3p_{3/2}$ BE of 465.0 eV. There is no evidence to link this resolved peak to either an impurity element or to satellite lines from any of the elements present. Clearly, this BE would seem to be far too high to be zero-valent Ru. Even though this positive BE shift could be due to strong atomic-relaxation effects of small Ru particles, a shift of 3.9 eV relative to bulk Ru^0 is much greater than the estimated relaxation energy shift of 1.0-1.25 eV calculated for Ru $3p_{3/2}$ (19). However, neither the $3d_{5/2}$ BE nor previous results (9,10,24,26) suggest the existence of significant amounts of non zero-valent Ru. The apparent great ionicity of the Ru species is obvious from the BE shift relative to that for bulk RuO_2 (+ 2.7 eV) and to that for highly dispersed RuO_2 (+ 2.4 eV). There is even a shift of + 1.5 eV relative to the Ru $3p_{3/2}$ BE in $Ru(NH_3)_6^{3+} NaY$. Such a shift can not be due just to small clusters of Ru^0 inside the supercages, otherwise a similar BE would have been exhibited by the RuNaY-VI-R1 catalyst. This great apparent ionicity of the Ru species suggests that this Ru species may be interacting with an electronegative atoms such as framework oxygen atoms. The electron density of oxygen in the sodalite cages is greater than that in the supercages and on the external surface of faujasite (9,27). Therefore, Ru would be expected to have a greater tendency to interact with the framework oxygen atoms in the sodalite cages. This was recently suggested by Pearce, et al. (9). However, the results of Pearce et al. would seem to indicate that, upon exposure to O_2 at ambient, the Ru is removed permanently from the sodalite cages. As stated

earlier, it is not known whether this removal is related to static reduction in H_2 . Thus, it is suggested that the Ru $3p_{3/2}$ BE of 465 eV found for RuNaY-R1 and RuHY-R1 corresponds to reduced (at least partly) Ru highly dispersed and probably located in the sodalite cages. In this location and by virtue of the symmetry of the Ru p orbitals, interaction of the Ru with the highly electronegative framework oxygens having only partially filled p orbitals results in a large shift in the Ru $3p_{3/2}$ BE as a result of FSCI. This size of this shift is probably also affected by atomic-relaxation of the small Ru "entities".

The Ru $3p_{3/2}$ BE's of RuNaY-R1 and RuHY-R1 located at 462.3 and 462.6 eV, respectively, are suggested to be due to small reduced Ru particles located in the supercages and perhaps on the external surface. This location is in good agreement with the BE found for RuNaY-VI-R1 prepared from $Ru_3(CO)_{12}$ (462.0 eV). The positive shift in BE's on going from RuNaY-VI-R1 to RuNaY-R1 to RuHY-R1 may be related to the increasing acidity of the support and hence to some metal-zeolite interactions. However, since ΔBE 's relative to bulk Ru^0 of 0.9 -1.5 eV are in the range of the ΔBE due to the change in the atomic-relaxation energy of Ru $3p_{3/2}$ (ca. 1.25 eV) (19), these differences could reflect slight differences in particle size.

Finally, the Ru $3p_{3/2}$ BE's of RuNaY-R1 and RuHY-R1 located at 458.8 and 460.5 eV, respectively, are shifted -2.2 and -0.5 eV relative to bulk Ru^0 . It is now known that alkali promotion of Ru/SiO_2 results in a negative shift of the Ru $3p_{3/2}$ BE (19). However, the Ru $3d_{5/2}$ BE is also shifted negatively, which was not the case for zeolite-supported Ru. Thus, one is not able to conclude that there is a simple promotion effect of the Na^+ cations in the zeolite. Also, no such downshifting in BE was seen for the highly dispersed RuNaY-VI-R1 catalyst even though it had a significantly higher Na^+

concentration in the zeolite. In addition, this negative BE shift for RuHY-R1 can not be completely attributed to an effect from residual Na^+ ions because the remaining Na^+ ions in HY should be mainly in the hexagonal prisms which can not be reached by Ru species. Even though the detailed mechanism for the FSCI between Ru and the zeolite is not well understood, it seems likely that the symmetry of the Ru p orbitals also favors FSCI with elements having filled or partially filled s and p orbitals such as Na, H, Al and Si. Therefore, it is concluded that this lowest BE corresponds to a reduced species of Ru which, as a result of the method of preparation, development of acid centers, and possibly neutralizing cation type, interacts with the zeolite in such a way so as to decrease the BE of the Ru $3p_{3/2}$ core electrons without greatly affecting the Ru $3d_{5/2}$ BE.

The stability of the Ru species having the $3p_{3/2}$ BE of 465 eV even for extended periods of reduction (R2) can be seen in Tables 3 and 4. The other two species of Ru in RuNaY also appeared to change little. However, these other two species in RuHY appeared to form more or less bulk Ru^0 upon extensive reduction, possibly as a result of sintering.

Bulk-like Ru^0 was observed for RuNaY-OxR and RuHY-OxR. This bulk-like Ru^0 has been attributed to large Ru particles on the external surfaces of the Y-type zeolite. The lack of significant Ru-zeolite interaction is presumably due to the fact that the Ru exists primarily as very large particles on the external surface of the zeolite.

Na/Zeolite Ratio

The RuNaY catalyst contained approximately 3.1 wt % Ru which corresponds to about 30% of the exchange capacity. It can be seen in Table 3 that following ion-exchange to form $[\text{Ru}(\text{NH}_3)_6]^{3+}$ NaY the Na/zeolite ESCA intensity

ratio fell from 0.74 (for NaY) to 0.17, corresponding to a decrease in Na of 77%. However, upon decomposition and reduction this ratio stabilized at around 0.40 corresponding to a decrease in Na relative to NaY of ca. 45%. ESCA is essentially a surface technique and is only able to sample the outer 2 nm or so of the zeolite. Thus, these results indicate that during exchange $\text{Ru}(\text{NH}_3)_6^{3+}$ is possibly preferentially exchanged to higher concentrations in the outer regions of the zeolite. Upon heating Na^+ is able to re-establish a more uniform concentration. The greater decrease in Na relative to NaY (45%) compared to the decrease necessary to account for Ru exchange (30%) had perhaps two causes: during Ru exchange from an aqueous solution it is possible that some proton-Na exchange also occurred (10), and/or the concentration of Na in site I in the hexagonal prisms remained disproportionately high as the result of low mobility.

The Na/zeolite intensity ratio for the RuHY catalyst (Table 4) remained approximately constant relative to the original NH_4Y zeolite. This indicates that most of the exchange of $\text{Ru}(\text{NH}_3)_6^{3+}$ was with NH_4^+ .

Thermal Stability of Ru in the Zeolite

The thermal stability and the migration tendency of Ru on ion-exchanged zeolites were studied as a function of Ru-zeolite interaction and pretreatment conditions. The migration tendency of Ru can be gauged by the surface ESCA atomic ratio of Ru/zeolite. Formation of large Ru particles on the external surface of the zeolites results from sintering and migration of Ru from inside the zeolite cavities during thermal treatment. The ESCA intensity of the metal particles on the external surface of the zeolite is greatly enhanced compared to the metal within the internal cavities of the zeolite (10) due to the surface-sensitive nature of ESCA.

Ru/zeolite atomic ratios for RuNaY catalysts under various treatments are listed in Table 3. These Ru/zeolite ratios represent the surface concentration of Ru on the external surface and in the outermost supercages of NaY. The freshly exchanged $[\text{Ru}(\text{NH}_3)_6]^{+3}\text{NaY}$ had a Ru/zeolite ratio of 0.0126. After treatments under the conditions of D, R1 and R2, the Ru/zeolite ratios increased to 0.0151, 0.0198 and 0.0207, respectively. However, after the RuNaY catalyst was pretreated using OxR conditions, a drastic enhancement of surface Ru/zeolite ratio resulted.

A systematic comparison of changes in the surface Ru concentration for RuNaY catalyst as a function of pretreatment can be made using the increase in Ru concentration on the surface of the catalyst pretreated under D, R1, R2 and OxR conditions (Table 1) relative to the surface concentration of the decomposed catalyst, i.e.

$$\frac{\Delta I}{I_D} = \text{relative surface Ru concentration} = \frac{(I_{\text{Ru}})_i - (I_{\text{Ru}})_D}{(I_{\text{Ru}})_D} \quad (3)$$

where $(I_{\text{Ru}})_i$ represents the Ru/zeolite atomic ratios and $i = \text{D, R1, R2 and OxR}$.

Very small changes in the surface Ru concentration between RuNaY-R1 and RuNaY-R2 are seen, suggesting that the Ru species are thermally stable at extended reduction times. This is consistent with the fact that identical Ru $3p_{3/2}$ spectra of RuNaY-R1 and RuNaY-R2 were observed. The drastic increase in surface Ru concentration for RuNaY-OxR is related to formation of bulk-like Ru^0 on the external surface of the zeolite due to oxidation. Since the RuNaY-OxR had a similar reduction time as RuNaY-R2, the Ru migration after OxR treatment can be attributed to the effect of oxidation and formation of bulk RuO_2 (10,24). It has previously been concluded that sintering of supported Ru

under oxygen-containing atmospheres happens as a result of the migration of Ru oxide (31).

The results for RuHY (Table 4) would appear to be somewhat different. After a slight increase in surface Ru concentration after re-reduction R1, that concentration remained essentially constant, even following treatment O_xR and the formation of Ru particles with bulk Ru⁰ characteristics (as determined by ESCA). H₂ chemisorption results indicated that in the reduced catalysts the average Ru particle size was greater in RuHY (ca. 2.7 nm) than in RuNaY (1.6 nm). Two possible causes for the apparent lack of increase in surface Ru concentration can be proposed. The first is related to a possible greater amount of defect structures (holes) in the HY support as a result of dehydration at 400°C during decomposition and reduction. This would follow because of the greater concentration of hydroxyl groups in that support. As a result significant sintering of the Ru could take place on the inner surface (holes) where large particles of Ru would form and be trapped. The second possibility is related to the fact that the ESCA sampling depth of Ru is approximately 1.6 nm (32). As the size of Ru particles exceeds this size the intensity of the Ru ESCA bands would become a weak function of any increase in Ru amount as a result of migration from within the zeolite. This would be especially true if the number of Ru particles on external zeolite surface and in the first supercages decreased as a result of agglomeration.

These results demonstrate the difficulty in using ESCA intensities for supported metals to determine change in surface concentrations without additional relevant results obtained by other techniques.

SUMMARY AND CONCLUSIONS

It has been demonstrated that the ESCA Ru 3p_{3/2} band is more sensitive than the Ru 3d_{5/2} band to the state of Ru and its interaction with the zeolite

support. The nature of the zeolite-supported Ru, as evidenced by the $3p_{3/2}$ band, is in good agreement with previous IR results (2,4).

RuNaY catalysts prepared by incipient wetness exhibits completely bulk Ru^0 behavior following reduction. This is in agreement with other results which indicate that the Ru exists primarily as large particle on the external surface of the zeolite (5).

RuNaY catalysts prepared by vapor impregnation of $Ru_3(CO)_{12}$ have Ru $3d_{5/2}$ and $3p_{3/2}$ bands which indicate that, following reduction, one species of Ru exists which is in the form of very small crystallites < 1 nm in diameter. These ESCA results are in excellent agreement with other IR and chemisorption results (4,5).

Characterization by ESCA of RuNaY catalysts prepared by ion-exchange illustrates the usefulness and even the necessity to take note of the Ru $3p_{3/2}$ band as well as the more intense $3d_{5/2}$ band. While both the Ru $3d_{5/2}$ and Ru $3p_{3/2}$ bands indicated the present of only one type of Ru (highly dispersed RuO_2) following reduction and exposure to air (D), the Ru $3p_{3/2}$ band of the highly dispersed reduced catalyst (R1) indicated the presence of 3 species of Ru, in agreement with IR results (2). The Ru $3d_{5/2}$ band did not indicate, however, such a complexity. It is concluded that the highest $3p_{3/2}$ BE and the lowest are related the zeolite-metal interactions, the latter being related to the interaction of Ru with more electropositive elements of the zeolite. The middle $3p_{3/2}$ BE could be easily related to small crystallites of Ru^0 . Much more work is needed before complete assignment of these bands can be made. The utility of using both Ru $3p_{3/2}$ and $3d_{5/2}$ bands can be seen from the fact that, without the knowledge of the $3d_{5/2}$ BE, it would have been easy to assign the $3d_{3/2}$ BE of 465 eV to a highly cationic species of Ru. If such a species existed, it would have also shifted greatly the $3d_{5/2}$ BE.

The ESCA results for RuNaY also indicated that ion-exchange with NaY may initially be more concentrated to the exterior of the zeolite. However, upon thermal treatment the concentration of Na appears to become more homogeneous throughout the zeolite.

While migration of Ru to the external surface of the zeolite could be followed as a function of pretreatment conditions for RuNaY, the results for RuHY indicated the possible difficulties in interpretation. These difficulties could arise as a result of the development of holes within the zeolite structure or "particle size"- "electron escape depth" considerations.

Finally, the results from this study fully support the existence of a strong configuration interaction of the Ru 3p core electrons with the valence 4d electrons (11).

ACKNOWLEDGMENTS

Funding for this study was provided by the National Science Foundation under Grant CHE 8108495 and by the Office of Fossil Energy, U.S. Department of Energy, under grant #DE-FG22-81PC40774.

REFERENCES

1. Jacobs, P.A., Verdonck, J., Nijs, R., and Uytterhoeven, J.B., in Hydrocarbon Synthesis from Carbon Monoxide and Hydrogen, ed. by E. W. Kugler and F.W. Steffgen, Adv. Chem. Ser. (ACS) 178, 15 (1979).
2. Goodwin, J.G., Jr., and Naccache, C., J. Catal. 64, 482 (1980).
3. Blackmond, D.G., and Goodwin, J.G., Jr., J.C.S. Chem. Comm., 125 (1981).
4. Goodwin, J.G., Jr. and Naccache, C., Appl. Catal. 4, 145 (1982).
5. Chen, Y.W., Wang, H.T., and Goodwin, J.G., Jr., J. Catal., in press.
6. Chen, Y.W., Wang, H.T., and Goodwin, J.G., Jr., J. Catal., in press.
7. Chen, Y.W., Wang, H.T., Goodwin, J.G., Jr., and Shiflett, W.K., to be published.
8. Wang, H.T., Chen, Y.W., and Goodwin, J.G., Jr., Zeolites, in press.
9. Pearce, J.R., Mortier, W.J., and Uytterhoeven, J.B., J.C.S. Faraday Trans. I 76, 403 (1980).
10. Pedersen, L.A., and Lunsford, J.H., J. Catal. 61, 39 (1980).
11. Kowalczyk, S.P., Ley, L., Martin, R.L., McFeely, F.R., and Shirley, D.A., Faraday Soc. Disc. 60, 7 (1975).
12. Proctor, A., private communication.
13. Ng, K.T., and Hercules, D.M., J. Phys. Chem. 80, 2094 (1976).
14. Wu, M., and Hercules, D.M., J. Phys. Chem. 83, 2003 (1979).
15. McEvoy, A.J., and Gissler, W., Phys. Status Solidi A 69, K91 (1982).
16. Bonzel, H.P., and Krebs, H.J., Surface Sci. 117, 639 (1982).
17. Kim, K.S., and Winograd, N., J. Catal. 35, 66 (1974).
18. Fuggle, J.C., Madey, T.E., Steinkilerg, M., and Menzel, D., Surface Sci. 52, 521 (1975).
19. Shyu, J.Z., Goodwin, J.G., Jr., and Hercules, D.M., to be published.
20. Kerkhof, F.P.J.M., and Moulijn, J.A., J. Phys. Chem. 83, 1612 (1979).
21. Scofield, J.H., J. Electron Spectrosc. and Rel. Phenom. 8, 129 (1976).
22. Haynes, H.W., Jr., Catal. Rev. - Sci. Eng. 17, 273 (1978).
23. Goodwin, J.G., Jr., J. Catal. 68, 227 (1981).

24. Verdonck, J.J., Jacobs, P.A., Genet, M., and Poncalet, G., *J.C.S. Faraday I* 76, 403 (1980).
25. Beatham, N., and Orchard, A.F., *J. Electron Spec. and Rel. Phenom.* 16, 77 (1979).
26. Clausen, C.A., III, and Good, M.L., *Inorg. Chem.* 16, 816 (1977).
27. Smith, J.V., in *Zeolite Chemistry and Catalysis* ed. by J.A. Rabo, *Adv. Chem. Ser. (ACS)* 171, Am. Chem. Soc., 1978, chap. 1.
28. Martin, R.L., and Shirley, D.A., in *Electron Spectroscopy Theory, Techniques and Applications*, ed. by C.R. Brundle and A.D. Baker, Academic Press, NY, 1977, Chap. 2.
29. Minachev, Kh.M., and Isakov, Ya.I., in *Zeolite Chemistry and Catalysis*, ed. by J.A. Rabo, *Adv. Chem. Series (ACS)* 171, Am. Chem. Soc., 1978, Chap. 10.
30. Vadrine, J.C., Dufaux, M., Naccache, C., and Imelik, B., *J.C.S. Faraday Trans. I* 74, 440 (1978).
31. Fiedorow, R.M.J., Chahar, B.S., and Wanke, S.E., *J. Catal.* 51, 193 (1978).
32. Penn, D.R., *J. Electron Spectrosc. and Rel. Phenom.* 9, 29 (1976).

TABLE 1

Abbreviated Names Used in This Study

| <u>Name</u> | <u>Pretreatment Conditions</u> |
|----------------|---|
| Fresh | Freshly exchanged $[\text{Ru}(\text{NH}_3)_6]^{3+}$ - zeolite catalyst precursor |
| Decomposed (D) | Freshly exchanged catalyst precursors decomposed in vacuum at $0.5^\circ\text{C}/\text{min}$ increasing from ambient to 400°C , followed by reduction in H_2 at 400°C for 2 hours, and then storage in a desiccator. |
| R1 | Decomposed catalysts reduced stepwise in H_2 in intervals of 50°C from room temperature to 200°C then reduced at 400°C for 2 hours. The time at each temperature was 30 minutes. |
| R2 | R1 catalysts additionally reduced at 400°C in H_2 for 4 hours. |
| OxR | R1 catalysts oxidized in dry air at 400°C for 1 hour and then reduced under the same conditions as R2. |

TABLE 2

ESCA Data for Impregnated RuNaY Catalysts

| <u>Sample#</u> | <u>C 1s</u> | <u>Al 2p</u> | <u>Ru 3d_{5/2}</u> | <u>Ru 3p_{3/2}</u> | <u>Atomic Ratio Ru/zeolite x 10³</u> |
|----------------|-------------|--------------|----------------------------|----------------------------|---|
| RuNaY-IW-R1** | 284.7 | 74.6 | 280.0 | 461.0 | 15.3 |
| RuNaY-VI-R1*** | 284.8 | - | 281.0 | 462.0 | 13.1 |

*Pretreatment conditions are listed in Table 1

**IW = incipient wetness impregnated RuNaY catalysts, wt% Ru = 2.0%, H₂ chemisorption data indicated that the average particle diameter of Ru was 6 nm (5).

***VI = vapor impregnated RuNaY catalysts, wt% Ru = 1.0%, average particle diameter determined by H₂ chemisorption was < 1.0 nm (5).

TABLE 3

ESCA Data for RuNaY

| Sample | Binding Energies (eV) | | | | | Atomic Ratio* | | |
|---|-----------------------|-------|-------|----------------------|--|---------------------------------|---------------|--|
| | C 1s | Al 2p | Na 2s | Ru 3d _{5/2} | Ru 3p _{3/2} | Ru x 10 ³ zeolite | Na zeolite | ($\frac{Al}{I}$) ^{**} Ru |
| Na ^a support | 284.8 | 74.8 | 64.7 | - | - | - | 0.74 | - |
| Freshly exchanged [Ru(NH ₃) ₆] ³⁺ NaY | 285.1 | 74.5 | 65.5 | 282.2 | 463.5 | 12.6 | 0.17 | - |
| RuNaY-D | 284.7 | 74.7 | 64.4 | 281.1 | 462.6 | 15.1 | 0.44 | 0 |
| RuNaY-R1 ^c | 284.7 | 74.9 | 64.7 | 280.5 | 465.0(16.8) ^b 462.3(45.5) 458.8(37.7) | 19.8 | 0.36 | 0.31 |
| RuNaY-R2 | 284.6 | 74.8 | 64.5 | 281.3 | 465.0(20.2) 462.3(42.8) 459.2(37.0) | 20.7 | 0.40 | 0.37 |
| RuNaY-OxR | 284.1 | 74.9 | 64.9 | 279.9 | 461.1 | 34.1 | - | 1.36 |

*: Ratios calculated based on equation 2

**: Calculated using equation 3

a: Si/Al ratio calculated from ESCA data is 2.44

b: Numbers in parentheses represent % of the peak in the Ru 3p_{3/2} region obtained from the best curve fits with weighted variances of 3.3 and 1.7, respectively, for RuNaY-R1 and RuNaY-R2, assuming FWHM's 3.4 and 3.5 eV for -R1 and -R2 samples, respectively. BE's are ±0.15 eV, r.s.d. for % of peak is ±10%.c: H₂ chemisorption data indicate that Ru particle diameter was ca. 16 nm (8).

TABLE 4

ESCA Data for RuHY

| Sample | Binding Energies (eV) | | | | | | Atomic Ratio* | |
|------------------------------|-----------------------|-------|-------|----------------------|--|---------------------------------|---------------|--------------------|
| | C 1s | Al 2p | Na 2s | Ru 3d _{5/2} | Ru 3p _{3/2} | Ru x 10 ³ zeolite | Na zeolite | $\frac{Al}{Ru}$ ** |
| NH ₄ Y support | - | 74.8 | 64.3 | - | - | - | 0.053 | 0 |
| RuHY-D | 284.7 | 75.1 | 64.4 | 281.1 | 463.1 | 11.9 | 0.047 | 0 |
| RuHY-R1** | 284.5 | 75.0 | 64.6 | 280.8 | 465.0(23.8) ^b 462.6(44.2) 460.5(32.0) | 14.9 | 0.045 | 0.25 |
| RuHY-R2 | 284.5 | 74.6 | - | 280.7 | 464.7(29.8) 461.1(70.2) | 14.6 | - | 0.21 |
| RuHY-OxR | 285.0 | 74.9 | - | 280.1 | 461.2 | 15.1 | - | 0.27 |

*: Ratios calculated based on equation 2.

**: Chemisorption data indicates the average particle diameter of Ru was < 2.7 nm (8).

***: Calculated using equation 3.

a: Si/Al ratio = 2.44, calculated from ESCA data.

b: Numbers in parentheses represent % of the peak in the Ru 3p_{3/2} region obtained from the best curve fits with weighted variances, respectively, of 1.9 and 1.0 for -R1 and -R2 samples assuming FWHM = 3.6 eV for both cases. BE's are ±0.15 eV, r.s.d. for the % of peak is ±10%

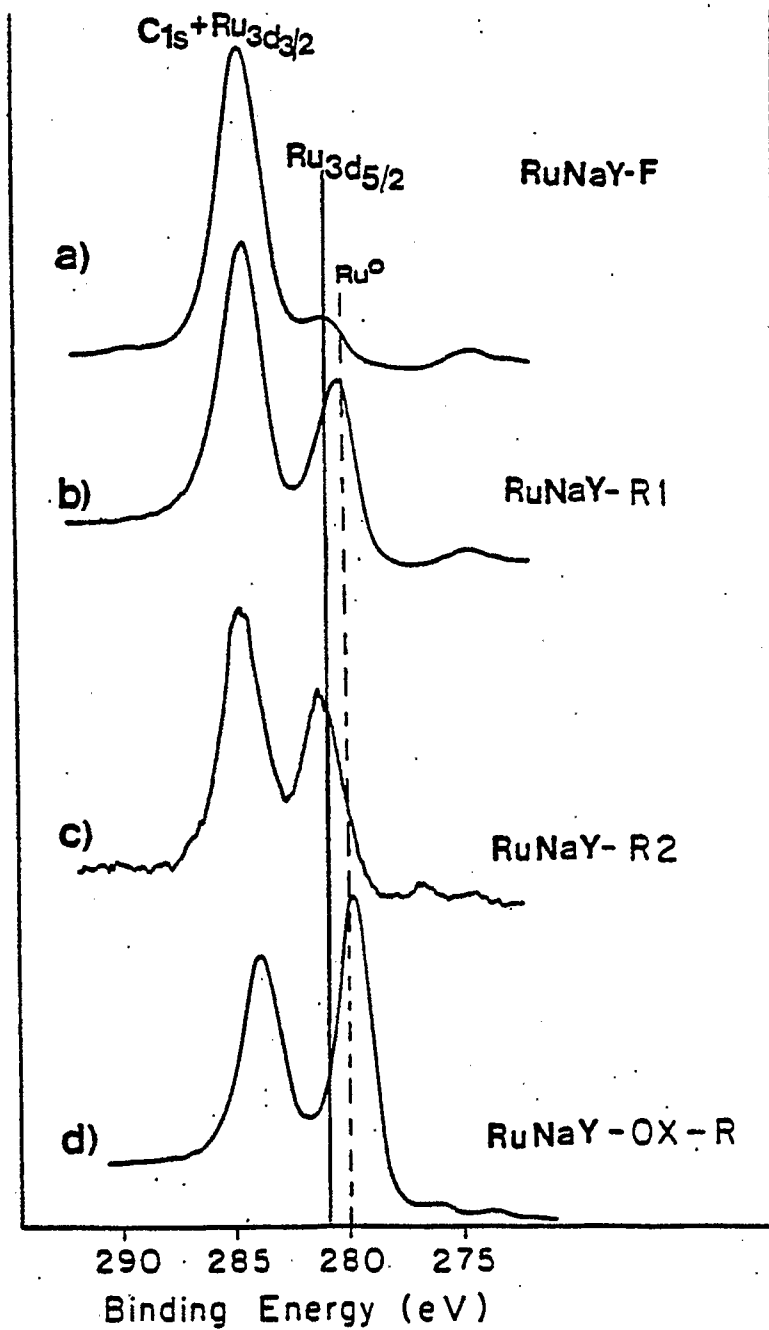


FIGURE 1: Ru $3d_{5/2}$ ESCA Spectra of Ion-Exchanged RuNaY Catalysts (3.1 wt% Ru)

(a) RuNaY-D (b) RuNaY-R1 (c) RuNaY-R2 (d) RuNaY-OxR

(The pretreatment conditions of D, R1, R2 and OxR are listed in Table 1).

ESCA Spectra of Ru $3p_{3/2}$ of RuNaY Catalysts

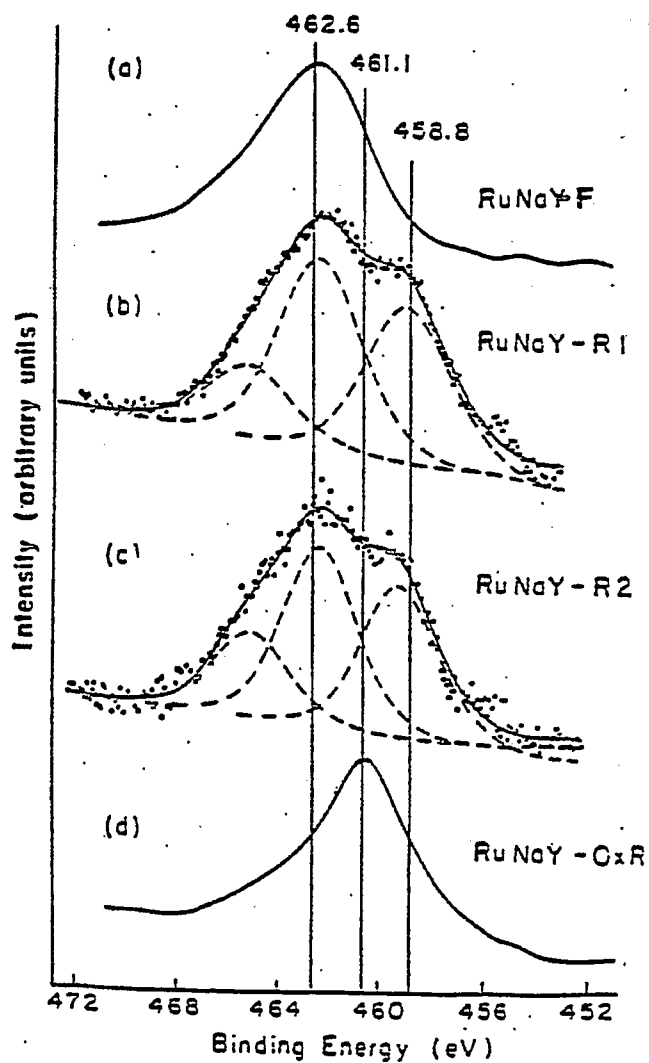


FIGURE 2: Ru $3p_{3/2}$ ESCA Spectra of Ion-Exchanged RuNaY Catalysts (3.1 wt% Ru).

(a) RuNaY-D (b) RuNaY-R1 (c) RuNaY-R2 (d) RuNaY-OxR

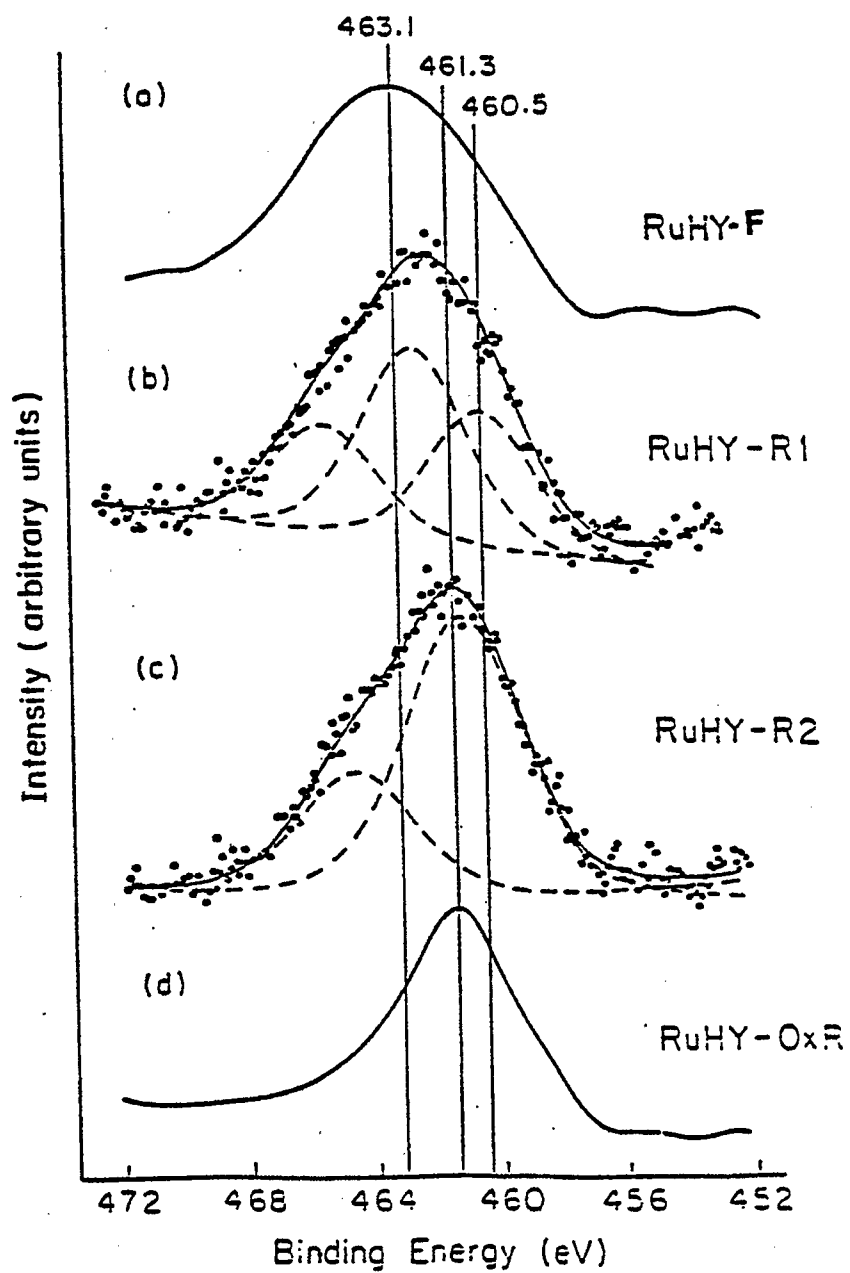


FIGURE 3: Ru $3p_{3/2}$ Spectra for Ion-Exchanged RuHY (3.1 wt% Ru)

(a) RuHY-D (b) RuHY-R1 (c) RuHY-R2 (d) RuHY-OxR

STRUCTURE AND PROPERTIES OF ZEOLITE-SUPPORTED
 $\text{Ru}_3(\text{CO})_{12}$ CATALYSTS

Liu Fu and James G. Goodwin, Jr.

ABSTRACT

An investigation of catalysts linking traditional heterogeneous and traditional homogeneous ones has been carried out. $\text{Ru}_3(\text{CO})_{12}$ was supported on NaY Zeolite via vapor impregnation of the support in a partial vacuum. The hydrogenolysis of cyclopropane over NaY-supported $\text{Ru}_3(\text{CO})_{12}$ was found to result in the complete decarbonylation of the carbonyl and also to produce a large amount of sintering of the metal even though the overall reaction temperature in the micro-reactor did not exceed 136°C . The zeolite-supported Ru clusters proved to have quite different catalytic properties from Al_2O_3 -supported Ru for the hydrogenolysis of cyclopropane to propane and for the hydro-isomerization of 1-butene. In addition, these supported clusters exhibited greater catalyst stability.

Introduction

There has been considerable interest in the past few years in the "heterogenizing" of homogeneous catalysts as a way of combining the advantages of both homogeneous and heterogeneous catalysts. This process normally consists of attaching a transition metal complex to a support. Of great importance to the full understanding of such a heterogenized catalyst is knowledge about the catalytic activities and selectivities of the supported carbonyl or cluster. In addition, it is important to determine the stability of the supported carbonyl and its possible decarbonylation under reaction conditions.

Ruthenium is well known as a heterogeneous catalyst. In addition, there are numerous studies¹⁻¹⁰ where Ru complexes were found to be effective homogeneous catalysts. A number of studies have been reported for $\text{Ru}_3(\text{CO})_{12}$ supported on SiO_2 ¹¹⁻¹³, Al_2O_3 ¹²⁻¹⁸, TiO_2 ¹⁸, and Y zeolites^{13,19-20}. Carlini et al.²¹ have studied complexes of Ru(II) having N- and P-donor linear polymeric ligands. Robertson and Webb¹¹ have investigated the hydrogenation of 1-butene over catalysts prepared from silica-supported $\text{Ru}_3(\text{CO})_{12}$. They found that the active catalyst in the temperature range studied (80° - 142°C) was a Ru subcarbonyl containing five carbonyl ligands per Ru triad. The supported complex was activated by heating it in vacuo at temperatures above 80°C at which time there was loss of carbonyl groups. Exposure to air of both the supported $\text{Ru}_3(\text{CO})_{12}$ and the various activated samples yielded samples containing no CO groups. Neither the originally supported $\text{Ru}_3(\text{CO})_{12}$ nor the oxidized catalyst exhibited any catalytic activity for the hydrogenation, hydroisomerization, or isomerization of 1-butene at temperatures from 80 - 142°C.

All carbonyls, supported or not, decompose upon heating to high enough temperatures. Supported carbonyls may pass through a number of stabilized subcarbonyl species as the temperature is raised. However, the stability of particular supported carbonyl species is dependent, typically, upon the support and possibly upon the atmosphere. Smith et al.²² investigated the stability of nickel carbonyl supported on phosphinated silica and found that $\text{Ni}(\text{CO})_3 - \text{L} - \text{SiO}_2$ was totally decarbonylated on heating under vacuum at temperatures greater than 150°C , where L was a phosphine group attached to the silica. Bartholin et al.²³ found that a number of supported complexes formed from $\text{Rh}_2\text{Cl}_2(\text{CO})_4$ and several phosphinated silicas produced metallic Rh upon prolonged heating in H_2 at only $25 - 100^\circ\text{C}$. Commereuc et al.²⁴ have studied $\text{Fe}(\text{CO})_5$, $\text{Fe}_3(\text{CO})_{12}$, and $(\text{HFe}_3(\text{CO})_{11})^{-1}$ supported on Al_2O_3 , La_2O_3 , MgO , and SiO_2 . Following thermal activation of these catalysts under a mixture of CO and H_2 at 10 bars and $180 - 270^\circ\text{C}$, small Fe particles less than 2 nm were present. After 90 hrs of F-T reaction at these conditions, T.E.M. showed the presence of very large Fe particles 20 - 50 nm in diameter.

A number of investigations into the stability of supported $\text{Ru}_3(\text{CO})_{12}$ have also been reported. Gallezot et al.¹⁹ investigated the loss of CO by HY-supported $\text{Ru}_3(\text{CO})_{12}$ in a closed, evacuated cell. They found that $\text{Ru}_3(\text{CO})_{12}$ began to lose CO at temperatures as low as 140°C but that a subcarbonyl having the proportions of $\text{Ru}_3(\text{CO})_9$ was stable between 200° and 300°C . Above 300°C , the carbonyl lost more and more CO ligands as the temperature was raised until none remained at 440°C . Robertson and Webb¹¹ found, however, that $\text{Ru}_3(\text{CO})_{12}/\text{SiO}_2$ lost some CO as low as 70°C when heated in flowing H_2 . Additional CO ligands were removed at 130 and 170°C . Recently, Hunt et al.¹⁸ have reported that 60 - 85% of the original carbonyl ligands can survive heat treatment under vacuum at 180°C [$\text{Ru}_3(\text{CO})_{12}$ on Al_2O_3] and at 250°C [$\text{Ru}_3(\text{CO})_{12}$

on TiO_2]. Very few studies of the modification of supported Ru carbonyls under catalytic reaction conditions have been done. In their classic study, Robertson and Webb¹¹ studied the reactions of 1-butene with hydrogen over $\text{Ru}_3(\text{CO})_{12}/\text{SiO}_2$ at 80 - 140°C. They did not see any indirect evidence for the total decarbonylation of the supported cluster. Otero-Schipper et al.²⁵ have investigated ethylene hydrogenation over polymer-bond analogs of

$\text{H}_4\text{Ru}_4(\text{CO})_{12-x}(\text{PPh}_3)_x$ at 50 - 90°C and 1 atm. They found no changes in the IR spectra following reaction suggesting that the originally prepared Ru_4 carbonyl clusters were largely preserved intact.

This paper reports the results of the catalytic activities and selectivities of $\text{Ru}_3(\text{CO})_{12}$ supported on NaY zeolite for the hydrogenolysis of cyclopropane to propane and for the hydro-isomerization of 1-butene. Research was also carried out on the same catalysts to determine the stability of the carbonyl under reaction conditions at relatively low temperatures.

Experimental

The supported complex was prepared by impregnation via the vapor phase of $\text{Ru}_3(\text{CO})_{12}$ of NaY zeolite, previously dried under vacuum at 450°C. This impregnation process took place in an evacuated, sealed pyrex cell held at a temperature of 80°C for several weeks. This temperature ensured that the vapor pressure of $\text{Ru}_3(\text{CO})_{12}$ was high enough for reasonably rapid adsorption of it on the zeolite but was not high enough to cause decomposition of the carbonyl. This preparation process was also used to produce Al_2O_3 - and SiO_2 -supported $\text{Ru}_3(\text{CO})_{12}$. After impregnation the zeolite had a yellow color. Visual examination of the particles of zeolite indicated that, especially for the large particles, the adsorbed carbonyl was more concentrated toward the

exterior. Thus, some large zeolite particles had centers which were white, indicating low concentrations of the carbonyl. The maximum amount of $\text{Ru}_3(\text{CO})_{12}$ able to be impregnated into the zeolite by this method seemed to be such that the % Ru in the catalyst was on the order of 1.5 wt %. However, loadings of 0.6 - 0.8 wt % Ru were usually used. A Ru/ Al_2O_3 catalyst was prepared also from $\text{Ru}_3(\text{CO})_{12}$. After impregnation of the alumina by $\text{Ru}_3(\text{CO})_{12}$ the catalyst was heated at 500°C under vacuum to decompose the carbonyl and form the reduced supported metal.

The Ru catalysts were examined closely at three conditions: as prepared, following direct decomposition at 400°C under vacuum of the prepared catalyst, and following reaction at 136°C over the supported carbonyl. Catalytic reactions were carried out at 1 atm in a flow, differential reactor and the products analyzed by gas chromatography. The catalysts were pretreated in flowing H_2 for 19 hours at 90°C or the temperature of reaction if higher than 90°C . A feed stream of 0.3 l/hr of 1-butene, 3.0 l/hr of H_2 , and 6.7 l/hr of N_2 was used for the hydroisomerization of 1-butene. For the hydrogenolysis of cyclopropane, the same proportions were used with cyclopropane replacing 1-butene. The flow rate used was sufficient to prevent bulk diffusion limitations.

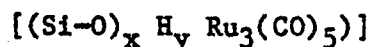
IR spectroscopic studies of the catalysts was carried out using greaseless and gas-tight IR cells made of pyrex with CaF_2 windows. Sample discs for IR investigation were prepared having diameters of 1.8 cm and weights between 10 and 20 mg. The Ru concentrations in the catalysts were determined by atomic absorption spectroscopy. These catalysts were also examined by gas volumetry (H_2 chemisorption), and transmission electron microscopy (T.E.M.).

Results and Discussion

A. Stability of $\text{Ru}_3(\text{CO})_{12}/\text{NaY}$

After preparation, the supported carbonyl exhibited an IR spectrum consistent with the undecomposed carbonyl¹³. Table 1 shows the effect of the support and method of preparation on the IR frequencies of the CO groups. The type of support greatly affects the relative intensity of the bands in addition to causing slight shifts in the band frequencies.

$\text{Ru}_3(\text{CO})_{12}/\text{NaY}$ (catalyst A in Table 2), which was yellow in color and had been exposed to air, changed to reddish-grey upon heating in H_2 at 90°C for 19 hours. It is known that $\text{Ru}_3(\text{CO})_{12}$ will react with H_2 to form a relatively stable Ru carbonyl hydride²⁶⁻²⁷. Robertson and Webb¹¹ have concluded that the pink catalytically active form of $\text{Ru}_3(\text{CO})_{12}/\text{SiO}_2$ can be represented as



Since this complex exhibited a color similar to that found for $\text{Ru}_3(\text{CO})_{12}/\text{NaY}$ following pretreatment in H_2 it may be suggested that a similar type of hydride existed for that case. However, the NaY supported complex may have contained more CO ligands since it was not pretreated under vacuum at $80^\circ - 150^\circ\text{C}$ like the SiO_2 -supported complex was.

Heating this Ru-carbonyl-hydride/NaY further in H_2 and carrying out the hydrogenolysis of cyclopropane over it at 136°C for four hours resulted in a change in the color of catalyst to grey and the development of a Ru particulate structure (catalyst C in Table 2). These Ru particles had an average diameter of 2.5 nm as determined by electron microscopy. Exposure of $\text{Ru}_3(\text{CO})_{12}/\text{NaY}$ to air for a prolonged period at 25°C resulted in the complete

oxidation of Ru and the removal of all CO ligands -- as detected by IR spectroscopy (catalyst D in Table 2). This was also found to be the case for $\text{Ru}_3(\text{CO})_{12}/\text{SiO}_2^{11}$ even though unsupported $\text{Ru}_3(\text{CO})_{12}$ is stable in air at room temperature. Neither supported $\text{Ru}_3(\text{CO})_{12}$ nor oxidized $\text{Ru}_3(\text{CO})_{12}$ was observable by electron microscopy. Reduction of this supported oxide in H_2 at 90°C for 19 hours resulted in the formation of catalyst E, which can be assumed to be highly dispersed, reduced Ru metal clusters.

Heating $\text{Ru}_3(\text{CO})_{12}/\text{NaY}$ (not exposed to air) under vacuum at 400°C for 2 hours resulted in the complete decomposition of the carbonyl and the formation of some Ru particles having diameters between 1.0 - 2.0 nm, as determined by electron microscopy (catalyst F in Table 2). H_2 chemisorption revealed the % dispersion of Ru to be approximately 100 % and IR spectra indicated no CO ligands remaining.

Decarbonylation and significant sintering of the supported carbonyl complex occurred during the hydrogenation of cyclopropane at 136°C . More sintering of the reduced metal happened under these conditions than during vacuum decomposition at 400°C . Decarbonylation and sintering of the Ru were probably facilitated by some localized heating effects in the catalyst particles during this exothermic reaction, even though the overall reactor temperature was maintained at 136°C and the catalyst granules had diameters of only ca. $3 \times 10^{-6}\text{m}$. Decarbonylation may possibly have been also due in part to slow reaction and incorporation of the CO ligands in product molecules. Certainly, it is known that supported carbonyls can be oxidized at ambient condition in air even when the unsupported carbonyls are air stable. It is thus highly probable that the carbonyl ligands react with H_2 or even organic molecules and are removed from the complex.

B. Catalytic Activity and Product Selectivity

1. Hydrogenolysis of Cyclopropane

Reduced Ru/Al₂O₃ was chosen as a standard of comparison in this study since alumina- and silica-supported Ru catalysts have been the most common type of Ru metal catalysts studied in the past. The hydrogenolysis of cyclopropane was utilized since it may exhibit many different types of concomitant processes: ring opening, hydrogenation, and fragmentation to ethane and methane. The catalysis of this reaction by Ru/SiO₂ has been previously studied²⁸. It was found in that study that, in addition to hydrogenation, there was significant fragmentation of cyclopropane in the temperature range 0-80°C.

As can be seen in Table 3, Ru/Al₂O₃ was slightly more active for this reaction at 90°C than the NaY-supported Ru clusters. However, both NaY-supported catalysts E and B yielded products consisting of 90% or more of propane. The rest of the products consisted of ethane (7-10%) and negligible quantities of methane. It is somewhat surprising that more methane was not observed since the fragmentation of cyclopropane should produce at least as many moles of methane as of ethane. While catalyst E suffered a 44% decline in its activity over a four hour period which might have been due to coking or poisoning of the catalyst by CH₄, catalyst B exhibited essentially no decline in its activity. Even catalyst E, however, showed less of a decline in activity than the Ru/Al₂O₃, which had a 60% decline in activity for the same period. This difference in activity decline is probably best explained by the difference in the degree of fragmentation on the respective catalysts. Increase in the temperature of reaction over catalyst B to 136°C resulted in a 65% conversion of the cyclopropane and a product distribution of 38% propane, 17% ethane, and 45% methane. Some of the 44% decrease in activity of this

catalyst under this reaction at 136°C could be explained by a decrease in dispersion since after reaction this catalyst consisted of supported Ru particles having an average diameter of 2.5 nm.

Table 4 shows a comparison of relative selectivities of the catalysts for the hydrogenolysis of cyclopropane at 90°C. It is interesting to note that at that temperature, the ratio of propane to ethane in the product stream was 4 times greater for the zeolite-supported Ru clusters than for the Ru/Al₂O₃. This ratio is indicative of the fact that fragmentation is a less important reaction on those zeolite-supported clusters. Another point of interest is the difference in the removal of propylene from the gas stream, the propylene being initially present in the cyclopropane stream as an impurity. While Ru/Al₂O₃ and catalyst E reduced the amount of propylene by 30-40%, catalyst B, the supported carbonyl, brought about a 94% reduction in the amount of propylene. Finally, catalyst E was more active (per g Ru) than either Ru/Al₂O₃ or catalyst B. However, the activity of Ru/Al₂O₃ per g of Ru was not lower due to the fact that it was less highly dispersed than the supported cluster catalysts since H₂ chemisorption measurements showed that the Ru of Ru/Al₂O₃ was initially 100% dispersed. Catalyst B was obviously less active than catalyst E.

2. Hydroisomerization of 1-butene

For the hydroisomerization of 1-butene a comparison was made between Ru/Al₂O₃ and catalyst E (Table 5). Ru/Al₂O₃ was found not to be active at 25°C to any measurable extent. However, an increase in the temperature to 90°C resulted in a 99% conversion of the 1-butene to mostly butane. Catalyst E on the other hand was active at 25°C yielding a 4% conversion of 1-butene with a product distribution of 63% t-butene-2, 29% c-butene-2 and only 8% butane. Increasing the reaction temperature to 90°C produced a 52% conversion

with the product distribution remaining essentially the same as at 25°C. At 112°C, 94% conversion was achieved; however, fragmentation of the hydrocarbons began to occur and butane became the main product (85%). Both of these catalysts exhibited much less stability under this reaction than under the hydrogenolysis of cyclopropane. The result of E is contrary to that found by Robertson and Webb¹¹ for SiO₂-supported oxidized Ru₃(CO)₁₂. Their catalyst was not active at all for this reaction at temperatures from 80° - 140°C. This difference is probably due to one of the following: method of preparation, support, or method of pretreatment. However, since oxygen has been shown to inhibit the isomerization of 1-butene over platinum black²⁹ it is likely that Robertson and Webb's supported oxide of Ru may not have been sufficiently reduced during catalyst pretreatment and reaction to activate it. The NaY-supported Ru oxide was probably reduced to form metal clusters.

Conclusions

This study had demonstrated the possibility for preparing active, zeolite-supported Ru catalysts from Ru₃(CO)₁₂. The vacuum-impregnation method used here would seem to have an advantage over the methods previously used in the preparation of Ru/Al₂O₃¹⁴ and Ru/SiO₂^{11, 14} from Ru₃(CO)₁₂ since no solvent was needed and catalyst preparation was carried out completely in vacuo. This, needless to say, reduces the chance for impurity intrusions into the preparation scheme. Furthermore, Anderson et al.¹⁴ found that no adsorption of Ru₃(CO)₁₂ from a methylene dichloride solution took place if the support had been pretreated in vacuo at temperatures as high as 357°C. No such effect was noted for the preparation method used here.

Ru carbonyl catalysts and Ru metal cluster catalysts supported on NaY zeolite have been shown to have unique catalytic properties compared to a more traditional Al_2O_3 -supported Ru catalyst. These supported cluster catalysts are of interest because of their stability under reaction and their selectivities vis-a-vis the hydrogenolysis of cyclopropane to propane and the hydro-isomerization of 1-butene. The results also show that, while a supported carbonyl such as $\text{Ru}_3(\text{CO})_{12}$ may retain CO ligands at relatively moderate temperatures under vacuum or a non-reacting gas, complete decarbonylation can occur at those temperatures or even lower under reaction conditions. Also, under reaction conditions, not only decarbonylation but also sintering of the metal clusters can result.

References

1. Halpern, J., Harrod, J. F., and James, B. R., *J. Am. Chem. Soc.* 88, 5150 (1966).
2. L'Eplattenier, F., and Calderazzo, F., *Inorg. Chem.* 6, 2092 (1967).
3. Hirai, H., Sawai, H., Ochiai, E., and Makishima, S., *J. Catal.* 17, 119 (1970).
4. James, B. R., and Markham, L. D., *J. Catal.* 27, 442 (1972).
5. Lyons, J. E. *J. Catal.* 28, 500 (1973).
6. Pennella, F., and Banks, R. L., *J. Catal.* 35, 73 (1974).
7. Holah, D. G., Hughes, A. N., Hui, B. C., and Kan, C. T., *J. Catal.* 48, 340 (1977).
8. Takagi, Y., Teratani, S., Takahashi, S., and Tanaka, K., *J. Mol. Catal.* 2, 321 (1977).
9. Porta, F., Cenini, S., Giordano, S., and Pizzotti, M., *J. Organomet. Chem.* 150, 261 (1978).
10. Frediani, P., Matteoli, U., Bianchi, M., Piacenti, F. and Menchi, G., *J. Organomet. Chem.* 150, 273 (1978).
11. Robertson, J., and Webb, G., *Proc. R. Soc. Lond. A.* 341, 383c (1974).
12. Kuznetsov, V. A., Bell, A. T., and Yermakov, Y. I., *J. Catal.* 65, 374 (1980).
13. Goodwin, J. G., and Naccache, C., *J. Mol. Catal.* 14, 259 (1982).
14. Anderson, J. R., Elmes, P. S., Howe, R. F., and Mainwaring, E. E., *J. Catal.* 50, 508 (1977).
15. Smith, A. K., Theolier, A., Basset, J. M., Ugo, R., Commereuc, D., and Chauvin, Y., *J. Am. Chem. Soc.* 100, 2590 (1978).
16. Brenner, A., and Hucul, D. A., *J. Am. Chem. Soc.* 102, 2484 (1980).
17. Knozinger, H., Zhao, Y., Tesche, B., Barth, R., Epstein, R., Gates, B. C., and Scott, J. P., *Faraday Disc.* 72, paper 4 (1981).
18. Hunt, D. J., Jackson, S. D., Moyes, R. B., Wells, P. B., and Whyman, R., *J. Chem. Soc., Chem. Comm.* 85 (1982).
19. Gallezot, P., Courdurier, G., Primet, M., and Imelik, B., in *Molecular Sieves II*. ed. by Katzer, J. R., ACS Symp. Series 40, 144 (1977).
20. Ballivet-Tkachenko, D., and Tkatchenko, I., *J. Mol. Catal.* 13, 1 (1981).

21. Carlini, C., Braca, G., Ciardelli, F., and Sbrana, G., *J. Mol. Catal.* 2, 379 (1977).
22. Smith, A. K., Basset, J. M., and Maitlis, P. M., *J. Mol. Catal.* 2, 223 (1977).
23. Bartholin, M., Graillat, C., Guyot, A., Coudurier, G., Bandiera, J., and Naccache, C., *J. Mol. Catal.* 3, 17 (1977/78).
24. Commereuc, D., Chauvin, Y., Hugues, F., Basset, J. M., and Olivier, D., *J. Chem. Soc., Chem. Comm.* 154 (1980).
25. Otero-Schipper, I., Lieto, J., and Gates, B. C., *J. Catal.* 63, 175 (1980).
26. L'Eplattenier, F., Mathys, P., and Calderazzo, F., *Inorg. Chem.* 9, 342 (1970).
27. Eady, C. R., Johnson, B. F. G., and Lewis, J., *J. Organomet. Chem.* 57, C85 (1973).
28. Dalla Betta, R. A., Cusumano, J. A., and Sinfelt, J. H., *J. Catal.* 19, 343 (1970).
29. Ragaini, V., *J. Catal.* 34, 1 (1974).

Table 1: IR Results for Ru₃(CO)₁₂

| catalysts | preparation method | Band Freq. (cm ⁻¹) |
|--|---|---|
| Ru ₃ (CO) ₁₂ /SiO ₂ | vap. impreg. | 2110w, 2079m (sh), 2067s, 2033vs, 1995w (sh) |
| Ru ₃ (CO) ₁₂ /SiO ₂ | soln. impreg. (Ref. 11) | 2065, 2035, 2010 |
| Ru ₃ (CO) ₁₂ /Al ₂ O ₃ | vap. impreg. | 2134w, 2063vs, 2030m, 1997s, 1986w (sh) |
| Ru ₃ (CO) ₁₂ /NaY | vap. impreg. | 2119w, 2070w (sh), 2058vs, 2025s, 2010 (sh) |
| Ru ₃ (CO) ₁₂ | in CH ₂ Cl ₂ soln. (Ref. 11) | 2060, 2029, 2007 |

Table 2: Modification of Ru₃(CO)₁₂/NaY

| Catalyst Modification | Composition | Treatment | Color | T. E. M. |
|-----------------------|--|---|--------------|-----------------------------|
| A | Ru ₃ (CO) ₁₂ /NaY | After preparation | Yellow | No metal structures >1.0 nm |
| B | Similar to [(Si-O) _x H _y Ru ₃ (CO) ₅] | heating in H ₂ at 90°C for 19 hours | reddish-grey | -- |
| C | Ru/NaY | hydrogenolysis of cyclopropane at 136°C for 4 hours | grey | 2.5 nm particles |
| D | RuO ₂ /NaY | Air/25°C/months | grey | -- |
| E | highly dispersed metal clusters | H ₂ /90°C/19 hours | grey | -- |
| F | Ru/NaY | 400°C under vacuum | grey | 1.0 ~ 2.0 nm |

Table 3: Hydrogenolysis of Cyclopropane

| Catal. | loading (% Ru) | T(°C) of Reaction | %conv. (4 hrs.) act. in 4 hrs. | % decrease | Main Products* (%) |
|-----------------------------------|----------------|----------------------|-----------------------------------|----------------|------------------------------|
| | | | | | |
| | | | | <u>Propane</u> | <u>Ethane</u> <u>Methane</u> |
| Ru/Al ₂ O ₃ | 1.04 | 90 | 1.6 | 60 | 67 17 16 |
| E | 0.56 | 90 | ca. 1 | 44 | 90 10 ca. 0 |
| B | 0.8 | 90 | ca. 1 | stable | 93 7 ca. 0 |
| B + C | 0.8 | 136 | 65 | 44** | 38 17 45 |

* Some propane formed by hydrogenation of propylene impurity in cyclopropane stream.

** Ru particles 2.5 nm in diameter (avg.) formed during the reaction.

Table 4: Relative Selectivities of Catalysts for the Hydrogenolysis of Cyclopropane[#]

| catal. | Propane/ loading(%Ru) | Propylene (200 min)/ Ethane | propylene (0) | Propane/ propane (Ru/Al ₂ O ₃) |
|-----------------------------------|--------------------------|--------------------------------|---------------|--|
| Ru/Al ₂ O ₃ | 1.04 | 2.61 | 0.63 | 1.0 |
| E | 0.56 10.10 | | 0.69 | 2.64 |
| B | 0.8 11.97 | | 0.06 | 0.788 |

[#] At 90°C after 200 min. of operation and based on existing amounts in [moles/(sec. gRu)]

Table 5: Hydro-isomerization of 1-Butene

| Catalyst* | T(°C) of Reaction | % Conv. | Main Products |
|-----------------------------------|----------------------|---------|--|
| Ru/Al ₂ O ₃ | 25 | 0 | None |
| " | 90 | 99 | butane, small amounts of t-butene-2 and c-butene-2 |
| E | 25 | 4 | 63% t-butene-2, 29% c-butene-2, 8% butane |
| E | 90 | 52 | hydroisomerization remained the main reaction in similar proportions as found at 25°C |
| E | 112 | 94 | cracking of HC's began to occur, butane main product (85%) with 10% t-butene-2 and 5% c-butene-2 |

* All catalysts deactivated fairly rapidly.

CHARACTERIZATION OF RU ZEOLITE CATALYSTS BY A
HYDROGENOLYSIS TEST REACTION NETWORK

D.J. Sajkowski, J.W. Schwank and J.G. Goodwin, Jr.

Abstract

The activity of a series of RuNaY zeolites with different ruthenium loadings has been investigated in a flow reactor using the hydrogenolysis of ethane, propane and cyclopropane as test reactions.

The RuNaY catalysts showed similar activity in ethane and propane hydrogenolysis compared to Ru/SiO₂ catalysts. However, the activity of the RuNaY catalysts for cyclopropane hydrogenolysis was by orders of magnitude higher than that of Ru/SiO₂. The RuNaY samples showed high selectivity toward propane formation, an effect which was previously observed on highly dispersed Ru/SiO₂ catalysts. It was observed that cyclopropane was sieved out of the reactant stream by the zeolite structure at the cyclopropane hydrogenolysis temperature. This effect was absent in the case of ethane and propane at their respective hydrogenolysis temperatures. A peculiar discontinuity in the cyclopropane Arrhenius plot was attributed to cyclopropane adsorption in the zeolite.

Introduction

Interactions between the metal and its support have been of interest in the field of catalysis for many years. The combination of high metal dispersions and the unique chemical environment provided by zeolites makes metal loaded zeolite systems interesting candidates for investigating metal-support interactions. Hydrogenolysis reactions of hydrocarbons have found wide application for probing the catalytic behavior of metals (1,2). The activities of hydrogenolysis catalysts appear to be very sensitive to the type of metal used as well as to structural and electronic properties of the catalyst.

Hydrogenolysis reactions have been extensively used as test reactions for Ru catalysts (3-11). However, little work has been reported on the hydrogenolysis activity of zeolite-supported Ru (12). On the other hand, a number of hydrogenolysis studies have dealt with other zeolite-supported metals, in particular Pt (13-15). Tran Manh Tri et al. (14) correlated the n-butane hydrogenolysis activity with the electrophilic character of platinum in PtY. Neopentane hydrogenolysis was one of the test reactions used by Dalla Betta and Boudart (10) to investigate PtY. They concluded that support interactions leading to electron deficient platinum were at least partially responsible for the increased activities of the catalysts. Naccache et al. (15) reported that the activity of platinum for ethane hydrogenolysis did not appear to depend upon whether the metal was supported on SiO₂ or Y zeolite. However, in cyclopropane hydrogenolysis, large activity increases were observed and attributed to the effect of the electrostatic field of the zeolite (15). Thus, different hydrogenolysis reactions can be more or less sensitive to structural or electronic properties of supported metal catalysts.

A useful combination of test reactions should be the hydrogenolysis of ethane, cyclopropane, and propane. Ethane hydrogenolysis is a structure sensitive reaction which can also provide information about the electronic properties. Cyclopropane can undergo parallel reactions leading to differences in product selectivity and can act as a very sensitive probe. Propane hydrogenolysis complements the cyclopropane hydrogenolysis in assessing the conditions necessary for secondary reactions. While this set of reactions has been proven valuable for characterizing Pt catalysts (15), it has the potential for providing even more information about ruthenium. First, ruthenium has a smaller ionization potential than platinum, and therefore, support interactions should be more pronounced with ruthenium. Secondly, cyclopropane hydrogenolysis over platinum produces only propane. The same reaction conducted over ruthenium produces ethane and methane as well as propane. Consequently, selectivity patterns may be determined when using this test reaction over ruthenium. These selectivity patterns have been extensively explored on a variety of supported ruthenium catalysts other than Ru zeolites (4,7,8). This previous work is an excellent framework to determine the influence of zeolite interactions on the properties of ruthenium. In addition, cyclopropane hydrogenolysis over RuNaY might elucidate the contribution of the electrostatic field effect on product selectivity. To this end, a series of ion-exchanged RuNaY catalysts was subjected to this set of ethane, cyclopropane, and propane hydrogenolysis test reactions.

Experimental

The RuNaY zeolite catalysts used in this study were prepared by two methods. Ruthenium was ion exchanged into NaY using an aqueous solution of $\text{Ru}(\text{NH}_3)_6\text{Cl}_3$. The exchanged $[\text{Ru}(\text{NH}_3)_6]^{3+}$ complex was decomposed in ultra high

vacuum on heating the catalyst up to 400°C at a rate of 1°C/min. The metal was then reduced at 450°C in hydrogen and subjected to the various chemisorption characterizations as outlined in Table 1. 1% RuNaY was also prepared by vapor impregnation of NaY with Ru₃(CO)₁₂. Details of this preparation procedure are given by Goodwin and Naccache (16). The preparation method and characterization of Ru/SiO₂ has been described previously (4,6).

A flow reactor containing up to 100 mg of catalyst sample was operated at atmospheric pressure (1 atm = 101.3 kPa) to obtain kinetic data on the catalysts. Prepurified hydrogen was passed through a palladium/asbestos reactor maintained at 400°C. Ultra high purity helium was passed over copper turnings maintained at 300°C. Each gas was then further purified using a molecular sieve trap maintained at liquid nitrogen temperature. High purity ethane, propane and cyclopropane were used without further treatment.

The analysis of the products and the reactants was carried out by gas chromatography. The G.C. column was a 3 m copper tube filled with silica gel (100-120 mesh), operated at 80°C.

Prior to pretreating the catalysts, the reactor was flushed with H₂ at room temperature for ten minutes. The catalysts were then slowly heated over a two hour period from room temperature to 320°C in flowing H₂ and then held at this temperature in flowing H₂ for 19 hours. Following reduction the reactor was cooled down to reaction temperature in flowing H₂.

The procedure outlined above was also used for NaY zeolite samples with the exception that helium was substituted for the hydrogen. This was also done for NH₄Y to dehydrate it and to remove ammonia, in order to form HY zeolite.

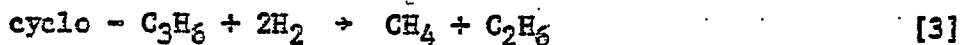
A "run" consisted of passing the appropriate reactant mixture over the catalyst and sampling the product stream after 120 sec. of reaction. In the

case of the cyclopropane hydrogenolysis experiments the reaction period was reduced to 70 sec. in order to avoid deactivation intrusions. Immediately after sampling, the flow of hydrocarbon and helium was stopped and hydrogen was passed over the catalyst at 200°C for 1/2 hour. The run was then repeated to check for deactivation. If there was no evidence for deactivation, further runs were conducted with intermittent 1/2 hour regeneration at 320°C. This procedure was sufficient for regeneration, even if signs of deactivation had been observed.

All the data used to calculate turnover numbers and subsequently kinetic parameters were obtained at conversions of less than 10%. Rate orders were determined by varying the partial pressure of one of the reactants at constant temperature. Deactivation characteristics of the catalysts were studied by passing the reactants continuously over the catalyst for 1 - 2 hours and sampling the products at 10 minute intervals.

RESULTS

The following test reactions were used in this study:



Reaction rates were determined using the following expression:

$$N_x = \frac{F_R}{A_s} \times \frac{\text{molecules}}{(\text{Ru surface atom}) \times \text{sec}} \quad [7]$$

N_x is the turnover number in molecules of reactant converted according to reactions [1] through [6], symbolized by the subscript x. F_R represents the flow rate of the reactant in molecules per second, A_g is the number of ruthenium atoms on the surface of the catalyst as determined by H_2 chemisorption, and α stands for the fraction of reactant being converted according to reactions [1] through [6].

In the cyclopropane hydrogenolysis, the percentage selectivity (S_2) for propane formation via reaction [2] was determined using the following expression:

$$S_2 = \frac{N_2}{N_2 + N_3 + N_4} \times 100 \quad [8]$$

In the case of propane hydrogenolysis, the percentage selectivity (S_5) for ethane formation via reaction [5] was calculated by means of the expression:

$$S_5 = \frac{N_5}{N_5 + N_6} \times 100 \quad [9]$$

Kinetic parameters for ethane hydrogenolysis were obtained for the RuNaY zeolites and the 3.86% Ru/SiO₂. Those parameters are given in Table 2. The rate expression could be fit to the following power law equation:

$$r = A \cdot \exp\left(-\frac{E_A}{RT}\right) (P_{Et})^m (P_{H_2})^n \quad [10]$$

Figure 1 shows the ethane hydrogenolysis activities of 0.19% RuNaY and 3.86% Ru/SiO₂. The 0.19% RuNaY was only moderately more active than the

Ru/SiO₂ catalyst over the temperature range studied. A strong similarity of the kinetic parameters among all the catalysts was found (Table 2).

However, the RuNaY zeolites displayed much higher activities than Ru/SiO₂ in cyclopropane hydrogenolysis. On the zeolites, quantitative kinetic data could only be obtained on the 0.19% RuNaY sample, the catalyst having the lowest metal loading. All the other zeolite supported Ru samples were so active that even by lowering the reaction temperature to 0°C, increasing the flow rate to the maximum possible for the reactor system, and decreasing the amount of catalyst in the reactor to 10 mg, 100% conversion was obtained. This represented an increase in activity by more than an order of magnitude over the activity of all other ruthenium catalysts previously studied. In fact, the activity for even the 0.19% RuNaY, which was the least active of the Ru zeolites in this study, was one order of magnitude greater than the highest activity ever reported on a Ru/SiO₂ catalyst (5). Figure 2 is a comparison of the 0.19% RuNaY's activity with other ruthenium catalysts reported in the literature (5).

The jump in the activity of the 0.19% RuNaY at a temperature of about 40°C, as can be seen in Figure 2, is remarkable. The Arrhenius plot for this catalyst shows a discontinuity in turnover number by almost an order of magnitude, separating two straight lines of somewhat similar slopes within experimental error. This abrupt change in turnover number was shown to be not due to deactivation and was reproducible. The discontinuity was observed regardless of direction of the temperature change or random T change. The apparent activation energies on either side of the discontinuity were found to be 21.7 and 28.8 ± 4 kcal/mole (1 kcal = 4.184 kJ) for the higher and lower temperature ranges respectively. Both of these activation energies appear to be significantly higher than the activation energies for Ru/SiO₂, Ru/MgO and

Ru sponge previously reported in the literature (5). These previous catalysts had much larger pore diameters than NaY. Therefore, effects of diffusion can be safely ruled out as the only cause of the discontinuity.

Even under non-differential conditions, it may be possible to determine selectivity patterns for the primary reactions, provided that secondary reactions can be ruled out. The results for propane selectivity are shown in Figure 3 for two RuNaY catalysts and the 3.86% Ru/SiO₂ catalyst. Data for the two other catalysts are taken from reference (5) and are shown for comparison. Methane/ethane ratios were close to unity for temperatures less than 180°C for the zeolite catalysts.

The catalysts follow two trends. The Ru sponge and the 3.86% Ru/SiO₂ both have propane selectivity-temperature curves which decrease as the temperatures increases above 110°C. The zeolite catalysts and the highly dispersed 0.6% Ru/SiO₂ all maintain higher selectivities at higher temperatures.

The activity of RuNaY for cyclopropane hydrogenolysis showed an induction period at temperatures less than 60°C. When reactants were passed over 100 mg of any of the zeolite catalysts and the product stream sampled at 120 sec., no products or cyclopropane were observed. However, at later times, the expected products and unreacted cyclopropane appeared. The sieving effect was also observed on pretreated NaY and HY. This shows that the effect is not dependent upon the presence of ruthenium. This behavior was not observed in either the ethane or propane hydrogenolysis experiments at their reaction temperatures. An investigation of the deactivation characteristics of the RuNaY catalyst was carried out at different reaction temperatures for the cyclopropane hydrogenolysis reaction. There was no influence of deactivation

on selectivity, however, the activity dropped and leveled off as a function of reaction time. A typical plot is presented in Figure 4.

Propane hydrogenolysis experiments were performed on the 0.76% Ru/NaY and the 3.86% Ru/SiO₂ catalysts. A comparison of these two catalyst's activities is shown in Figure 5. The difference between the activities of the two catalysts is modest. The energy of activation was 31 ± 4 cal/mole for the 0.76% RuNaY. This is in agreement with previously published values of the energy of activation over conventionally supported ruthenium (4). The rate order for hydrogen was also determined on the 0.76% RuNaY. It was found to be -2.0, similar to that previously reported for Ru/SiO₂ (4). However, the selectivity behavior of the 0.76% RuNaY catalyst was different from that of the 3.86% Ru/SiO₂. Figure 6 shows that on Ru/SiO₂ the selectivity for ethane formation declined at higher temperatures, while the 0.76% RuNaY exhibited 100% ethane selectivity over the temperature range studied.

DISCUSSION AND CONCLUSIONS

Within the temperature range studied in this work, the blank NaY and HY supports proved to be inactive for both hydrogenolysis and isomerization reactions. This indicated that the ruthenium surface provided the active sites for breaking the C-C bonds. To probe for a potential influence of the zeolite support on the properties of the active ruthenium sites, a comparison of the selectivity patterns of RuNaY catalysts with conventionally supported Ru catalysts was made. In the propane hydrogenolysis, RuNaY showed 100% selectivity for ethane formation via reaction [5], while the selectivity of the 3.86% Ru/SiO₂ catalysts decreased at higher temperatures (Figure 6) due to the onset of reaction [6]. However, this difference in selectivity does not necessarily indicate an influence of the zeolite. It can adequately explained on the basis of a particle size effect which was found in the previous study

of propane hydrogenolysis on a series of conventionally supported ruthenium catalysts (4). Reaction [6], the exclusively methane producing reaction, becomes dominant on catalysts with low dispersions (Figure 6) where a modified reaction mechanism seems to apply (4).

The selectivity patterns in the hydrogenolysis of cyclopropane can be interpreted in a similar fashion in terms of ruthenium particle size (5). At low temperatures, the selectivity S_2 of RuNaY did not appear to be different from Ru/SiO₂ or ruthenium sponge (Figure 3). It would appear, however, that the electrostatic field of the zeolite may facilitate the ring opening of the cyclopropane molecule by perhaps inserting a negative charge into a low lying sigma orbital of cyclopropane, as postulated by Naccache et al. (15). Such an insertion would destabilize the strained cyclopropane ring and would favor ring opening but not breaking of the chain. Thus, the presence of the zeolite would be expected to increase the rate of ring opening, after which Ru would be able to hydrogenate the intermediate to propane. This indeed seems to occur. While the reaction rate was more than one order of magnitude greater than that of comparable catalysts, the zeolite-supported Ru catalysts still maintained high selectivity S_2 for propane formation even at temperatures above 110°C (Figure 3). Such a selectivity is typical for ruthenium catalysts having high dispersions. It was previously noted that the selectivity S_2 at temperatures greater than 110°C was dependent on the ruthenium particle size in the case of conventionally supported ruthenium catalysts (5). The complete hydrogenolysis of cyclopropane into three molecules of methane via reaction [4] required large ruthenium particle sizes. The onset of reaction [4] at temperatures greater than 110°C was responsible for the decline in selectivity S_2 of Ru/SiO₂ and ruthenium sponge having low dispersions. Reaction [4] was absent on the RuNaY catalysts within the temperature range studied. This was

to be expected in view of the high ruthenium dispersion in the zeolite catalysts. For comparison, data for a highly dispersed 0.6% Ru/SiO₂ catalyst, taken from reference (5), are included in Figure 3; this Ru/SiO₂ catalysts had ruthenium particle sizes smaller than 30 Å and did not give rise to reaction [4] at these higher temperatures. The RuNaY catalysts showed somewhat higher selectivity S₂ than the highly dispersed 0.6% Ru/SiO₂ catalyst (5). It is likely that this small selectivity difference is due to the even higher ruthenium dispersion in the zeolite samples, rather than due to the influence of the electrostatic field of the zeolite. It is, however, impossible to differentiate between particle size and electrostatic field effect on the basis of our experimental data.

The catalytic activity of the RuNaY catalysts in the ethane hydrogenolysis was very similar to the activity of Ru/SiO₂ (See Table 2 and Figure 1). These results are consistent with literature reports on PtY catalyst where no significant difference between Pt/SiO₂ and PtY zeolite was detected (15). Similarly, the RuNaY samples showed only a slight increase in propane hydrogenolysis activity compared to Ru/SiO₂ (Figure 5). This increase is insignificant compared to the order of magnitude changes in turnover number which were previously observed on conventional ruthenium catalysts prepared on different supports (4).

In contrast to the ethane and propane hydrogenolysis results, the RuNaY catalyst showed a remarkable increase in cyclopropane hydrogenolysis activity by orders of magnitude compared to conventional Ru catalysts. In addition, the Arrhenius plot (Figure 2) shows a surprising discontinuity around 40°C. The discontinuity in the activity of RuNaY for cyclopropane hydrogenolysis as the reaction temperature increased past 40°C (Figure 2) can be easily explained. A TGA study (17) showed that this discontinuity occurs in the